DANMARKS OG GRØNLANDS GEOLOGISKE UNDERSØGELSE RAPPORT 1997/63

EFP-96
Fractures and rock mechanics, Phase 1

Geology

Anette Krogsbøll, Finn Jakobsen and Lena Madsen

GEOLOGICAL SURVEY OF DENMARK AND GREENLAND
MINISTRY OF ENVIRONMENT AND ENERGY

G E U S

DANMARKS OG GRØNLANDS GEOLOGISKE UNDERSØGELSE RAPPORT 1997/63

EFP-96
Fractures and rock mechanics, Phase 1

Geology

Anette Krogsbøll, Finn Jakobsen and Lena Madsen

GEOLOGICAL SURVEY OF DENMARK AND GREENLAND
MINISTRY OF ENVIRONMENT AND ENERGY

EFP-96
Fractures and rock mechanics, Phase 1

Geology

GEUS

EFP-96
Fractures and rock mechanics, Phase 1

Geology

GEUS

EFP-96
Fractures and rock mechanics, Phase 1

Geology

GEUS

EFP-96
Fractures and rock mechanics, Phase 1

Geology

GEUS

EFP-96
Fractures and rock mechanics, Phase 1

Geology

GEUS

EFP-96
Fractures and rock mechanics, Phase 1

Geology

GEUS

EFP-96
Fractures and rock mechanics, Phase 1

Geology

GEUS

EFP 96

Fractures and Rock Mechanics, Phase 1

Anette Krogsbøll, Finn Jakobsen and Lena Thrane.

GEOLOGY

List of contents

1. Introduction

This report contains the results of the research carried out by GEUS under EFP 96, Fractures and Rock Mechanics, Phase 1 (EFP J.nr. 1313/96-0007).

GEUS' involvement in this project includes 1) Geological description of the outcrop locality Hillerslev quarry, 2) Classification and geological description of all samples, 3) Standard core analysis for plugs taken from block samples, 4) Evaluation of the stress-/deformation history for Hillerslev and to a certain degree for the reservoirs and 5) Discussion of the relation between geological and geotechnical observations.

Samples from two offshore fields and two onshore localities have been analysed:

A) Stevns Klint	(Sample prefix S**)
B) Hillerslev quarry	(Sample prefix H**)
C) Tyra Field	(Samples 10-20)
D) Valhall Field, Tor Fm	(Samples 21-26)
E) Valhall Field, Hod Fm	(Samples 30-34)

The classification and geological description of all samples and standard core analysis have been carried out. A complete presentation of this work is presented in Appendix 1. In this section only extracted data is used for summing up the main conclusions of the work.

The main objective of this project is to relate geological descriptions of chalk types and fractures to rock mechanical properties. Therefore a detailed description of the fracture system of the Hillerslev quarry is carried out. In this phase of the project the sampling in the Hillerslev quarry has not been coordinated with the fracture system. Therefore no conclusions on the natural fracture system and rock mechanical properties are made. These topics will be examined in a planned phase 2 of the project.

The stress and deformation history of the chalk in Hillerslev quarry is described in chapter 3 under Chalk in the northern Jutland. Focus is on the Recent deformations during Holocene.

Finally, various relations between geological observations and geotechnical results have been evaluated.

2. Methodology

All the analysed samples were described geologically, both prior to test (original rock) and after test (test plug). The description and classification of the chalk follows the JCR nomenclature (JCR, 1996) supplemented by determination of texture variations using microscope and SEM. The nomenclature used for the texture is in this report based on the Folk (1962) and Embry and Klovan (1971) classifications.

The geological description comprises determination of chalk type, origin and diagenesis which is used for a subdivision of the chalks that might explain the variation in strength properties of the chalks. Key parameters are listed in table 2.1.

The description before test is made both on a macroscopic and a microscopic scale carried out on block material or plug trims. The macroscopic description includes primarily identification of among others lithotype, bioturbation, hardness and fractures.

The microscopic description includes determination of biogenic composition, texture and type and degree of cementation.

In addition porosity, permeability and the content of insoluble residue were carried out on all examined samples (with the exception of sample HL 91 and Block 50-3). Capillary pressure analysis were carried out on four samples (two from Hillerslev, one from Stevns and one from Valhall Hod).

The fracture description was attempted to follow the methodologies as described in Fritzen and Corrigan (1990) and by the Q-methodology describe by the Norwegian Geotechnical Institute (Løset, 1995). The fractures induced in the plugs, however, are not fully comparable to natural fractures. Also the condition of the plugs does not allow a detailed description. Therefore some modifications in the classification have been necessary.

After test, the plugs were described with respect to fracturing. A few attempts were made to clean the samples for further geological analysis, but the samples did fall apart in a way that porosity and permeability measurements and other analyses were unrealisable.

The stress and deformation history of Hillerslev is evaluated, primarily based on topographic elements in the area of the Thisted structure. Estimates of the impact from icecover and from Tertiary sediments have been established based on measurements of apparent preconsolidation stress for the four localities.

3. Chalk in northern Jutland

3.1 Introduction

The Upper Cretaceous and Danian of the Danish area are dominated by very pure, largely biogenic limestones. In the Early Maastrichtian global sea level high stand all of the danish territory was transgressed as the culmination of the period of 35 mill. years (Cenomanian-Maastrichtian) during which the chalk was deposited in a shallow seaway running from the Cretaceous Atlantic in the west to Poland in the east, bordered by the Fennoscandian Precambrian Shield and the Middle Europe islands (fig. 3.1; Håkansson et al., 1974). The near-shore areas were dominated by greensands and biocalcarenites passing into biomicrites or chalks towards the basin. In the earlier part of the Danian the marine accumulation was largely confined the Danish Basin (Håkansson & Thomsen, 1979) and the Central Graben in the present North Sea. Chalks in northern Jutland are basinal and occupies regions with salt induced highs as well as fault controlled inversion structures - much like the situation in the Central Graben.

The inversion took place during the Cretaceous and Early Tertiary along the Fennoscandian Border Zone, and due to subsequent regional Neogene upheaval and intensive Quaternary erosion, the location of the coastline to the north is not known. The chalk level now exposed is the result of up to 1000 metres of Neogene uplift and subsequent erosion (Japsen, 1993). Glacial influence is largely erosional in northern Jutland with only local internal deformation of the chalk sequence. The melting of the icesheet, however, has induced horizontal, largely bed-parallel deloading fractures of the near surface part of the chalk sequence.

Maastrichtian and Danian chalks and limestones are exposed in the sub-Quaternary surface in a zone across northern Jutland (fig. 3.2). Mostly the rocks are covered by glacial and postglacial deposits, but in a series of quarries and natural outcrops the chalks and limestones are readily accessible.

Main lithologies include a more or less continuous spectrum of biogenic carbonate sediments ranging between the two dominant end members, pelagic chalk and bryozoan limestone (Bromley, 1979). The insoluble residue is low, suggesting a low influence of terrestrial material. The chalk is intensively bioturbated with distinct burrows indicating deposition in mainly oxic conditions (Ekdale and Bromley, 1984). Sedimentation rate has been fairly high during the Maastrichtian (Håkansson et al., 1974). As a result of low to moderate post-depositional burial most onshore chalk has suffered surprisingly mild diagenesis and has retained a very high primary porosity.

3.2 The Thisted Dome

3.2.1 Introduction

The area between Thisted and Hanstholm occupies the crestal part of a broad, flat salt-induced dome. In this dome movements of the deep lying Zechstein salt commenced in Late Triassic time, have been active in the Holocene and may still be going on today (Hansen & Håkansson, 1980; Madirazza, 1981). As a result of the very late movements, chalk and limestones of Maastrichtian and Danian age are extensively exposed at the surface, in part without a cover of glacial sediments (fig. 3.3). The topography of the area is dominated by a hemi-circular line of prominent hills, capped by Danian limestones, while inside the hemi-circle Late Maastrichtian chalk is the youngest pre-Quaternary deposit present. The center of the structure is believed to be situated slightly north of Nors Sø (fig. 3.3).

Limestones in the Hanstholm Hill, on the northern side of the dome, dip gently towards the north, as confirmed by age differences of the bryozoan limestones at the north- and south-side of the hill, respectively (Hansen & Håkansson, 1980). Limestone in the Hjardemål Hill in the north-eastern part of the dome dips towards the northeast, and the area south of the lake Vandet Sø the limestone shows a generel dip towards the south (Andersen, 1944). However, the dips rarely exceed 5 degrees.

3.2.2 Stratigraphy

Due to its domal nature the Thisted Dome exposes a wide stratigraphic range of chalk at the surface. Preliminary biostratigraphical investigations indicate that the entire Maastrichtian system may be present, and possibly the center of the structure exhibit chalk of Late Campanian age (E. Håkansson, pers. com. 1996). Similarly a wide range of Danian sediments are exposed in the area, particularly along the northern and eastern perimeter. The basal Danian succession is exposed intermittently all around the dome (Håkansson & Hansen, 1979; Hansen, 1979). At the northern margin of the structure the Middle Danian zone NP3 is exposed on the beach NE of Hanstholm Hill (Thomsen, 1995), while the Late Danian zones NP8 and NP9 are exposed within the Hanstholm Harbour immediately NW of Hanstholm Hill (Hansen & Håkansson, 1979; Thomsen 1995).

3.2.3 Structural geology

Structural data from the area have been obtained at two scales. The large scale fault pattern of the Thisted Structure has been established from stereoscopic interpretation of aerial photographs covering an area of approximately 400 sq. km, while orientation on the numerous small scale fractures has been determined in outcrops.

Most prominent faults are compatible with the systems of radiating and concentric faults expected over a rising dome. The elongated Danian limestone hills are bounded by faults belonging to a concentric fault system and the hills are separated by wide gabs and intersected by narrow gullies representing a radiating fault system. A more chaotic fault pattern is found in the center of the dome with several fault bounded lakes, among which Nors Sø can be considered a collapse graben.

So far only a single topographically determined fault line has been documented through biostratigraphic investigation; i.e. a relative down-throw in excess of 50 m has been established for the block immediately west of Hanstholm (fig. 3.3; Hansen & Håkansson; 1980).

The small scale fracture orientation has been determined at selected localities in the Thisted Structure (fig. 3.3). Strike orientation of fractures measured in three different localities in the area are presented as rose diagrams on fig. 3.3. Two localities, the Thisted Quarry and Nye Kløv, are situated at the rim of the dome. In Thisted Quarry the ENE-WSW and the NW-SE orientations are easily explained as part of the overall radiating and concentric fault pattern whereas the relation of the N-S fracture orientation is less obvious. At Nye Kløv two orientations are dominating, one is following the NNE-SSW concentric faults pattern, whereas the other, NW-SE, parallels the major faults creating the gabs between the prominent hills both north and south of the locality. The dominating orientations in the Hillerslev quarry are ENE-WSW and NNW-SSE, which are in good accordance with the fault pattern detected in the immediate vicinity of the locality.

3.3 Hillerslev Quarry

The Hillerslev Quarry is an active chalk quarry located immediately southwest of the village Hillerslev in the eastern half of the Thisted Dome (fig. 3.3). Presently it provides the only good exposure within the central portion of the dome although it is located at some distance from the very center. The size of the quarry is approximately 500 sq. metres. The general tilt in the area is 4 degrees towards ESE.

A low quarry wall (approximately 4 m high and 45 m long) in the northern part of the quarry has been excavated and described in detail (fig 3.4). Fracture density and orientation have been determined along a horisontal line. The fracture description was associated with a series of one inch core plugs subsequently described and analysed for porosity and permeability.

3.3.1 Stratigraphy and lithology

The chalk in the quarry is of Late Maastrichtian age, belonging to the *humboldtii-stevensis* Zone (Brachiopod zone 9, E.Håkansson pers. com., 1996). It is a soft, weakly cemented mudstone/wackestone, composed almost exclusively of coccolithic material with subordinate amounts of skeletal material (foraminifera, bryozoans, echinoderms, molluscs) and a low content of silica, clay minerals and pyrite.

Horizontal bedding of the chalk is indicated by a slightly darker marly chalk and discontinuous layers of flint. The flint layers are traceable over larger areas and they are usefull as marker horizons. The individual beds occur as sheet like deposits with a lateral extension exceeding the length of the profile investigated. Omission surfaces are largely overprinted by late relaxation fractures, but one marked clayish fracture zone is found in the lower part of the horizontal profile. Thickness of the individual beds ranges from 10 to 50 cm as defined by relaxation fractures and from 20 to 40 cm if based on marly intervals.

Three different lithotypes have been recognized along the profile. Burrowed massive chalk mudstone is the most common lithotype found in most of the profile. Locally burrowed laminated chalk mudstone are seen and in the eastern part of the profile pebbly massive chalk mudstone (and skeletal wackestone) is dominating.

3.3.2 Diagenesis

Analysis of the chalk samples from North Jutland indicates that the chalk is more affected by compaction (mechanical diagenesis) than chemical diagenesis. The pore volume is dominated by intra fossil void.

Fine euhedral and subhedral cement crystals are found scattered in the pore space. Relatively few calcite spar crystals are associated with overgrowth of shell fragments. Syntaxial calcite overgrowth on coccolith platelets is normally scarce and the size of these crystalites is typically less than 2 μm.

Flint concretions amount to a small percentage of the total sediment volume and most silica within the chalk are found as cristobalite aggregates.

3.3.3 Porosity and permeability

The distribution of porosity and permability along the horisontal profile is illustrated in fig. 3.5. The average porosity is 47 % (with a range from 44 % to 52 %) and the average permeability is 8.1 mD (ranging from 5.1 mD to 13.4 mD).

The one inch core plugs and fracture data was sampled along the same line and the possible linkage between the variation in porosity and permeability and the position of fractures was investigated. However, low as well as high values of porosity and permeability are found associated with fractures and no consistency could be detected based on the present data set.

3.3.4 Fracture investigation

Information on fracture orientation (strike/dip) and fracture density was primarily sampled as a scanline profile from the excavated quarry wall (fig. 3.4). Data were supplemented with measurements of fracture orientation from other locations in the quarry.

3.3.5 Orientation

The orientation of numerous fractures in the quarry were measured as strike/dip and subsequently plotted in a Wulff projection (equal angle) as normals to fracture planes (fig. 3.6a) and as contours (fig. 3.6b). The fracture orientations are widely scattered, although some clustering is evident from the contour plot. A rose diagram of strike orientation (fig. 3.7a) shows that a high proportion of fractures are oriented ENE-WSW and with NNW-SSE as another important direction. Dip and dip direction of fractures has been plotted as histograms (figs. 3.8a and b) and dip direction as a rose diagram as well (fig. 3.7b). The majority of fractures are steeply dipping with a dominance of almost vertical fractures (fig. 3.8a).

Based on their dip fractures can be divided into two fairly distinct groups with little overlap: A group of low angle to horisontal fractures, dipping less than 30°, and a group of the much more numerous high angle fractures. The most likely origin of the low angle to horisontal fractures is glacigenic thrusting or simply deloading, which means they are late in origin and less relevant for subsurface conditions. These fractures are not considered further in the present investigation. The high angle fractures most likely originate from the structural growth of the dome and associated tectonic movements.

3.3.6 Scanline

A horisontal scanline profile, approximately 31 metres long, was sampled from the exposed quarry wall. As the majority of fractures are steep to very steep with a dip of 65° or more the horizontal line sampling employed is considered to be at a sufficiently high angle to the overall fracture orientation. In addition to the position of the fractures on the line the orientation (strike/dip) of each fracture has been determined. The density of fractures along the scanline is evident from fig. 3.9 where each measured fracture is marked by a vertical line.

The fractures have been divided into two sets according to their orientation and each set has been analysed individually. Coefficient of variation (CV) of the density for each subdirectional set has been calculated. CV values are 0.8 and 0.9 for the two sets indicating that the density of fractures are anticlustered approaching a random spacing (CV = 1 is random spacing). The close approximation to a random spacing of fractures is further confirmed by the spacing-frequency diagrams presented in fig 3.10. The density distribution of each subdirectional fracture set is close to straight lines indicating a negative exponential distribution for the two datasets investigated.

The histogram of density distribution of the two data sets (fig. 3.10) show that the majority of fractures are densely spaced.

3.4 Evaluation of stress and deformation history

During the Late Weichselian glaciation all of northern Jutland was covered by ice caps, and the topography, therefore, reflects the landscaping effects of glacier ice or melt water.

However, in the Thisted Dome, Maastrichtian and Danian chalks and limestones are exposed at the surface and to a large extent devoid of tills and glaciofluvial sediments. Moreover, the present surface topography displays a number of morphological features which are not readily compatible with glacial processes. Rather, it appears that most prominent topographic elements in the Thisted-Hanstholm area can be related to fault activities subsequent to the disapperance of the ice about 12,000 years ago.

The average upheaval of the area has been in the order of 2.5 mm/year in the center of the dome during the past 4000 years (Hansen & Håkansson, 1980). The relative magnitude of salt induced deformation has been established by comparing two previously horisontal reference surfaces, the Maastrichtian/Danian boundary (age 65 MY) and the maximum transgression surface (age 4000 years), with the present day sea level.

The Maastrichtian/Danian boundary is exposed in several localities around the margin and taking the local tilt into account, this points to a domal surface with a maximum near Nors Sø (Hansen & Håkansson 1980). Based on a conservative estimate of the local thichness of the Maastrichtian chalk, it appears that the Maastrichtian/Danian boundary level in the center of the dome has been raised approximately 300 m in relation to the margin during the last 65 MY; on average this amounts to a negligible yearly movement in the order of 0.005 mm/year or less (Hansen & Håkansson, 1980).

During the Holocene transgression the Thisted Dome was partly covered by the sea. The presence of erosive beach lines and beach ridges associated with this transgression allow the determination of the former maximum sea level over large parts of the dome. Deviation from the present sea level, therefore, provide information on deformation, which has affected the area, subsequent to the time of the maximum transgression which occured in the Thisted-Hanstholm area approximately 4000 years ago (Petersen, 1976).

In the Thisted-Hanstholm area the regional, isostatic land upheaval caused by uploading subsequent to the melting of the Late Weichselian ice cap is expected to be between 4 and 4.5 m above present day sea level (Mertz, 1924; fig. 3.3). However, throughout the area a substantial variation exists in the present level of the maximum Holocene transgression surface indicated by the altitude of beach lines. In most of the area the figures are significantly higher than expected, up to 15.7 m, whereas in other areas the figures are lower, down to 1.6 m (fig. 3.3). Thus, within this area a surface feature which was horisontal approximately 4000 years ago is now deformed with an amplitude exceeding 14 m (Hansen & Håkansson, 1980).

The fault controlled topography in combination with the deviation recorded between the actual, local levels of the maximum transgression and the expected, regional level confirms that the deep-seated salt surface in the Thisted-Hanstholm area has changed its shape significantly during Holocene. Thus, the calculated average yearly movement in the center of the dome is close 2.5 mm/year over the last 4000 years (Hansen & Håkansson, 1980).

4. Correlation with other chalk localities

4.1 Introduction

Samples for rock mechanical tests were taken in the Hillerslev quarry during a field trip in April, 1996. However, the feasibility of the fracture study is at present only primarily tested because the number of samples analysed for rock mechanical properties in this project is not sufficient to establish a model. In addition to the number of samples, the sampling itself was not closely related to the fracture distribution.

Despite the infeasibility of testing the fracture and rock mechanical model a comparison of the Hillerslev data with other localities has been carried out. These localities include : Stevns (outcrop), the Tyra Field and the Valhall Field (fig. 4.1). A detailed description of the samples are presented in Appendix 1.

4.2 Stratigraphy and lithology

All samples are related to the Maastrichtian Tor Formation or time equivalent except for 5 Valhall samples related to the Campanian to Turonian Hod Formation (fig. 4.2).

Each of the four localities comprises a rather uniform chalk type (with some differences between Valhall Tor and Valhall Hod). A few massive chalk mudstones are present in the Tyra and Valhall fields, but in general most of the samples can be classified as burrowed massive chalk mudstone. The samples exhibit a highly variable degree of bioturbation and type of trace fossil and most probably the chalk types from the various localities are different from each other due to different depositional and diagenetic history.

4.2.1 Depositional environment

The Maastrichtian chalks from all of the examined localities are relatively clean mudstones (with a sparse biomicritic wackestone texture). A large content of planktonic foraminifera indicates a primary autochthonous pelagic origin of the chalk. The amount of insoluble residue is relatively low, except for Valhall Hod, and suggest a low contribution of detrital material.

At Stevns the high content of bryozoans in the chalk indicates a marginal relatively shallow environment. The high intensity in bioturbation indicates that mainly oxic conditions have prevailed.

In Hillerslev a high content of calcispheres and relative low degree of bioturbation indicative of a starved euxenic depositional environment.

In the Tyra and Valhall fields the massive chalk mudstone with high density of hairline fractures are indicative of frequent mud flows e.g. reworking of the original chalks. Shear fractured zones typical for slumping are also present.

The Campanian to Turonian Valhall Hod samples comprise a large content of planktonic foraminifera indicative of predominantly autochthonous pelagic origin. The samples from the Valhall Hod have a high content of clay (kaolinite) and quartz, indicative of a high detrital supply from a nearby source area. A high density in bioturbation indicates that oxic conditions have prevailed.

In summary, the description of the chalk samples indicates the presence of three overall types of depositional situations but comprising more or less the same lithotype:

1) autochthonous pelagic chalk (burrowed massive chalk mudstone)	Stevns, Hillerslev
2) autochthonous pelagic chalk with high detrital supply (burrowed massive chalk mudstone)	Valhall Hod
3) allochthonous mud flows/slumps ((burrowed) massive chalk mudstone)	Tyra and Valhall Tor

4.2.2 Diagenesis

The diagenetic alteration seen in the samples from the same locality/well is relative uniform. However, the burial history and the formation of overpressure vary between the localities and the diagenesis is consequently affected in different ways. This has reinforced the original variation in chalk type caused by differences in depositional environment.

The outcropping chalk in Denmark is expected to mirror an overburden of 500-1000m prior to erosion and exposuring (Japsen, 1993), but in the Stevns and Hillerslev samples no severe compaction is seen. The chalks are highly porous weakly compacted with a relatively sparse cementation. Micrite cement crystals (< 3µm) prevail and only a few microspar crystals (5 - 20 µm) are seen. Foraminifera chambers are open. Microspar crystals exhibit rounded edges, suggesting etching.

The diagenesis give rise to a soft and medium consolidated chalk. A slightly higher degree of cementation is seen in the Hillerslev samples as compared to the Stevns samples.

The depth of burial in the Tyra and Valhall fields is approximately 2000 m and 2400 m, respectively. Compaction and subsequent dissolution of the chalk, however, have been retarded by pore pressure support (overpressure) reducing the effective vertical stress acting on the formation. In the Valhall field an effective depth of burial is estimated to be 395 m for the Tor Formation and 825 m for the Hod formation (Andersen, 1995). In the Tyra Field the overpressure is less than in the Valhall field and an effective overburden in the order of 1100 m is expected. (A more detailed discussion on overpressure is given in section 4.5)

In Valhall Tor the extreme overpressure has reduced the degree of compaction leaving a soft, medium consolidated and highly porous chalk. Only weak indications on pressure dissolution (dissolution seams and stylolites) are seen. The Valhall Tor chalk is dominated by both a large amount of well preserved coccoliths and fragments of coccoliths with little indication of overgrowth. Cementation consists of scattered micro-rhombs of calcite, rather than more pervasive cementation. Intraskeletal pores are seen to be largely filled with calcite spar. Occasional foraminifera chambers are open.

In the Tyra field the relative lower overpressure has resulted in some compaction, dissolution and subsequent recementation. In most of the examined samples mm-thick, high amplitude stylolites are seen. All of the Tyra samples are hard chalk with a high degree of consolidation. The chalk is dominated by a large amount of well preserved coccoliths and fragments of coccoliths with some overgrowth. Pervasive cementation dominate the samples and foraminifera chambers are filled with spar cement. In the matrix the cement crystals (3-5 μm) are generally larger than seen in the outcrop and Valhall samples. Microspar crystals (5-20 μm) are common.

The Valhall Hod samples are medium hard with a high degree of consolidation. The induration of the samples is a result of compaction rather than an effect of cementation. The Valhall Hod samples are characterized by a high content of insoluble residue (primarily kaolinite and quartz). The normal stable framework formed by grain support is hindered by the clay flakes and a very compact chalk is seen. In the clay rich samples the matrix comprises well preserved coccoliths tangled into each other. In the more clay poor samples disintegration of the coccoliths are common. The degree of cementation in the matrix is generally low and the crystal size is less than 3 μm. The fine crystal size is suggested to be a result of the high clay content which reduces the formation of large euhedral spar crystals. The obstruction in growth of calcite crystals caused by clay minerals are illustrated in figure 4.3. The figure shows a foraminifera chamber partly filled with micritic cement with intergranular clay minerals.

The diagenetic alteration observed within the examined samples indicates a relationship between cementation and depth of burial. An increase in depth of burial increases the compaction of the chalk and subsequent dissolution/stylolitisation and re-cementation. Pervasive cementation of spar crystals give rise to a hard, low porosity chalk. This is the situation for the Tyra samples.

The degree of compaction and dissolution are reduced in case of a significant overpressure which is the case in the Valhall field. The diagenetic alteration of the Valhall Tor is "restricted" to scattered calcite cementation similar to the Hillerslev and Stevns samples. The Valhall Tor, the Hillerslev and the Stevns samples appear all as soft, high porosity chalk.

A reduction in dissolution is also seen in clay rich chalk, as f. ex. in the Valhall Hod samples. Severe compaction is seen, but the compaction is primarily associated with a tighter packing of the chalk particles. Dissolution of the calcite particles are hindered by the smearing effect of the clay minerals. At the same time the clay minerals seem to prevent growth of spar crystals. Despite the lack of cement in the Valhall Hod samples, the compaction alone give rise to a medium hard, relatively low porosity chalk.

4.3 Porosity/permeability

As it is indicated from the geological description above the chalk types from the various localities/ formations appear differently, although with some similarities between Valhall Tor and the outcrop data. This subdivision in three groups is recognised when looking at the porosity/permeability data:

1) Stevns and Hillerslev	(43 - 46 %, 8 - 9 mD)
Valhall, Tor Formation	(43 - 45 %, 6 - 7 mD)
2) Tyra Field	(28 - 36 %, 1 - 4 mD)
3) Valhall, Hod Formation	(33 - 40 %, 1 - 5 mD)

Actually the porosity (and permeability) data suggest only 2 groups (figures 4.4 and 4.5):
Group 1: Outcrops and Valhall Tor
Group 2: Tyra and Valhall Hod

Whereas some similarities in diagenesis between outcrops chalks and the Valhall Tor samples can be justified from the present study, the diagenetic alteration of the Tyra and Valhall Hod chalks are quite different.

The effective depth of burial is most probably the same for outcrops and Valhall Tor and therefore the same conditions seem to have prevailed in these areas.

In the Tyra Field the porosity reduction is partly caused by pervasive cementation - a result of recementation of the dissoluted calcite from the intensive stylolitization.

In the clay rich Valhall Hod chalk the porosity reduction is primarily caused by compaction. The samples only encounter scattered cementation.

In figure 4.6 the porosity is plotted versus insoluble residue. The plot does not give any indication of a relationship between porosity and insoluble residue. Looking at the Valhall data separately (both Tor and Hod data), there seems to be a shift in trend when reaching values higher than 6 % insoluble residue, but at higher contents no major reduction in the porosity is seen. The shift in trend may be due to the different origin of the two sets of samples and may therefore not be correlated. From the available data set there are evidences of a direct impact of the content of insoluble residue on porosity. The controlling factor on the porosity distribution in argillaceous chalk is compaction. In this study the examined samples exhibit the same porosity range as highly cemented chalk.

Figure 4.7 shows the relationship between permeability and insoluble residue. Contrary to the porosity versus insoluble residue plot in fig. 4.6 there is a tendency for permeability reduction with increasing content of insoluble residue. However the number of data points are restricted due to broken samples. Especially the lack of Valhall Tor data makes the picture incomplete.

The diagenetic processes is normally reflected in both the hardness of the chalk and the porosity/ permeability values. This study, however, indicate that there is no unambiguous correlation between porosity and cementation which is seen comparing the Tyra and Valhall Hod data. Therefore porosities are not a perfect single parameter for determining the chalk type but should be compared with information as insoluble residue and texture. This should be taken into consideration when the rock mechanical properties of different chalk types are evaluated.

4.4 Fracturing

For identification of a possible relation between induration and fracturing the test plugs were examined after test. The fracture description was carried out on plugs after Multiple Triaxial Test, Unconfined Uniaxial Compression and Uniaxial Strain Compaction. Fracture type and surface were described and fracture angle determined. In addition the fracture surfaces on direct shear test plugs were described. Some uncertainty in the evaluation of the fracture description is to be expected because the tests have been carried out under different conditions and because normally only one sample from each locality have been tested by the same type of test.

The induced fractures in the samples are generally representing a fracture zone varying in thickness and characterised by a somewhat unclear surface following a large number of joints. The thickness of the fracture zone is dependent on block size and displacement. In the element samples the compression and displacement is of limited size and the fracture zone is generally less than 2 mm whereas the block tests gave rise to compaction up to 3 cm and caused severe displacement. The fracture zone is here recorded up to 2 cm. The fracture surface is rough, follows a high number of joint zones. No clean plane surface throughout the samples are seen, neither are slickensides, mineralised or non-mineralised.

Gliding planes in relatively hard chalk are seen. In these cases the chalk has been squeezed into paste and smoothed into a wavy surface (fig. 4.8)

The fracture angle seems to depend on the degree of induration. In the most cemented chalk from Tyra a well defined subvertical fracture system appears with an angle of 60-70^{o}. In the less cemented samples as Valhall Tor and Outcrop samples subhorizontal fractures is dominant. In Valhall Hod the examined sample is multifractured with both subhorizontal and subvertical fracture sets.

Special attention has been paid rock properties for stylolitic chalk. In this context the stylolites are divided into 3 groups (the description is made on plug level and the amplitude is a relative indication related to the examined samples):

1) Thin, low amplitude stylolites with varying density. This type is associated with a soft to medium hard loosely cemented chalk (samples # 21 and 24, Valhall Tor samples).

2) Medium thick, medium amplitude stylolites with varying density. These are associated with medium hard to hard, cemented chalk (sample # 10, Tyra sample).

3) Thick "accumulated" stylolite with varying amplitude. This type are often associated with hard intensely cemented chalk (sample # 20A, Tyra sample). Stylolite associated fractures are seen in this group.

The type of stylolite is dependent on clay content and pressure condition. Low content of clay induces stylolites, high clay content causes dissolution seams.

4.5 Stress and deformation history

The four localities have experienced different stress and deformation histories. A detailed description of the structural development, and thereby the stress and deformation history, requires an analysis of the topography of the overburden layers and analyses of compaction of the overburden layers also. That kind of study is possible for the offshore localities only, since there is no overburden on top of the chalk neither in Hillerslev nor in Stevns. However, the analyses are outside the scope of this work, and only simple considerations about depth of burial and major structural deformations have been included in the present study.

The geological history for the Tyra and Valhall fields is dominated by deposition of large amounts of sediments due to the formation of the Central Graben basin. During the last 65 million years thousands of meters of sediment have been deposited with a generally increasing sedimentation rate (Clausen et al., 1993, Foged et al, 1995). The overall picture of continued sedimentation has possibly been interrupted by a few small erosional or non-depositional periods - especially in the early Tertiary periods (Clausen et al., 1993). Nevertheless, the high sedimentation rates resulted in underconsolidated overburden layers and consequently overpressured chalks.

The depth of burial in the Tyra and Valhall fields are approximately 2050 m and 2400 m, respectively. Due to the high excess pore pressures the stress acting on the formation (effective stress) corresponds to an effective depth of burial much smaller than the actual depth. In the table below some simple estimations of equivalent depth of burial for Tyra and Valhall are given. Details of assumptions and equations are given in encl.1.

Field	Formation	Depth [m]	Pore pressure [MPa]	Overburden stress [MPa]	Effective overburden stress, [MPa]	Effective depth, [m]
Valhall	Tor	2400	44.5	47.8	3.3	390
	Hod	2700	46.4	53.8	7.4	810
Tyra	Tor	2050	30.7	41.7	11.0	1130

Table 4.1. Estimations of effective depth of burial

Uniaxial compaction tests (K_0 - consolidation) have been carried out for each chalk type (see enclosures 3.2, 3.5, 4.5, 4.8 and 4.10 in DGI part of the report). From such a test a preconsolidation stress (σ_{pc}) can be estimated, indicating the stress level at which the chalk shifts from elastic to plastic behavior. The shift in behavior represents the beginning of pore collapse due to increasing effective stress. If increase of effective stress would be the only explanation of porosity reduction the value of σ_{pc} would actually represent the maximum stress level experienced for the particular chalk. However, the porosity is reduced by for instance diagenetic processes and creep also. If a chalk shows high tendency to creep the value of σ_{pc} depends strongly on the applied deformation rate during testing (Krogsbøll, 1996): At high rates, like laboratory testing rates, σ_{pc} would be higher than for low rates. In those cases the value of σ_{pc} measured in the laboratory does not reflect the true preconsolidation stress which must be lower.

The apparent preconsolidation stresses $\sigma_{pc,l}$ measured in the laboratory at a deformation rate of 0.1 %/hr are compared to the preconsolidation stresses corrected for creep and referring to lower deformation rates (see Table 4.2). During production from a field the effective stress increases due to pore pressure reduction resulting in a deformation rate of approximately 1%/year (Ruddy et al., 1989). The rate caused by subsidence in the Central Graben is estimated to 0.1%/million years (Olsen, 1993). The values of preconsolidation stresses are compared to the in situ stress level σ_i for the different chalk types (from Table 4.1). The equations and the values used in this context are shown in Encl. 2.

Sample	ϕ [%]	$\sigma_{pc,l}$ [MPa] (0.1%/hr)	$\sigma_{pc,p}$ [MPa] (1%/year)	$\sigma_{pc,s}$ [MPa] (0.1%/MY)	σ_i [MPa]
Hillerslev, HL 106	47.8	4.5	3.3	1.6	~ 0
Stevns, SL 321	44.3	6	2.7	0.5	~ 0
Tyra, 16 B	32.9	55	45	30	11
Valhall, Tor 25	44.2	9	6.5	3.4	3.3
Valhall, Hod 32	37.2	20	14.5	7.8	7.4

Table 4.2. Effect of creep on preconsolidation stress.

It is seen from the results that chalk from Tyra seems to show a preconsolidation stress that can not be explained by effective stresses and creep effects only. It must be concluded that the Tyra chalk has either been exposed to higher effective stresses than known at the time, or has been subject to a cementation that has influenced the porosity decline. The latter is likely to be the case as discussed in section 4.2.2 about diagenesis. The conclusions in that section generally support the picture obtained in this section: It was concluded that Hillerslev chalk is more cemented than Stevns, and that the degree of cementation in Valhall Hod and Tor is generally low.

Based on the above considerations it must be concluded that the compressibility of a chalk is reduced by stress induced compaction and by cementation. And that the effect caused by cementation can be estimated when analyzing test results from uniaxial compaction tests. This kind of analysis contributes to a better understanding of the effect of cementation on rock mechanical properties.

The evaluation of preconsolidation stresses indicate that Hillerslev and Stevns chalk have been burried to an effective depth of less than 100 m. If it is asumed that the chalk was exposed to a higher deformation rate than was the case for offshore chalk, the effective depth might have been a few hundred meters. The icecover from the glaciation periods must have had an influence as well, but it seems likely that the pressure from the ice did not exceed 3-4 MPa. That corresponds to an icecover of 300 - 450 m.

5. Discussion

5.1 Outcrop analogue to reservoirs

Lithologically the Maastrichtian chalk at Stevns and Hillerslev are correlatives of the North Sea hydrocarbon reservoirs in the Tor Formation. Paleogeographically, however, Stevns Klint was located relatively close to the coast, while the Hillerslev and the North Sea chalks were deposited near the centre of the basin (fig. 4.1). This is reflected in the generally relatively high content of coarse skeletal grains from benthic organisms in Stevns Klint as well as in the number of omission surfaces as compared to the North Sea counterparts. The porosity in the outcrop data varies between 42-47% while gas matrix permeabilities range between 6-10 mD. The Tyra and Valhall values are generally lower and they vary over a broader range. This probably reflects differences in the postdepositional diagenetic and burial history.

Petrophysical and petrographical analyses on both outcrop chalk and reservoir chalk show a number of similarities with respect to the diagenesis. The porosity/permeability data from the Valhall Tor is falling in the same area as outcrop properties. In the case of chalks with a low clay content the type of cementation (based on SEM analysis) seems to be similar and both onshore and offshore data follow the same permeability vs. porosity trend, indicative of comparable changes in the pore systems associated with diagenesis. Petrographical and petrophysical analyses of outcrop chalk are therefore expected to be transferable to reservoir chalk.

The similarities between outcrop data and reservoir chalk is only valid to a certain limit. Some discrepancies from the general trend is seen. The change in petrophysical properties seems to be controlled by clay content and texture. Different depositional and diagenetic history has severe impact on the chalks giving rise to variations in compaction, cementation, fracturing ect. Therefore lithological differences may be taken into consideration when comparing outcrop data with reservoir chalk. It may however also be seen that in case of similar origin and composition there is a close relationship between petrophysical properties.

5.2 Fractures

The description of the fractures in the samples after test indicates that vertical and inclined fractures occur in the samples used in multiple triaxial tests. In these tests the chalk is compressed to shear failure several times.

The samples used in uniaxial strain compaction tests show horizontal fracture planes. These samples have not been exposed to shear failure and the fractures must be associated with the process of compaction.

The samples from Valhall show generally horizontal major fractures and lots of small fractures crossing the sample in almost any direction. This fracture pattern is most probably more controlled by the initial fractures in the samples than the type of test. The Valhall samples were all fractured more or less before testing.

The presence of stylolites seems not to influence the rock mechanical properties significantly. However, there is a tendency to a slightly decreased shear strength perpendicular to the stylolites. This is probably due to the small stylolite associated fractures perpendicular to the stylolite. It could be due to the bedding planes and not the stylolites as shear strength parallel to bedding planes normally is slightly higher than perpendicular to the bedding planes.

In some of the samples hairlines have been observed. Hairlines are typically perpendicular to bedding planes and are formed by small scale vertical flow in near surface sediments. The induced fractures are partly controlled by the hairlines. Parts of the fracture planes are coinciding with the hairlines. In sample SL321 the horizontal fractures are thrown in the hairline planes. The compression strength in first compression is 8% higher in SL311 (with hairlines) than in SL33 (without hairlines) which could indicate a positive effect of hairlines on strength. The amount of data is however very small and no clear evidence is found. Several of the Tyra samples have hairlines, but there is no samples without hairlines and at the same time initially unfractured. Consequently, no conclusions on effect of hairlines on strength are obtainable.

5.3 Natural fracture systems

The effect of natural (and initial) fractures on rock mechanical properties have been treated partly in this first phase of the project. Two large blocks of natural fractured Stevns chalk have been tested in a triaxial test and the results have been compared to element tests on unfractured chalk. Direct shear tests have been carried out on fractured and nonfractured samples. These test results are the first step in establishing a model for the influence of natural fractures on rock mechanical properties.

One of the purposes of this project was to establish a model of how variations in porosity, cementation, content of insoluble residue and perhaps other geological features influence the *formation* of natural fractures. If that should be possible a series of the same type of test should be performed with only one geological parameter (including location) changing from test to test.

5.4 Recommendations

- It is possible from the geological description to describe two occurences for the same porosity and permeability. The same subdivision has not been possible from the geotechnical analysis due to different test conditions. A continuation of the project therefore neccesarily has to include test analysis on a more extensive data set and carried out under exactly the same test conditions.

- In order to evaluate the influence of porosity alone on rock mechanical properties it is recommended to carry out a series of triaxial tests on Hillerslev chalk samples (at least 10). All samples should be from the same unit, with the same kind and degree of cementation. The presumably small variations in porosity are either indicated by the results and the effect can be measured, or if the variations are not reflected in the results an estimate of uncertainties of the triaxial test is obtained.
- In order to evaluate the influence of natural fracture systems it is recommended to carry out a series of tests on Hillerslev chalk samples, representing initially fractured chalk and chalk from different distances from initial fractures. In all cases the samples should be oriented in relation to the natural fracture system present.
- The shear failure criterion seems to depend on the degree of compaction. In order to improve the understanding and documentation of stress induced part of the compaction, it is recommended to carry out a series of uniaxial strain compaction tests at different deformation rates. A part of the test should be to evaluate how the horizontal stresses vary compared to the vertical during uniaxial strain compaction in elastic and plastic state (K_0 - variation).

6. References

Ali, N. and Alcock, T., 1994: Valhall Field, Norway - The First Ten Years. *In*: North Sea Oil and Gas Reservoirs - III , NTH, pp 25-40.

Andersen, S.A., 1944: Danmarks Geologi, vol. I., København.

Andersen, M., 1995: Petroleum Research in North Sea Chalk. Joint Chalk Research Phase IV, 1994-1996, Rogaland Research.

Bromley, R. 1979: Chalk and bryozoan limestone: Facies, sediments and depositional environments. *In:* Birkelund, T. & Bromley, R. (eds.), Symposium on Cretaceous-Tertiary boundary events 1, Proceedings, pp 16-32, Copenhagen.

Clausen, O.R., Korstgård, J.A., (1993). Tertiary tectonic evolution along the Arne-Elin Trend in the Danish Central Trough. Terra Nova, 5, 233-243, 1993.

Ekdale, A.A. & Bromley, R.G., 1984: Comparative ichnology of shelf-sea and deep-sea chalk. J. Paleontol., 58, pp 322-332.

Embry, A.F. and Klovan, J.E., 1971: A late Devonian reef tract on northeastern Bank Island, Northwest Territories. Can. Petrol. Geology Bull., 19, pp 730-781.

Foged, N., Krogsbøll, A., Hansen, C.F., Zinck-Jørgensen, K., Christensen, H.F., Jepsen, J.-E., (1995). Modelling of stresses and fractures in a reservoir. Final Report, EFP-93.Danish Geotechnical Institute and Geological Survey of Denmark.

Folk, R.L., 1962: Spectral subdivision of limestone types. *In*: Ham, W. E. (Ed.), Classification of Carbonate Rocks. Am. Ass. Petrol. Geologists Mem. 1, pp 62-84.

Fritsen, A. and Corrigan, T., 1990: Establishment of a Geological Fracture Model for Dual Porosity Simulations on the Ekofisk Field. In: North Sea Oil and Gas Reservoirs - II, NTH., pp 173-184.

Hansen, J.M., 1979: A new dinoflagellate zonation around the boundary. *In*: T. Birkelund, and R. Bromley (eds): Symposium on Cretaceous-Tertiary boundary events 1, Proceedings, pp 136-141.

Hansen, J.M. & Håkansson, E.,1980: Thistedstrukturens geologi - et “neotektonisk” skoleeksempel. Dansk geol. Foren., Årsskrift for 1979, pp 1-9.

Håkansson, E., Bromley, R. & Perch-Nielsen, K., 1974: Maastrichtian chalk of north-west Europe - a pelagic shelf sediment. *In*: K.J. Hsü & H.C. Jenkyns (Eds): Pelagic sediments. Spec. Publs. int. Ass. Sediments, 1, pp 211-233.

Håkansson, E. & Hansen, J.M., 1979: Guide to Maastrichtian and Danian boundary strata in Jylland. *In:* Birkelund, T. & Bromley, R. (eds.), Symposium on Cretaceous-Tertiary boundary events 1, Proceedings, pp 171-188, Copenhagen.

Håkansson, E. & Thomsen, E., 1979: Distribution and types of bryozoan communties at the boundary in Denmark. *In:* Birkelund, T. & Bromley, R. (eds.), Symposium on Cretaceous-Tertiary boundary events 1, Proceedings, pp 78-91, Copenhagen.

Håkansson, E. & Surlyk, F. (in press): Geology of Denmark. In: Moores, E.M. & Fairbridge, R.W. (Eds): Encyclopedia on World Regional Geology. Chapman & Hall.

Japsen, P. 1993: Influence of lithology and Neogene uplift on seismic velocities in Denmark: Implications for depth conversion of maps. AAPG Bull. V. 77, No. 2, 194-211.

JCR, 1996: Description and Classifiaction of Chalks, North Sea Region, Joint Chalk Research Phase IV. NPD.

Krogsbøll, A., 1996. Constitutive model with time dependent deformations. In contributions to Workshop on Computational Methods in Engineering Geology, Lund 1996.

Liboriussen, J., Ashton, P. & Tygesen, T. 1987: The tectonic evolution of the Fennoscandian Border Zone In Denmark. Tectonophysics, 137, 21-29.

Leonard, R.C. and Munns, J.W., 1987: Valhall. In: A.M. Spencer et al. (eds): Geology of the Norwegian Oil and Gas Fields. Graham & Trotman, pp 153-163.

Løset, F., 1995: Bruk av Q-metoden ved tunnelkartlegging. Intern rapport, NGI.

Madsen, L. and Zinck-Jørgensen, K., 1997: Faults and joints in chalk, Denmark: The Thisted Dome. GEUS rapport 1997/44.

Madirazza, I., 1981: Mere om Thisted saltstrukturen. Dansk Geol. Foren., Årsskrift for 1980, pp 83-87.

Mertz, E.L., 1924: Oversigt over de sen- og postglaciale niveauforandringer i Danmark. Danm. geol. Unders. II Rk., 41, 49 pp.

Olsen, A.S., 1993: Use of Geotechnical Methods in the Mathematical Simulation of Natural Fracture Development in Chalks. Ph.D. Thesis, Geological Survey of Denmark and Department of Geology and Geotechnical Engineering, Technical University of Denmark.

Petersen, K.S., 1976: Om limfjordens postglaciale marine udvikling og niveauforhold, belyst ved molluskfaunaen of C14 dateringer. Danm, geol. Unders., Årbog 1975, 75-103.

Ruddy, I., Andersen, M.A., Pattilli, P.D., Bishiawi, M., Foged, N., (1989). Rock Compressibility, Compaction, and subsidence in a high-porosity Chalk Reservoir: A Case Study of Valhall Field. Journal of Petroleum Technology, July 1989, pp 741-746.

Thomsen, E., 1995: Kalk og kridt i den danske undergrund. *In*: Nielsen, O. B. (ed): Danmarks geologi fra Kridt til i dag. Aarhus geokompendier nr. 1. Geologisk Institut. Aarhus Universitet.

ENCLOSURE 1

Effective depth of burial

Assumptions:

- Overburden gradients from Andersen (1995). Tyra is assumed to have same overburden gradient as Eldfisk.
- Brine gradient is assumed to be 0.46 psi/ft = 10.4 kPa/m, Andersen (1995).
- Valhall pore pressures are from Andersen (1995), Tyra pore pressure is from database at GEUS.
- Depth of the sea is as an average set to 50 m above both Tyra and Valhall.

Field	Formation	Depth, D [m]	Pore-pressure, P [MPa]	Overburden gradient, g_t [kPa/m]	Brine gradient g_w [kPa/m]	Overburden stress, OB [MPa]	Effective overburden stress, OB_e [MPa]	Effective gradient, g_e [kPa/m]	Effective depth, D_e [m]
Valhall	Tor	2400	44.5	20.1	10.4	47.8	3.3	9.7	390
	Hod	2700	46.4	20.1	10.4	53.8	7.4	9.7	810
Tyra	Tor	2050	30.7	20.6	10.4	41.7	11.0	10.2	1130

Equations used for calculations:

$g_e = g_t - g_w$ — Effective overburden gradient is the difference between overburden and brine gradients

$OB = (D-D_w)g_t + D_w g_w$ — Total overburden is a sum of weigth of sea water and sediments

$OB_e = OB - P$ — Effective overburden is the difference between total overburden and pore pressure

$D_e = D_w + OB_e/g_e$ — Effective depth of burial is a sum of water depth and contribution from effective overburden (which is independent of water depth).

ENCLOSURE 2

Correction of preconsolidation stress for creep effects

Basic data:

- Stress-strain curve for a uniaxial compaction test, including elastic and plastic states (vertical strain versus logarithmic vertical stress)
- Time curve for a creep test after the yield point (vertical strain versus logarithmic time)

Parameters: (Enclosure no. in paranthesis refer to DGI report)

$Q = d\varepsilon / d \log \sigma$ — Inclination of strain per decade of stress, measured in the plastic part of the stress-strain curve. (Encl.: 3.2p4, 3.5p4, 4.5p2, 4.8p2, 4.10p2)

$\sigma_{pc,l}$ — Preconsolidation stress, indicating the shift between elastic and plastic deformations (Encl.: 3.2p4, 3.5p4, 4.5p2, 4.8p2, 4.10p2)

$\varepsilon_s = d\varepsilon / d \log t$ — Creep parameter, indicating the change in strain per decade of time at a constant stress level (Encl.: 3.2p7, 3.5p8, 4.5p5, 4.8p6, 4.10p6)

T_0 — Time in creep test from when the relation between strain and logarithmic time is valid. Theoretical value from time curve. (Encl.: 3.2p7, 3.5p8, 4.5p5, 4.8p6, 4.10p6)

Assumptions:

- Laboratory deformation rate is $\varepsilon'_{lab} = 0.1$ %/hr
- Deformation rate caused by field production is $\varepsilon'_p = 1$%/year
- Deformation rate caused by subsidence and consequent increase in effective stress is $\varepsilon'_s = 0.1$ %/million years

Sample	$\sigma_{pc,l}$	Q	ε_s	T_0	σ	t_p	$\Delta\varepsilon_{cr,p}$	t_s	$\Delta\varepsilon_{cr,s}$	$\sigma_{pc,p}$	$\sigma_{pc,s}$
unit	MPa	%/dec. σ	%/dec. t	min	MPa	10^5 min	%	10^{12} min	%	MPa	MPa
HL106	4.5	23.8 *	1.07	200	6	2.44	3.30	2.44	10.8	3.27	1.58
SL321	6.0	23.8	2.59	450	6.9	5.91	8.08	5.91	26.2	2.75	0.47
16B	55	10.1 **	0.245	13	100	0.56	0.89	0.56	2.61	44.9	30.4
25	9	18.7	0.754	55	40	1.72	2.64	1.72	7.91	6.51	3.40
32	20	17.6 **	0.681	40	100	1.55	2.44	1.55	7.21	14.5	7.79

*: Value for Hillerslev could not be measured, Stevns data is used.

**: The curve is not linear in logarithmic plot - a best estimate is used.

Equations:

$$t_p = \frac{\varepsilon_s}{\varepsilon'_p \ln 10}$$

Time in creep test when deformation rate equals production deformation rate (Ruddy et.al. (1989)). Equivalent for subsidence rate.

$$\Delta\varepsilon_{cr,p} = \varepsilon_s \log\left(\frac{t_p}{T_0}\right)$$

Additional creep at time t_p (Ruddy et. al. (1989))

$$\sigma_{pc,p} = \sigma_{pc,l} 10^{\frac{-\Delta\varepsilon_{cr,p}}{Q}}$$

The correction of preconsolidation stress corresponds to a shift of virgin compaction curve, using a line parallel to the one measured in laboratory.

Figures

Figure captions

Figure 3.1: Palaeogeographic map of Central Europe and the North Sea area showing the maximum extension of the sea during Late Cretaceous. The map also shows the present-day extra-Alpine outcrops of chalks and related facies and areas with Late Cretaceous inversion.

Figure 3.2: Sub-Quaternary geological map of Denmark. (From: Håkansson & Surlyk, in press)

Figure 3.3: Geological map of the Thisted Dome. A rim of Danian sediments surrounds Maastrichtian chalk. Rose diagram of strike orientation of fractures from three localities are included (Madsen & Zink-Jørgensen, 1997)

Figure 3.4: Escavated quarry wall in the northern part of the Hillerslev Quarry.

Figure 3.5: a) Porosity distribution, b) Permeability distribution and c) Porosity/permeability cross plot.

Figure 3.6: Stereographic projections (Wulff) of fractures orientations from Hillerslev Quarry. a) normals to planes, b) contour plot.

Figure 3.7: Rose diagrams of fracture orientations from Hillerslev Quarry.
a) strike, b) dipdirection.

Figure 3.8 : Orientation/frequency histograms of fracture orientations from Hillerslev Quarry.
a) dip, b) dipdirection.

Figure 3.9: Horizontal scanline profile from Hillerslev Quarry. Fractures are marked by vertical lines.

Figure 3.10: Density distribution of fractures in the scanline profile, Hillerslev Quarry. Fractures have been divided into two sets based on their orientation. a) Spacing versus cummulative number showing almost straight lines for both fracture sets on a normal-log plot. b) histogram of spacing versus frequency for the two fracture sets.

Figure 4.1: Locality map.

Figure 4.2: Stratigraphic scheme showing the position of the chalk succession Stevns and Hillerslev compared to the North Sea reservoir sections.

Figure 4.3: Valhall Hod sample showing calcite cementation prohibited by clay. A) Thin section showing foraminifera chambers rimmed by micrite. B) SEM image of foraminifera chamber with clayminerals.

Figure 4.4: Porosity distribution of the examined samples grouped according to locality.

Figure 4.5: Permeability versus porosity plot.

Figure 4.6: Porosity versus insoluble residue plot.

Figure 4.7: Permeability versus insoluble residue plot.

Figure 4.8: Photo of gliding plane in relatively well cemented chalk (Tyra field).

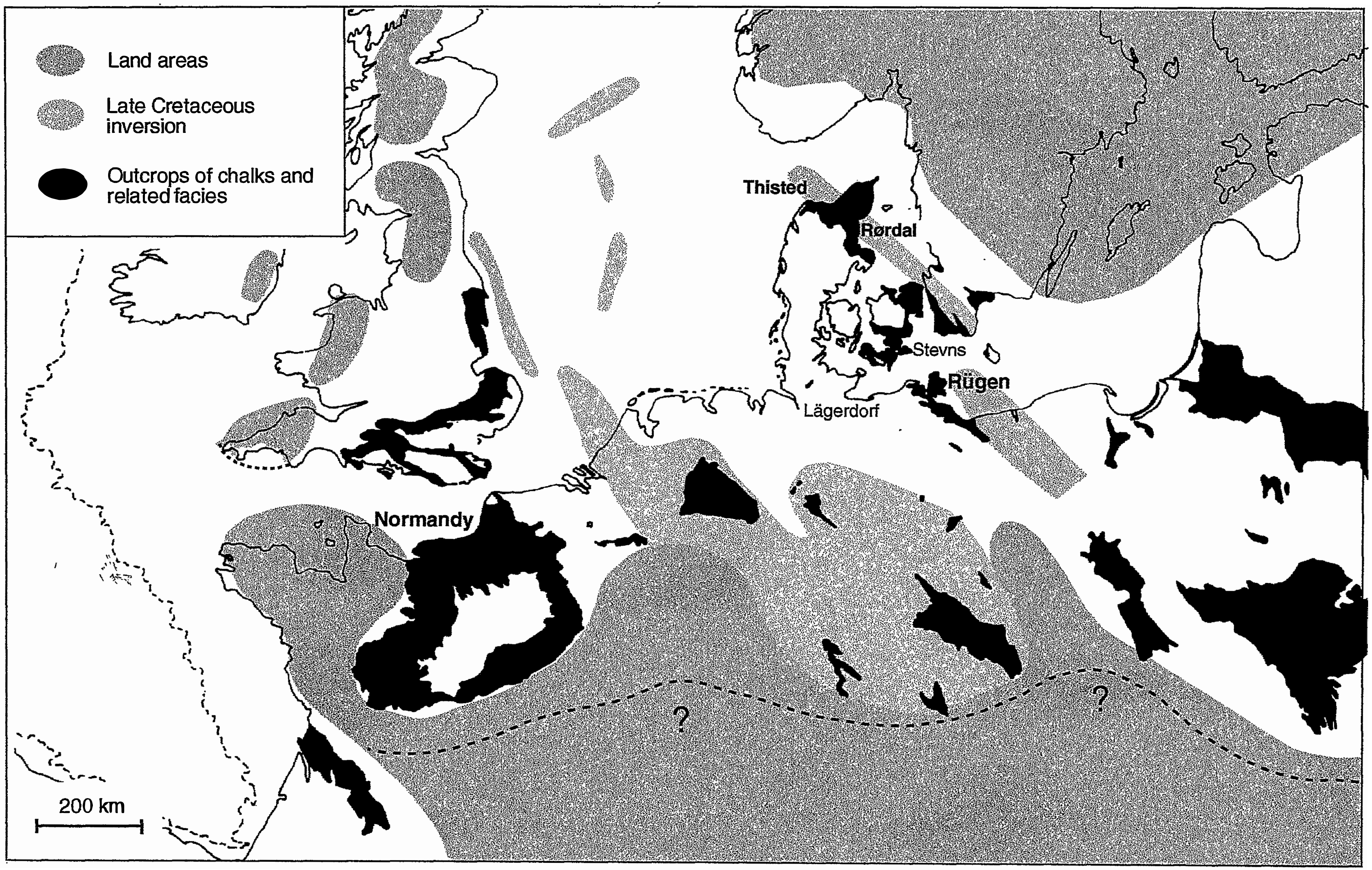
Land areas
Late Cretaceous inversion
Outcrops of chalks and related facies
Thisted
Rørdal
Stevns
Rügen
Lägerdorf
Normandy
?
?
200 km

Figure 3.1

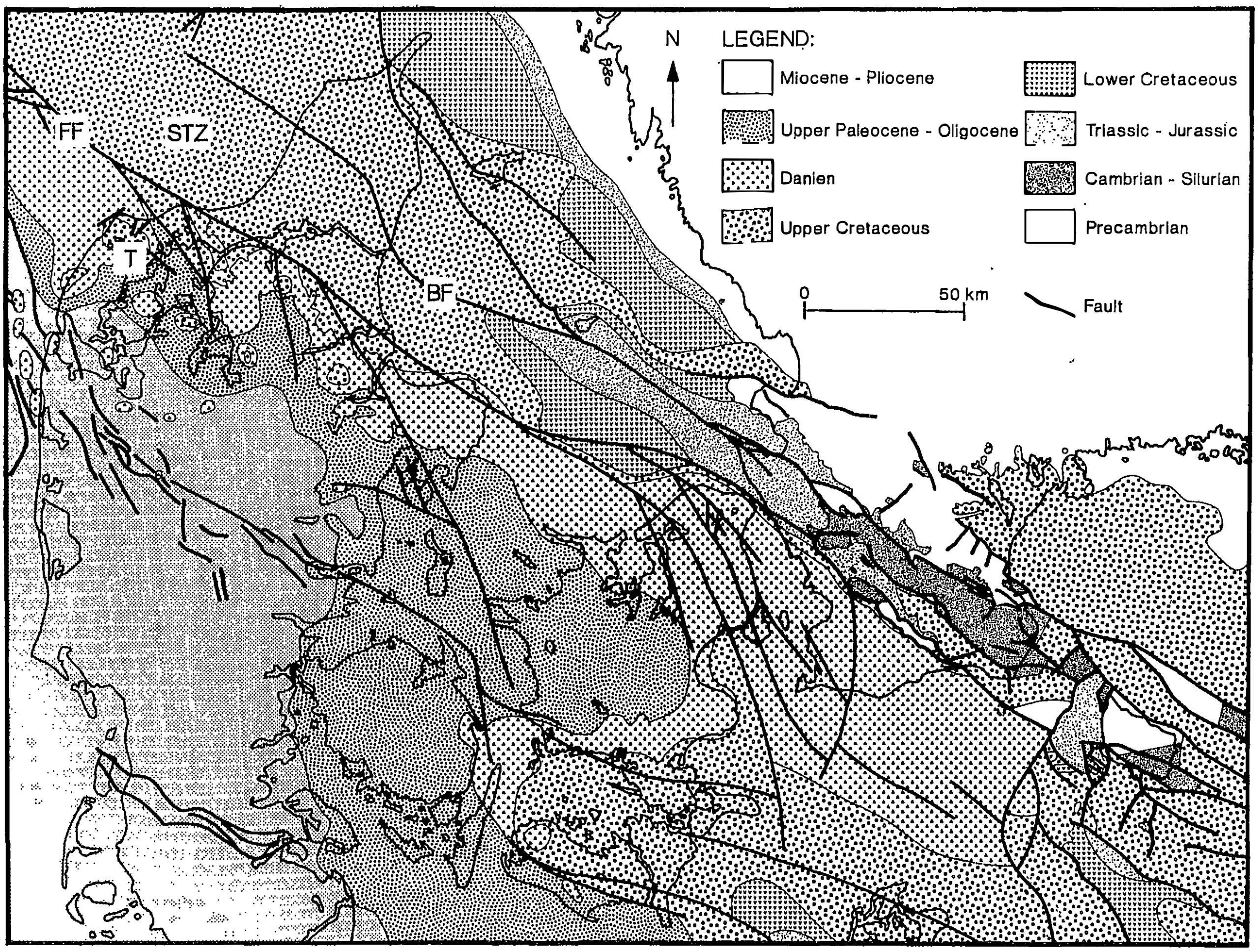

N
LEGEND:
Miocene - Pliocene
Upper Paleocene - Oligocene
Danien
Upper Cretaceous
Lower Cretaceous
Triassic - Jurassic
Cambrian - Silurian
Precambrian
0
50 km
Fault
FF
STZ
T
BF

Figure 3.2

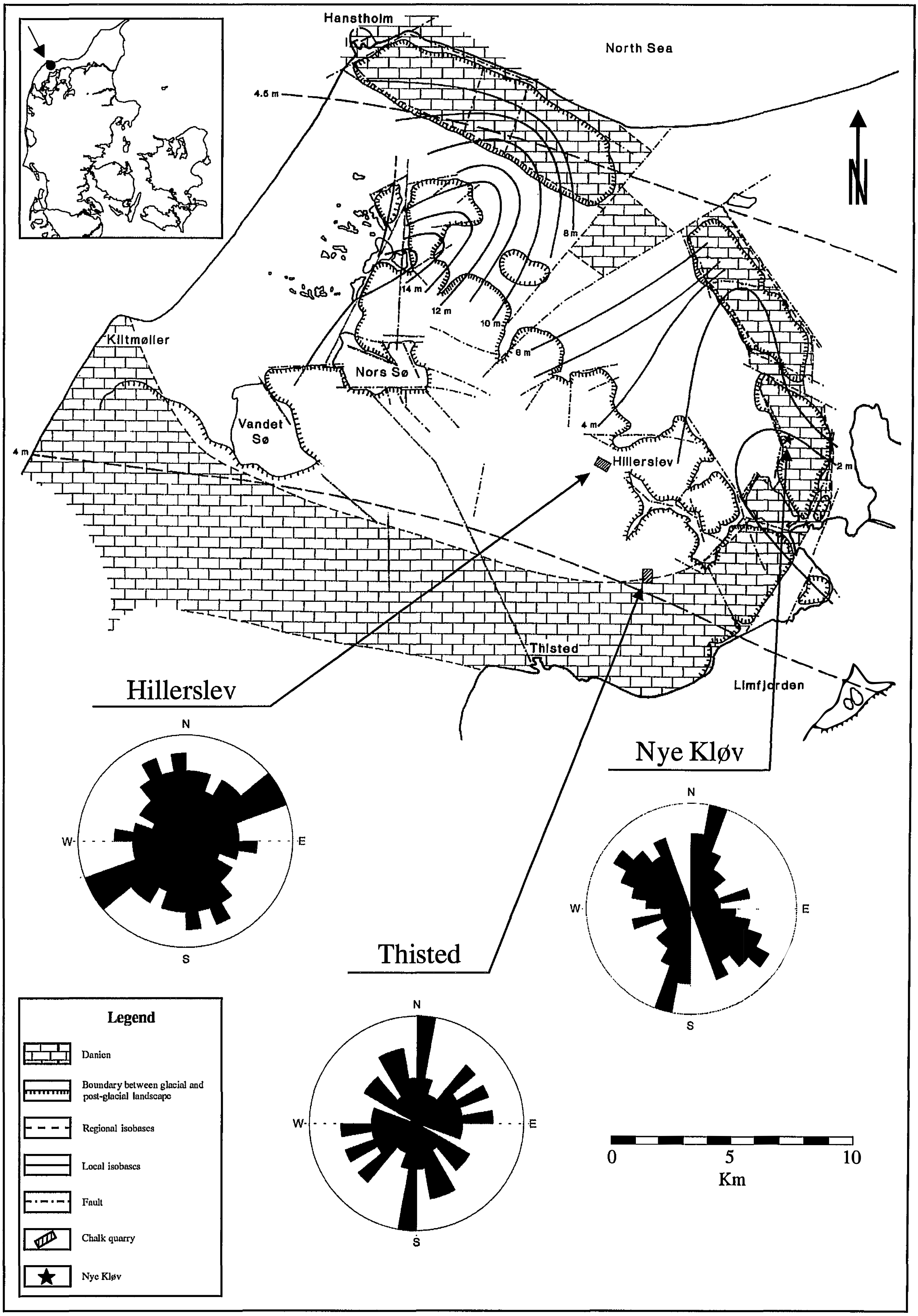
Hanstholm
North Sea
4.5 m
8 m
14 m
12 m
10 m
Kiltmøller
Nors Sø
Vandet Sø
4 m
Hillerslev
2 m
Thisted
Limfjorden
Hillerslev
Nye Kløv
Thisted
N
S
W
E
Legend
Danien
Boundary between glacial and post-glacial landscape
Regional isobases
Local isobases
Fault
Chalk quarry
Nye Kløv
0
5
10
Km

Figure 3.3

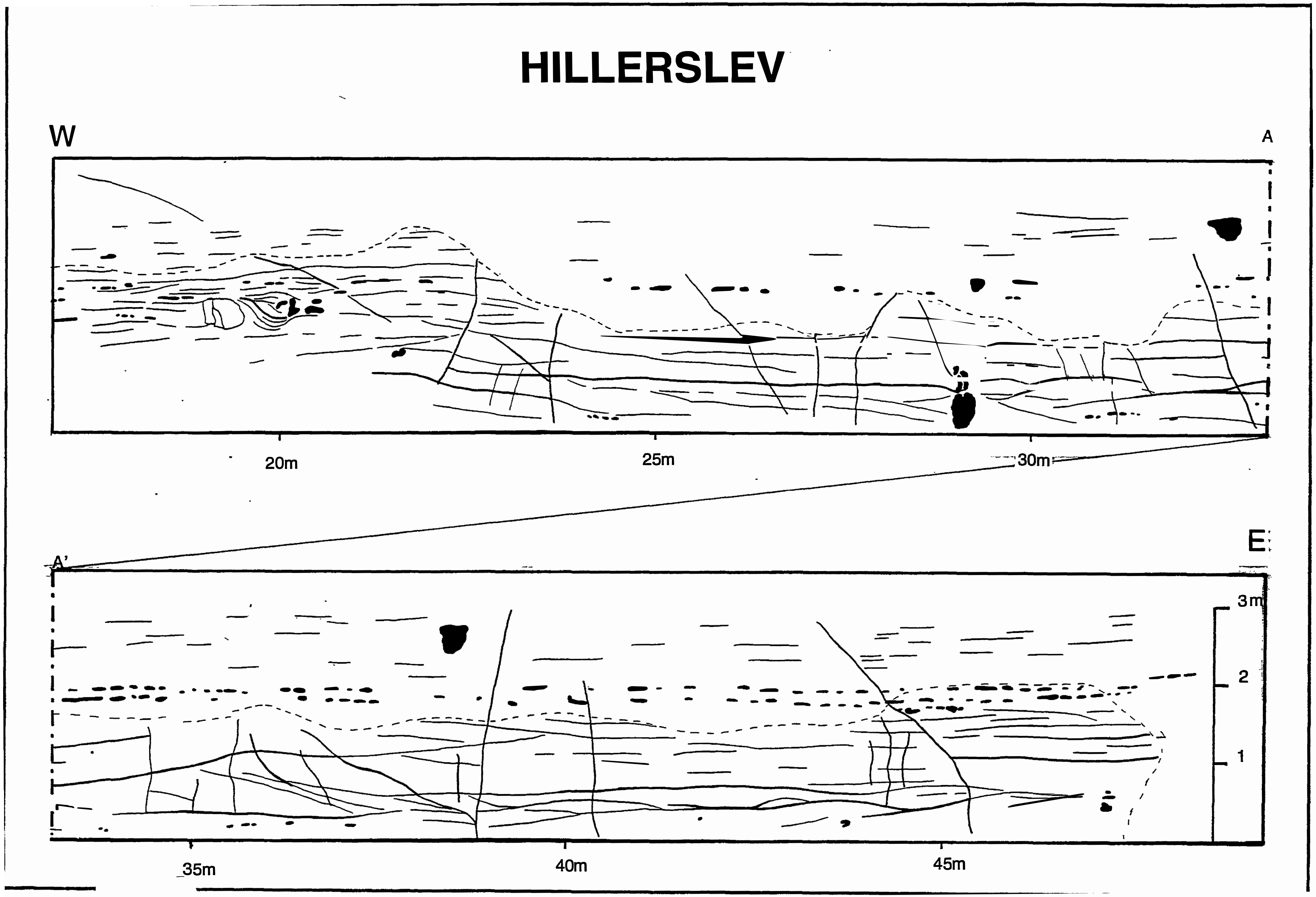

Figure 3.4

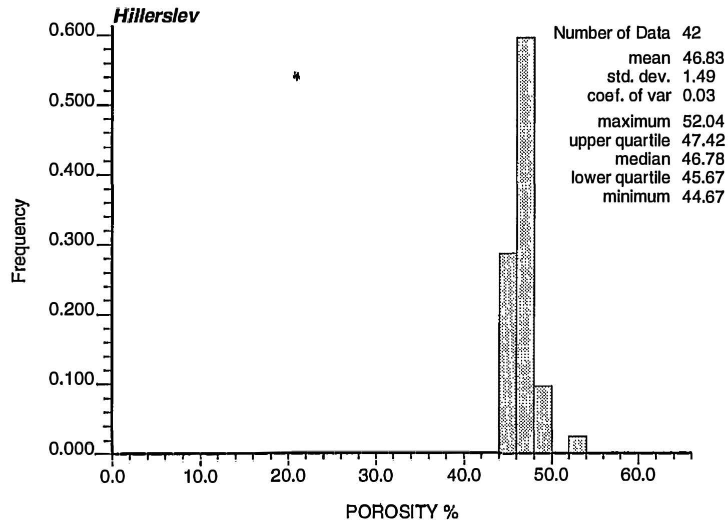
Hillerslev
Number of Data 42
mean 46.83
std. dev. 1.49
coef. of var 0.03
maximum 52.04
upper quartile 47.42
median 46.78
lower quartile 45.67
minimum 44.67
Frequency
POROSITY %

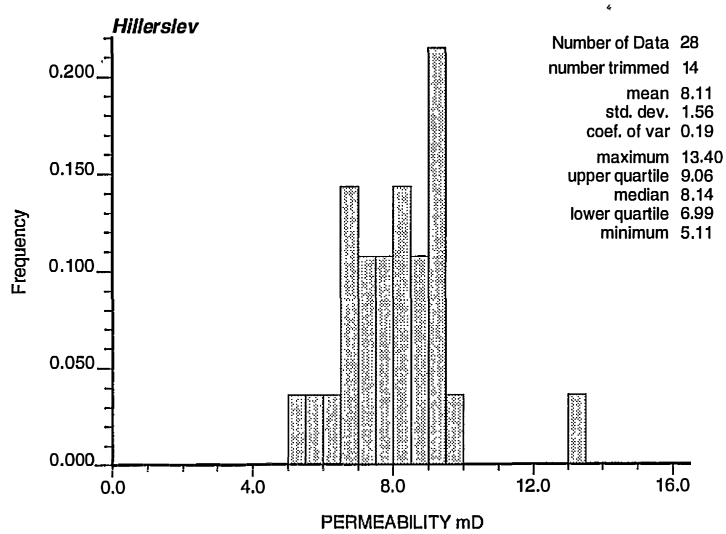
Hillerslev
Number of Data 28
number trimmed 14
mean 8.11
std. dev. 1.56
coef. of var 0.19
maximum 13.40
upper quartile 9.06
median 8.14
lower quartile 6.99
minimum 5.11
Frequency
PERMEABILITY mD

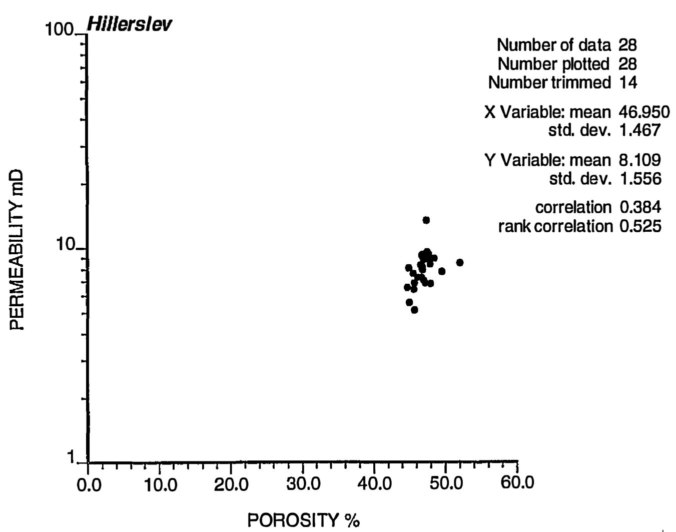
Hillerslev
Number of data 28
Number plotted 28
Number trimmed 14
X Variable: mean 46.950
std. dev. 1.467
Y Variable: mean 8.109
std. dev. 1.556
correlation 0.384
rank correlation 0.525
PERMEABILITY mD
POROSITY %

Figure 3.5

Hillerslev 1 & 2

Wulff projection

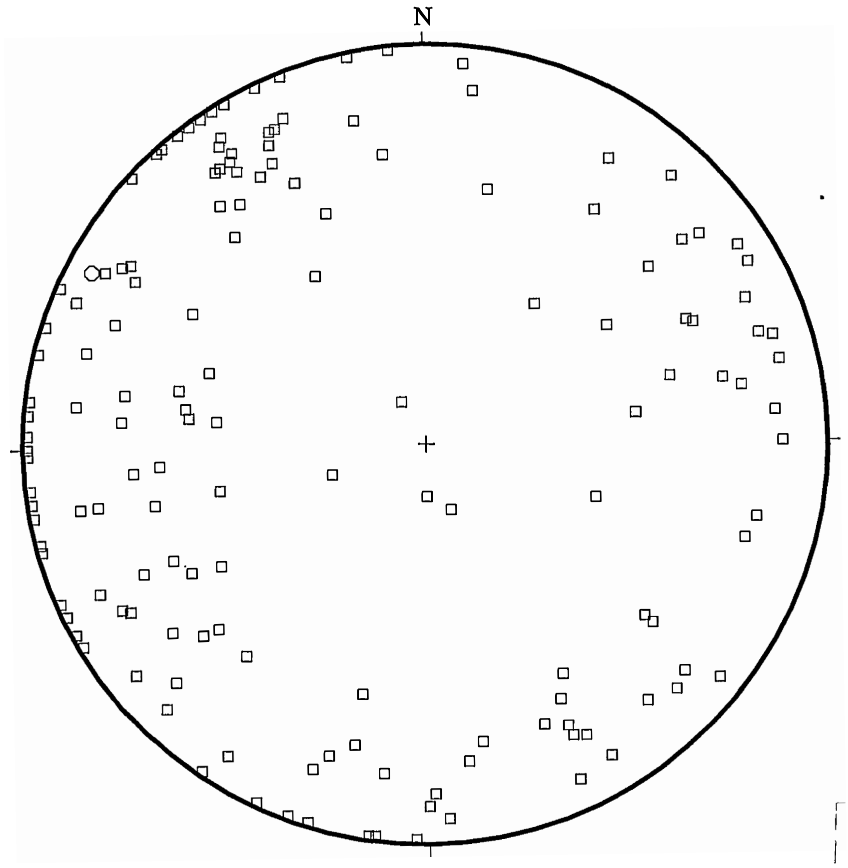

a

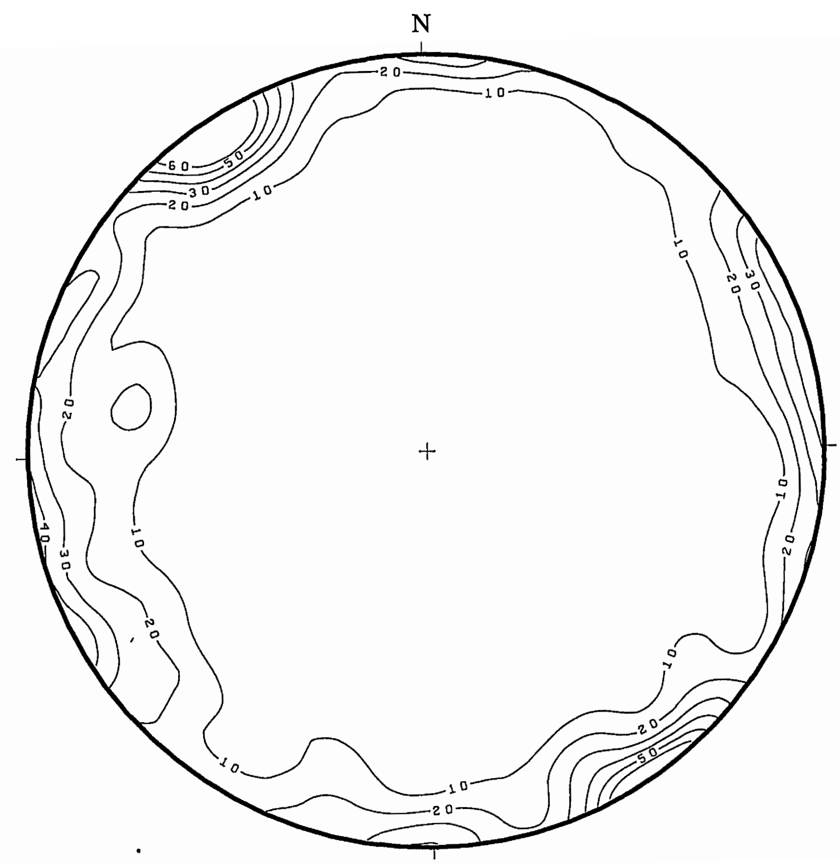

b

Figure 3.6

Hillerslev

Strike

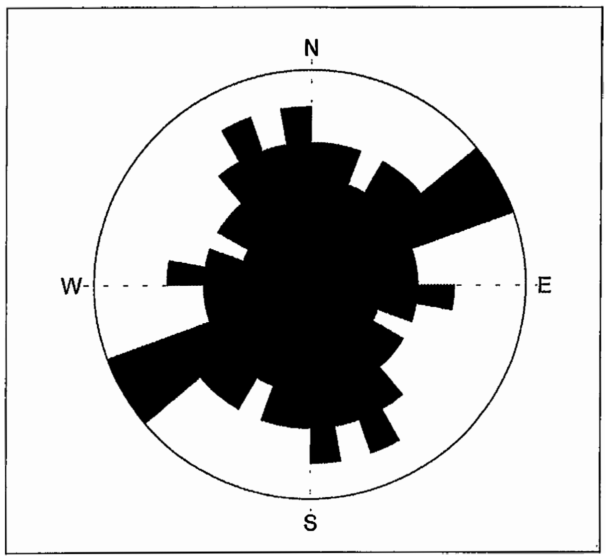

a

Dipdirection

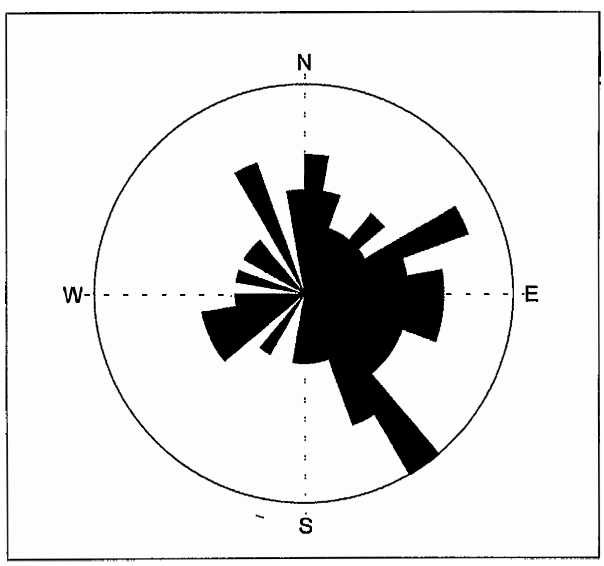

b

Figure 3.7

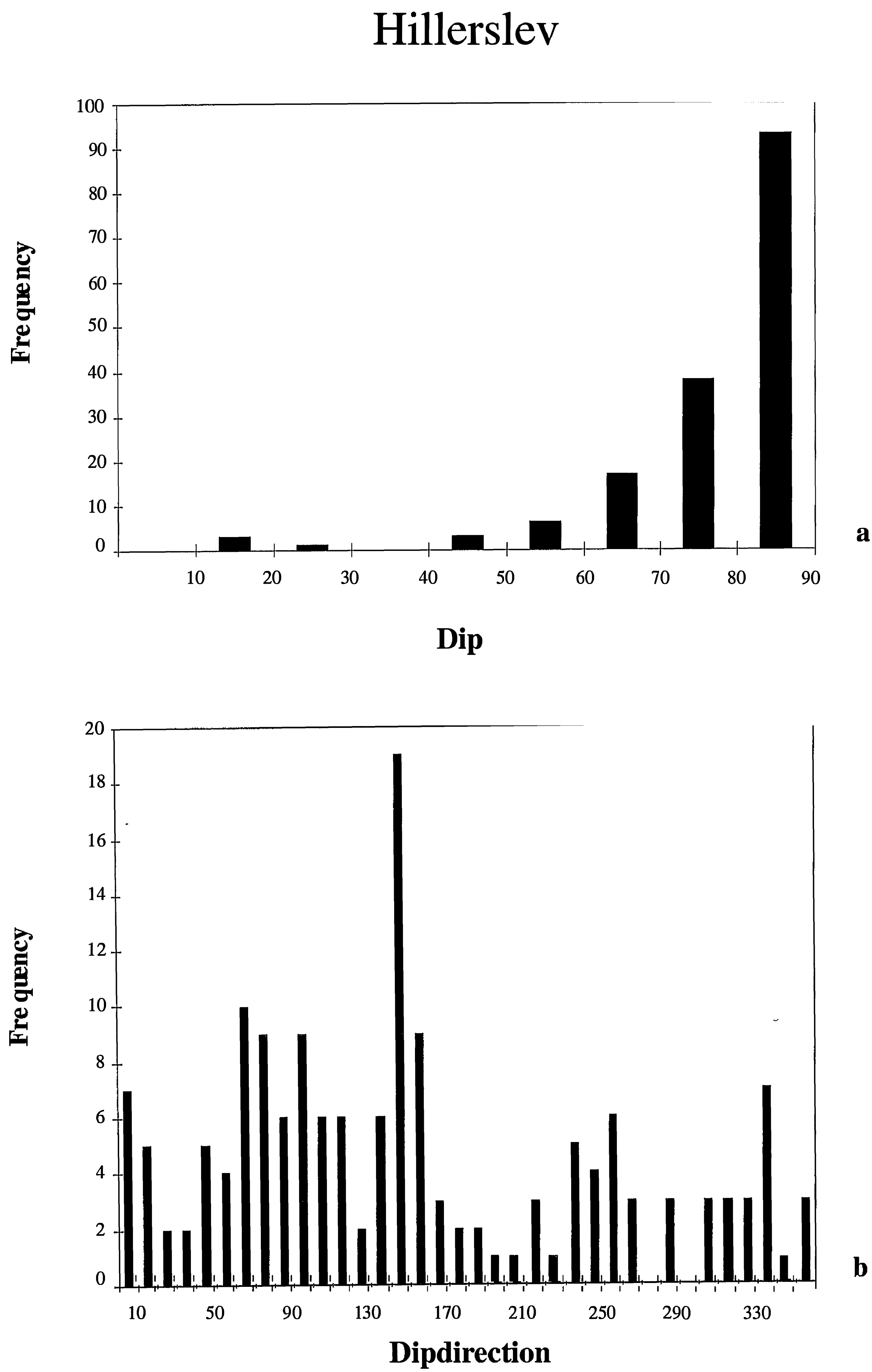

Hillerslev
Frequency
100
90
80
70
60
50
40
30
20
10
0
10
20
30
40
50
60
70
80
90
Dip
a
Frequency
20
18
16
14
12
10
8
6
4
2
0
10
50
90
130
170
210
250
290
330
Dipdirection
b

Figure 3.8

Figure 3.9

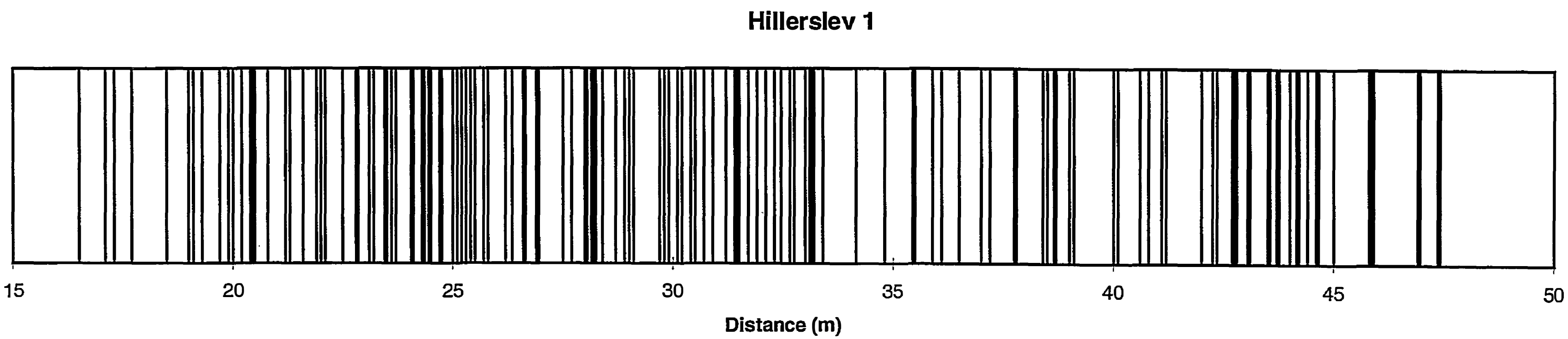

Hillerslev

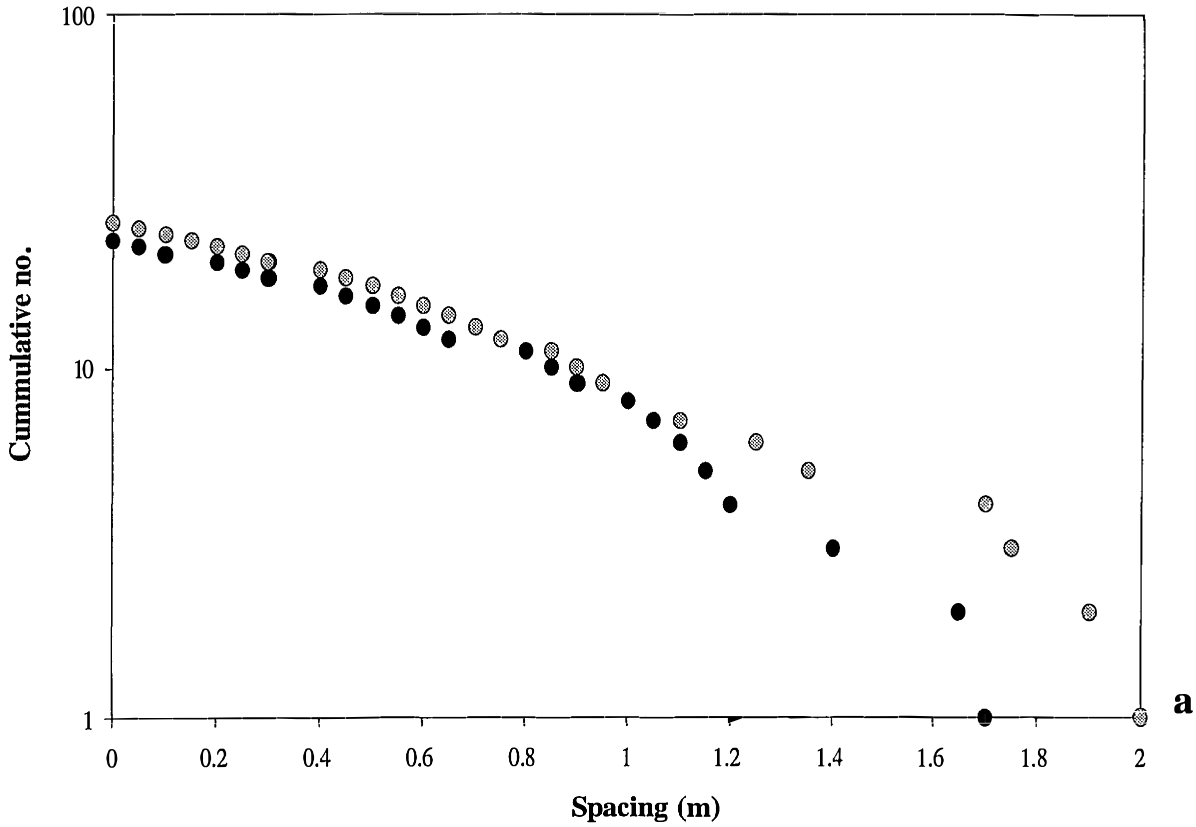

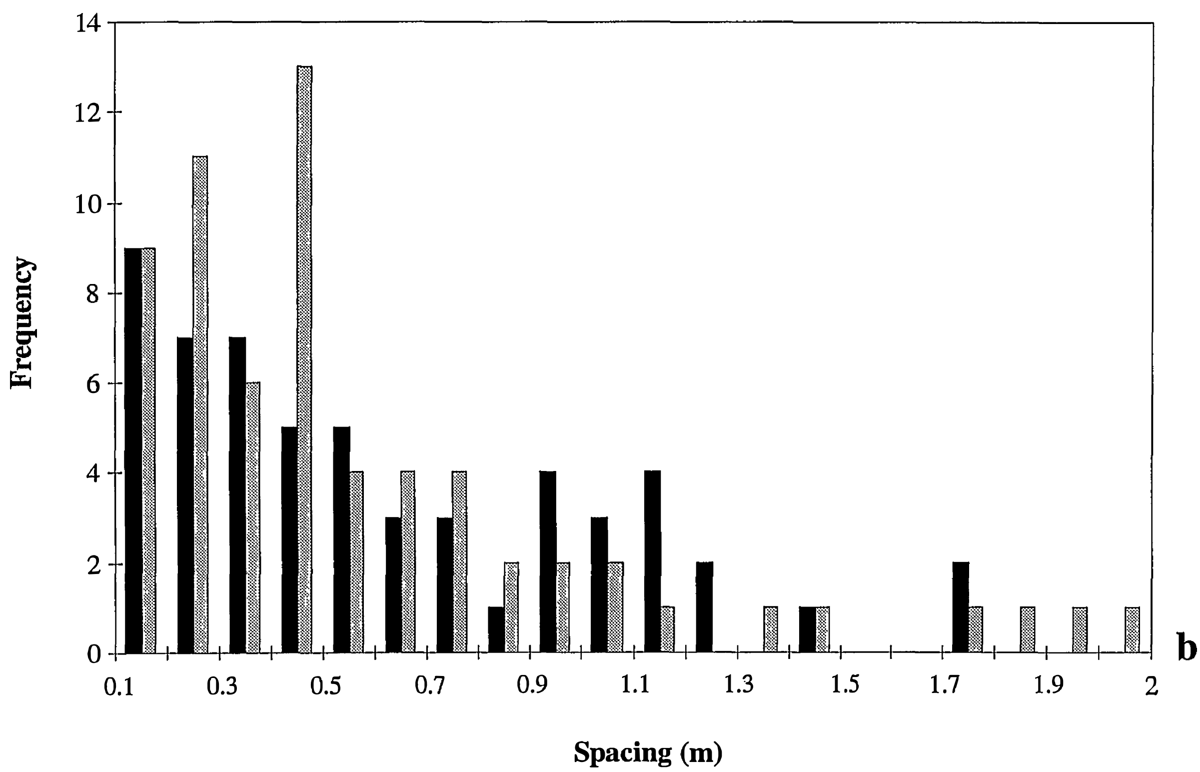

Figure 3.10

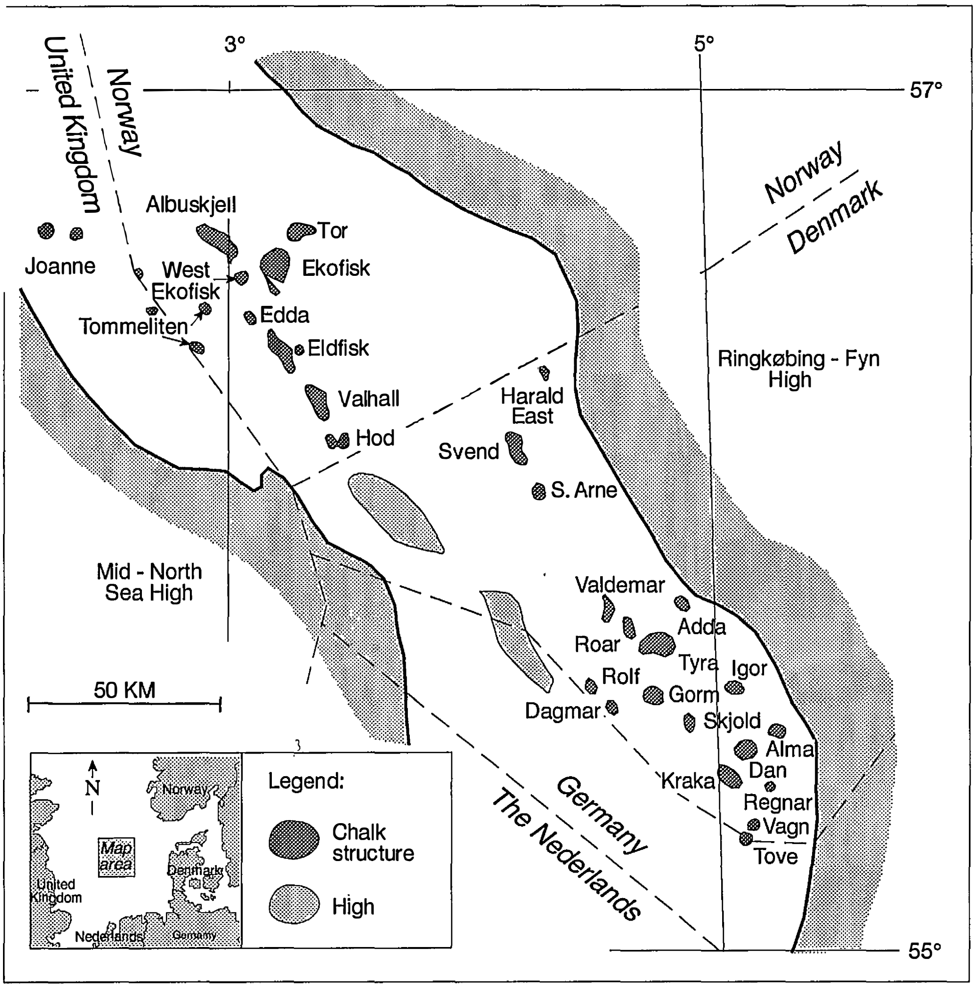

3°
5°
57°
55°
United Kingdom
Norway
Norway
Denmark
Albuskjell
Tor
Joanne
West Ekofisk
Ekofisk
Edda
Tommeliten
Eldfisk
Valhall
Hod
Harald East
Svend
S. Arne
Ringkøbing - Fyn High
Mid - North Sea High
Valdemar
Adda
Roar
Tyra
Igor
Rolf
Gorm
Dagmar
Skjold
Alma
Dan
Kraka
Regnar
Vagn
Tove
Germany
The Nederlands
50 KM
N
Norway
Map area
Denmark
United Kingdom
Nederlands
Germany
Legend:
Chalk structure
High

Figure 4.1

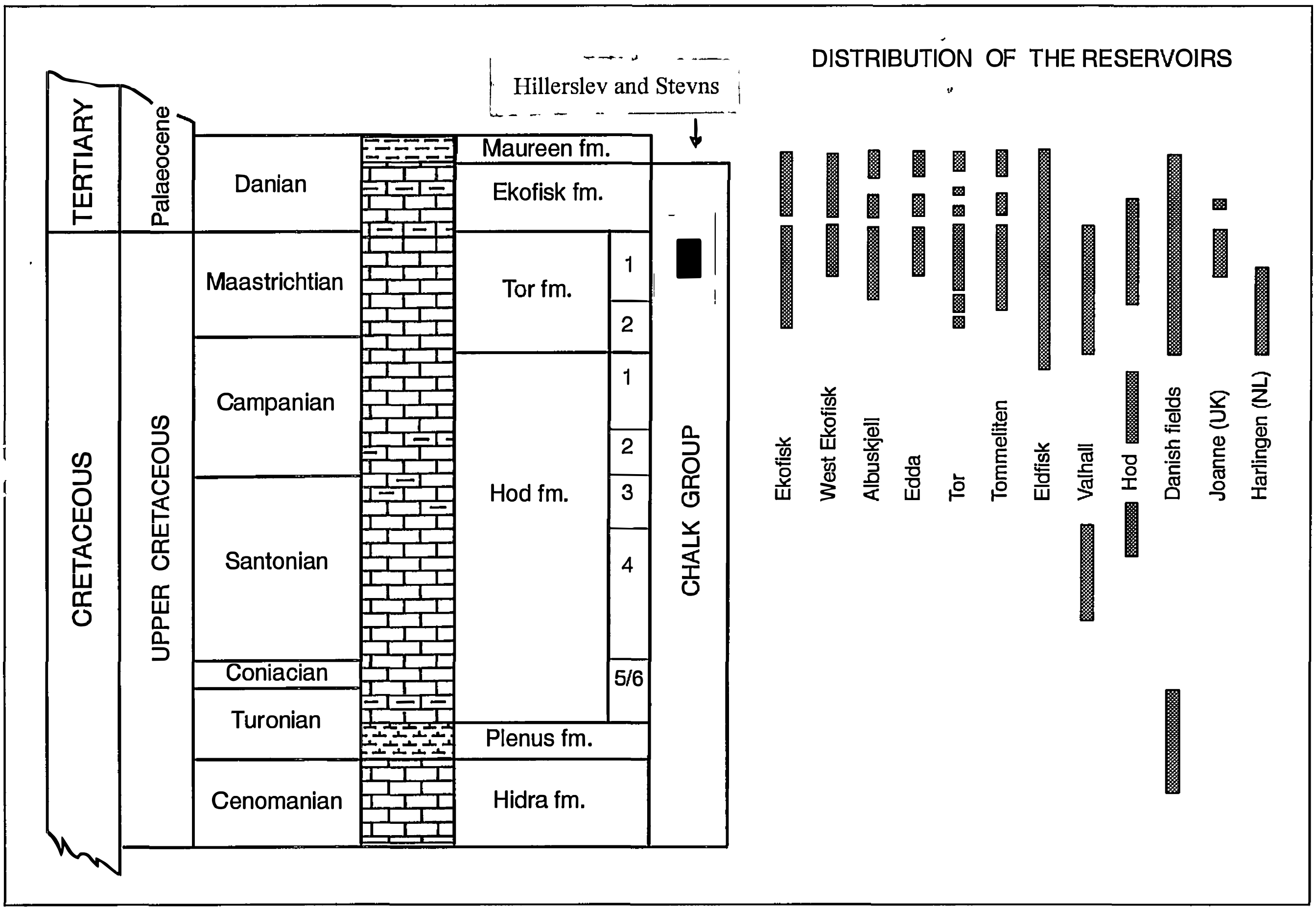

Modified from D'Heur (1993)

Figure 4.2

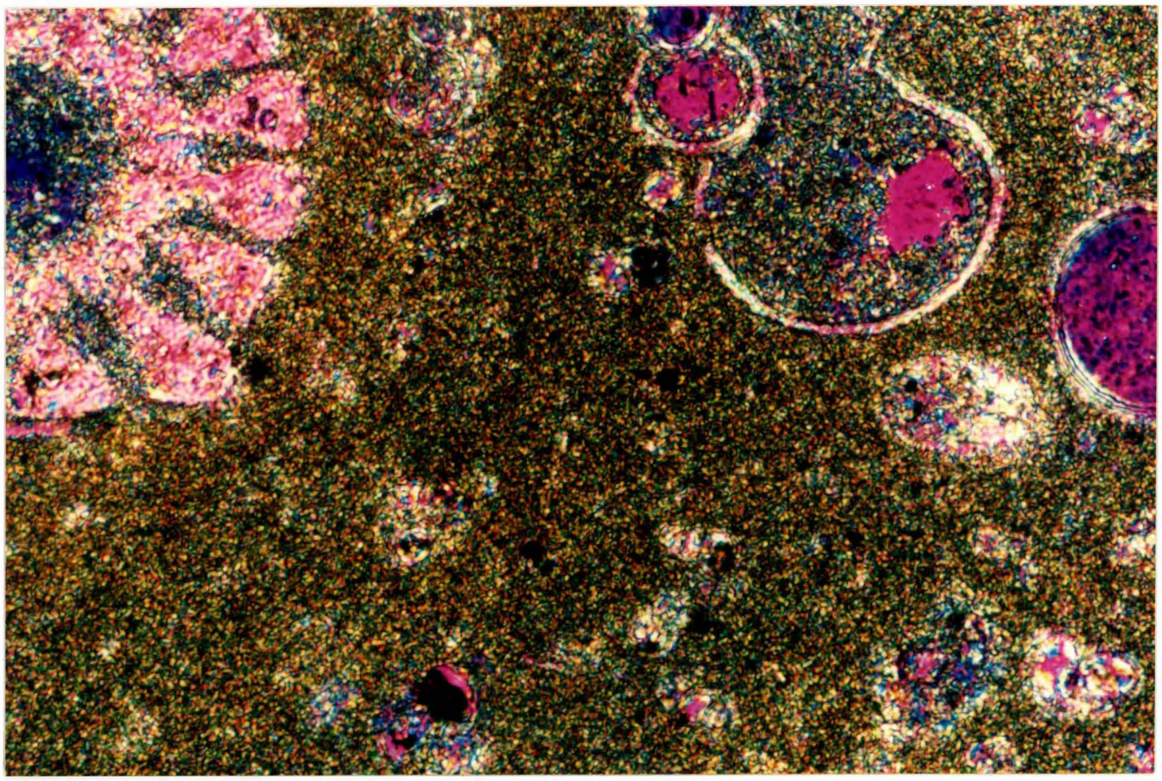

a

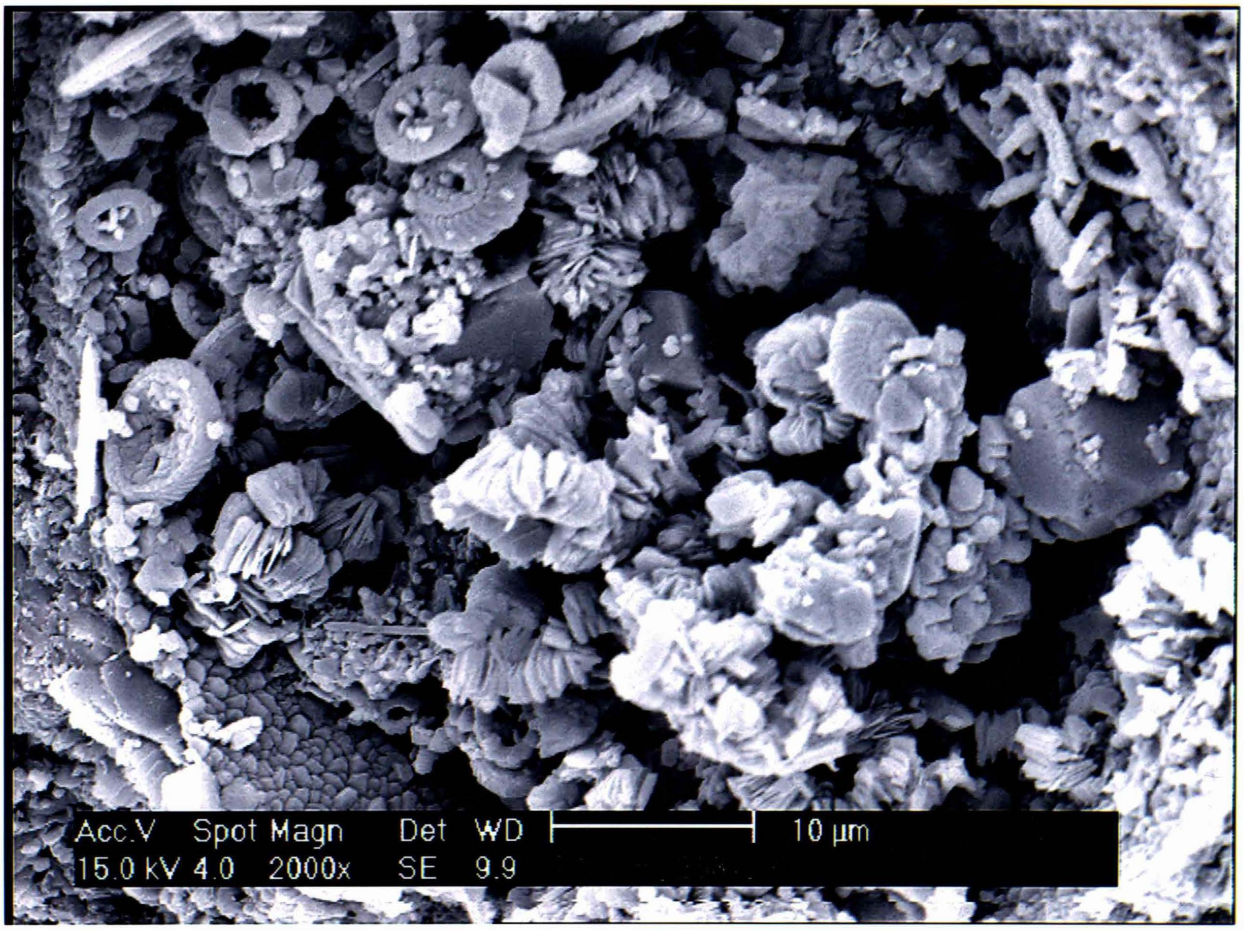

b

Figure 4.3

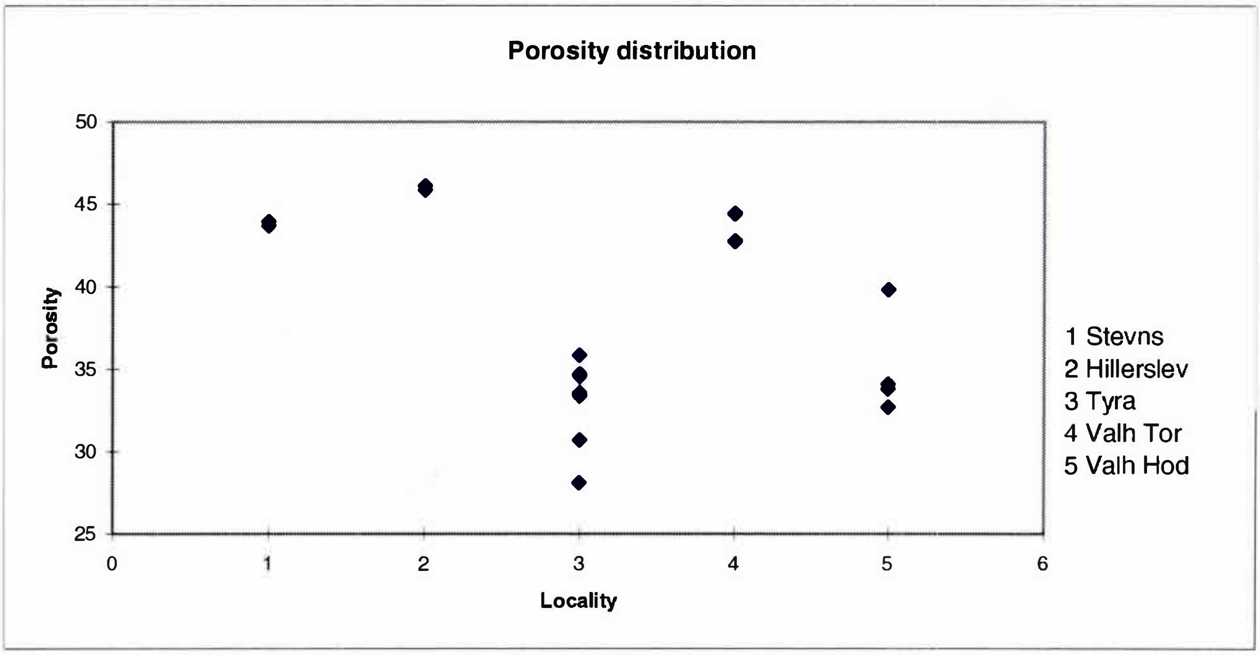

Figure 4.4

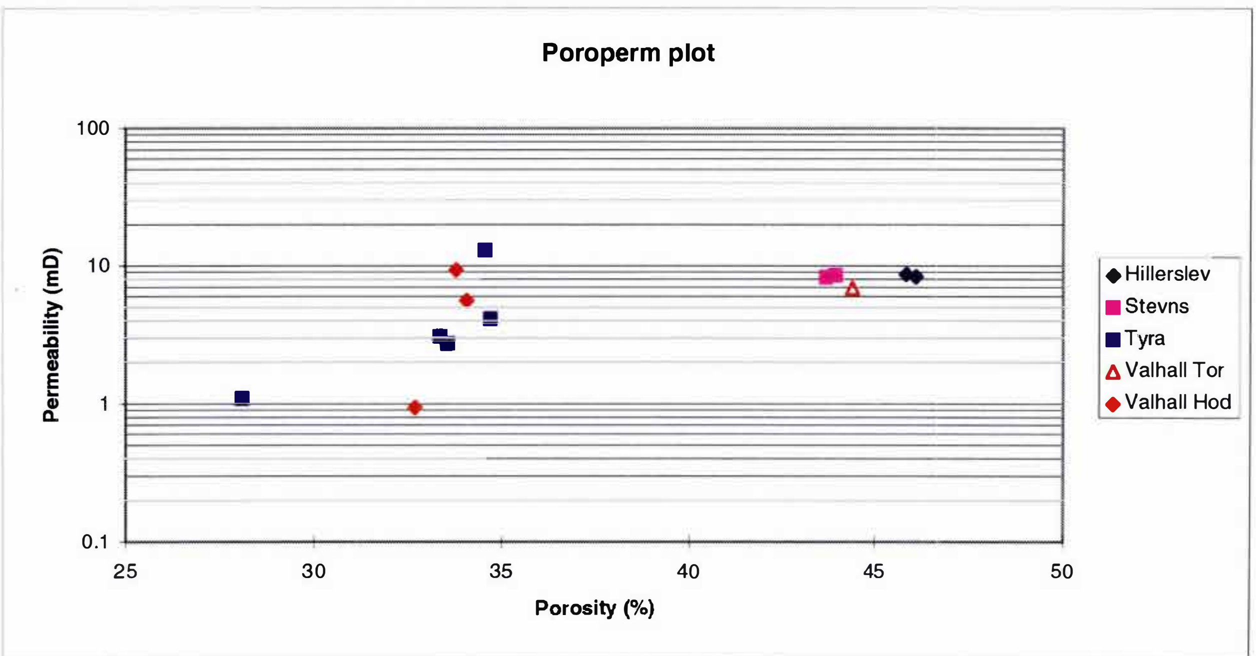

Figure 4.5

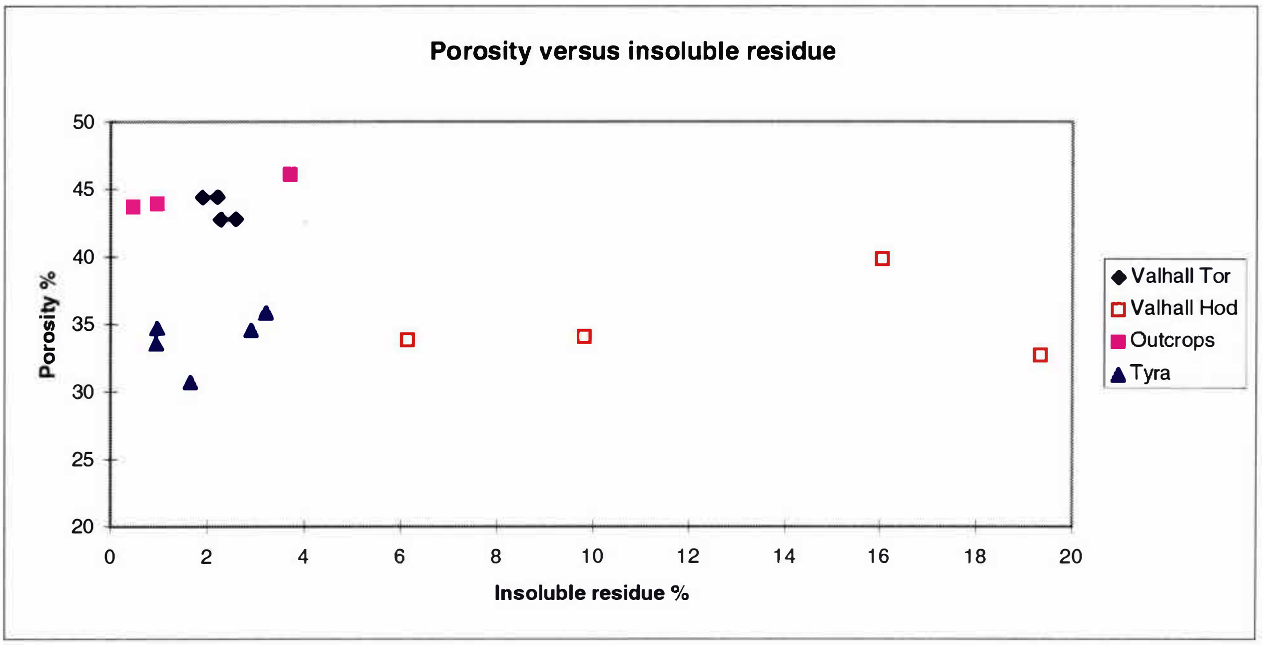

Figure 4.6

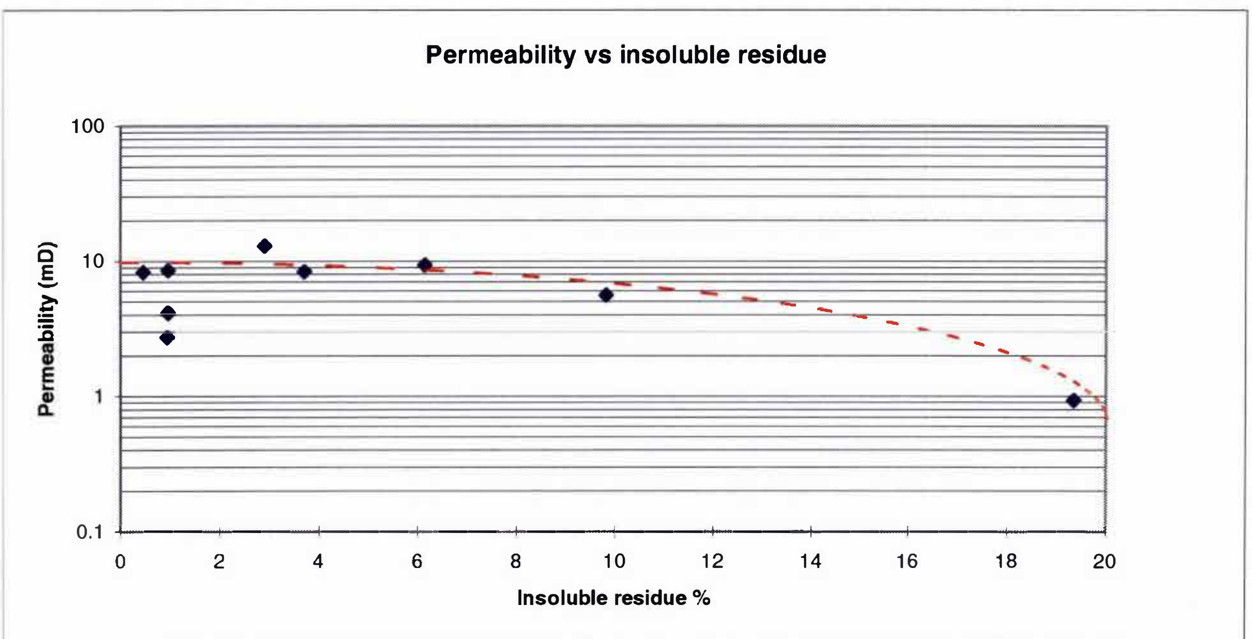

Figure 4.7

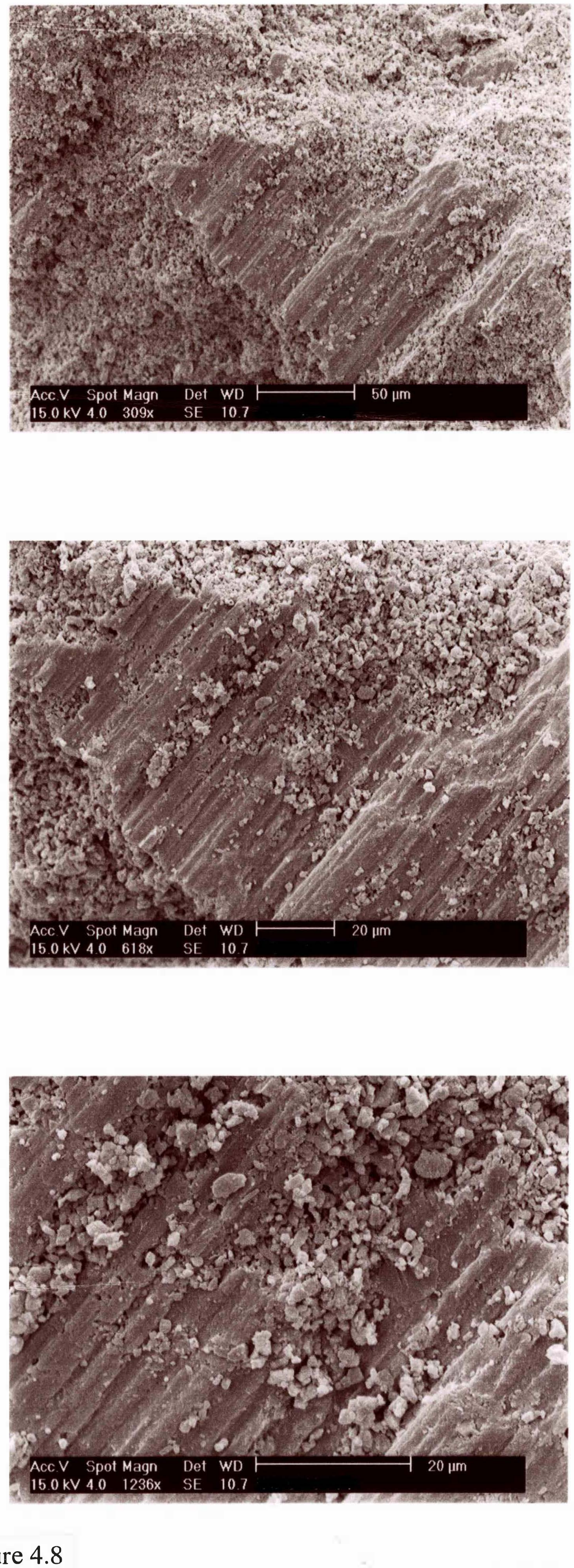
Acc.V Spot Magn Det WD 50 µm
15.0 kV 4.0 309x SE 10.7
Acc.V Spot Magn Det WD 20 µm
15.0 kV 4.0 618x SE 10.7
Acc.V Spot Magn Det WD 20 µm
15.0 kV 4.0 1236x SE 10.7

Figure 4.8

APPENDIX 1

Geological description

This appendix comprises the results from the geological description of plugs carried out at GEUS in the connection with the EFP-96 project "Fractures and Rock Mechanics, Phase 1".

Samples from two offshore fields and two onshore localities have been analysed:

A) Stevns	(Sample prefix S**)
B) Hillerslev quarry	(Sample prefix H**)
C) Tyra Field	(Samples 10-20)
D) Valhall Field, Tor Fm	(Samples 21-26)
E) Valhall Field, Hod Fm	(Samples 30-34)

All the analysed samples were described geologically, both prior to test (original rock or test plug) and after test (test plug). The geological description comprises determination of chalk type, origin and diagenesis which is used for a subdivision of the chalks that might explain the variation in strength properties of the chalks.

The description before test is made both on a macroscopic and a microscopic scale carried out on block material or plug trims. The macroscopic description includes primarily identification of among others lithotype, bioturbation, hardness and fractures. The microscopic description includes determination of biogenic composition, texture and type and degree of cementation.

The macroscopic description and classification of the chalk follow the JCR nomenclature (JCR, 1996) supplemented by determination of texture variations using microscope and SEM. The nomenclature used for the texture is in this report based on the Folk (1962) and Embry and Klovan (1971) classifications. It should be noted that the JCR nomenclature not always is transferable to plug level. F.ex. is bedding and stylolite density determined on a larger scale than plug level.

In addition porosity, permeability and the content of insoluble residue were carried out on all examined samples (except for sample HL 91 and Block 50-3). Capillary pressure analyses were carried out on four samples (two from Hillerslev, one from Stevns and one from Valhall Hod).

The fracture description was attempted to follow the methodologies as described in Fritzen and Corrigan (1990) and by the Q-methodology describe by the Norwegian Geotechnical Institute (Løset, NGI). The fractures induced in the plugs, however, is not fully comparable to natural fractures. Also the conditions of the plugs do not allow a detailed description. Therefore some modifications in the classification have been necessary. The fracture description in this study includes number of fracture sets, number of fractures, type (conjugated, horizontal and vertical) and dip angle.

After test, the plugs were described with respect to fracturing. A few attempts were made to clean the samples for further geological analysis, but the samples did fall apart in a way that porosity and permeability measurements and other analyses were unrealisable. Only with respect to block 50-1 from Stevns supplementary analysis was carried out.

The fractures induced during the multiple triaxial and uniaxial strain compaction tests is in this report visualised by markers on foil temporarily wrapped around the plug. Unfortunately not all plug remains were possible to describe due to poor conditions after test. The emphasis was made to illustrate the sedimentological features as lamination, bioturbation, hairline fractures and stylolites, which is believed to represent zones of weakness in the plug. The legend used for the drawings of fractures is shown on the page A-5.

In connection with direct shear test the plugs have only been described with respect to fracture planes. The shear induced fracture surfaces are normally not possible to display.

The test carried out on the different samples is listed in table App.-1. It should be noticed that not all test-types have been carried out under the same conditions. Therefore the variation in fractures is not necessarily related to differences in lithology alone.

A summary of the key parameters is listed in Table App.-2.

Table App.-1: List of samples

Locality	**Original samples**	**Tests and test plug number**			
		Multiple triaxial test	Uniaxial strain compaction	Direct shear test	Triaxial model test
Stevns	Block 3	SL 311, SL 33	SL 321	SV 312, SV 341	
Stevns	Megablock 1				50-1
Stevns	Megablock 3				50-3
Hillerslev	Block 8		HL 82	HL 81A, HL 81B	
Hillerslev	Block 9			HL 91	
Hillerslev	Block 10	HL 107	HL 106		
Tyra Field		13A, 13B, 14A, 16	16B	10, 11A, 11B, 20A, 20B	
Valhall, Tor		21, 23	25	22, 24, 26	
Valhall, Hod		31	32	33, 34	

Locality / Sample no.	Lithofacies	Trace fossils / Ichnogeneous	Hairline fractures	Defor-mation	Stylolites density **	Stylolites amplitude **	Fractures styl. assoc.	Fractures open	Hardness	Cemen-tation	Insoluble residue	Porosity	Perm. air	Density	Test type	Fractures before test set/no	before test type	before test angle	after test set/no	after test type	after test angle	length (cm)	surface	Comment
Stevns																								
SL 311	B.M.C.M	Th, Pl, Zoo	+						+	+	0.47	43.69	8.275	2.7	MTT	0/ 0			1/3	sv, o	75	11/8	undulat.	
SL 312	B.M.C.M	Th, Pl, Zoo	+						+	+	0.47	43.69	8.275	2.7	DST									
SL321	B.M.C.M	(Th, Pl, Zoo)	+						+	+	0.47	43.69	8.275	2.7	USC	0/ 0			1/3	h	10	2.5	smooth	
SL33	B.M.C.M	Th, Pl							+	+	0.47	43.69	8.275	2.7	MTT	0/ 0			1/ 2	sh	10-25	5	-	
SV 341	B.M.C.M	(Th, Pl, Zoo)	(+)						+	+	0.47	43.69	8.275	2.7	DST									
Plug 50-1	B.M.C.M	Th, Pl, Zoo	+						+	+	0.97	43.96	8.562	2.705	TMT	2/ >2	h/v, o		multi	c	80	50	uneven	
Plug 50-3	B.M.C.M	Th, Pl, Zoo	+						+	+					TMT	2/ >3	h/sv, o		multi	c	60-70	50	uneven	
Hillerslev																								
HL 81A	B.M.C.M	Pl, Zoo							+	+	3.72	46.11	8.308	2.696	DST									
HL81B	B.M.C.M	Pl, Zoo							+	+	3.72	46.11	8.308	2.696	DST									
HL82	B.M.C.M	Pl, Zoo							+	+	3.72	46.11	8.308	2.696	UUC	0/ 0			1/3	v+sv	75-90	8	rough	
HL 91	B.M.C.M	Th, Pl, Zoo						+	+	+					DST									
HL 106	B.M.C.M	Th, Pl, Zoo							+	+	4.45	45.85	8.675	2.696	USC	1/ 1	sh, o		2/>5	sh	15		smooth	
HL107	B.M.C.M	Th, Pl, Zoo	(+)						+	+	4.45	45.85	8.675	2.696	MTT	0/ 0			1/ 1	c, o	70		rough	
Tyra																								
10	M.C.M		+		+++	+++	+	+	+++	++++	3.22	35.85		2.701	DST								smooth	
11A	B.M.C.M	Zoo, Pl	++		+++	++		+	+++	+++	2.92	34.58	13.0 *	2.704	DST									* broken
11B	B.M.C.M	Zoo, Pl	++		+++	++		+	+++	+++					DST								styl-contr	
13A	D.M.C.M	Ch	+++	Shear					+++	++++	0.97	34.72	4.13	2.707	MTT	0/ 0			2/ 5	i, o	55	9		
13B	D.M.C.M	Pl, Th	+++	Shear					+++	++++					MTT	1/ 2	c, o		2/ 4	sh/v	60	11		
14A	D.M.C.M	Zoo, Pl, Th, Ch		Shear					+++			28.11	1.09	2.708	MTT	2/ 4	o	40+v	2/ 4	i, sv	60	6		
16	(B)M.C.M	Ch	++		++	+		+	+++			33.37	3.07	2.708	MTT	1/ 2	c, o		2/ 5	c, p, o	65 -70	8/10	rough	
16B	(B) M.C.M	Ch	++		++	+		+	+++	+++	0.95	33.58	2.711	2.71	USC	?								
20A	B.M.C.M	Pl, Ch	+		+++	+++	+	+	+++	++++	1.65	30.71		2.698	DST								slick, rou	
20B	B.M.C.M	Pl, Ch	+		+++	+++	+	+	+++	++++					DST								smo-rou	
Valhall																								
Tor Fm																								
21	(B.) M.C.M	Pl			+	+			+	+	2.16	44.41	6.894	2.705	MTT	1/ 3	sh, o	10-20	2/ 4	sh/v,	5-15	5		
22	D.M.C.M	Pl, Ch	+++++	Shear				+	+		1.91	44.42		2.703	DST									
23	D.B.M.C.M	Ch	+++++	Shear				+	+		2.97				MTT	2/ 2	sv/sh	25/60	3/ 4	sh, o	20/60	5	smo-rou	
24	D.B.M.C.M	Ch	+++++	Shear	+	+			+		2.59	42.79		2.687	DST									
25	D.M.C.M	Ch?	+++++	Shear					+		2.21	44.45		2.699	USC	-			-					
26	D.B.M.C.M	Ch	+++++	Shear					+	+	2.28	42.77		2.706	DST									
Hod Fm																								
31	B.L.A.M	Th, Ch, Pl, Zoo						?	++	+	16.07	39.83		2.702	MTT	2/ 3	sv/sh	70 + h	multi	c, o	20/70			
32	B.L.A.M	Th, Zoo, Pl	++					+	++	+	19.36	32.71	0.932	2.704	USC	-			-					
33	B.L.A.M	Th, Pl, Ch, Zoo	+					+	++	+	9.83	34.09	5.578	2.702	DST									
34	B.L.A.M	Ch, Pl						+	++	+	6.16	33.81	9.344 *	2.694	DST									* broken
	Abbreviated	Th: *Thalassinoides*							Scale 1-4:	Scale 1-5					DST: Direct shear test									
	JCR nomencl.	Pl: *Planolites*			** plug level definition				+ soft						USC: Uniaxial strain compaction									
		Zoo: *Zoophycos*							++ medium hard						MTT: Multiple triaxial test					C: conjugated		(I: inclined)		
		Ch: *Chondrites*							+++ hard						TMT: Triaxial model test					H: horizontal		(S: sub)		
									++++ very hard						UUC: Unconfined uniaxial compression					V: vertical		(S:sub)		
																				O: open P: parallel				

Summary table

LEGEND

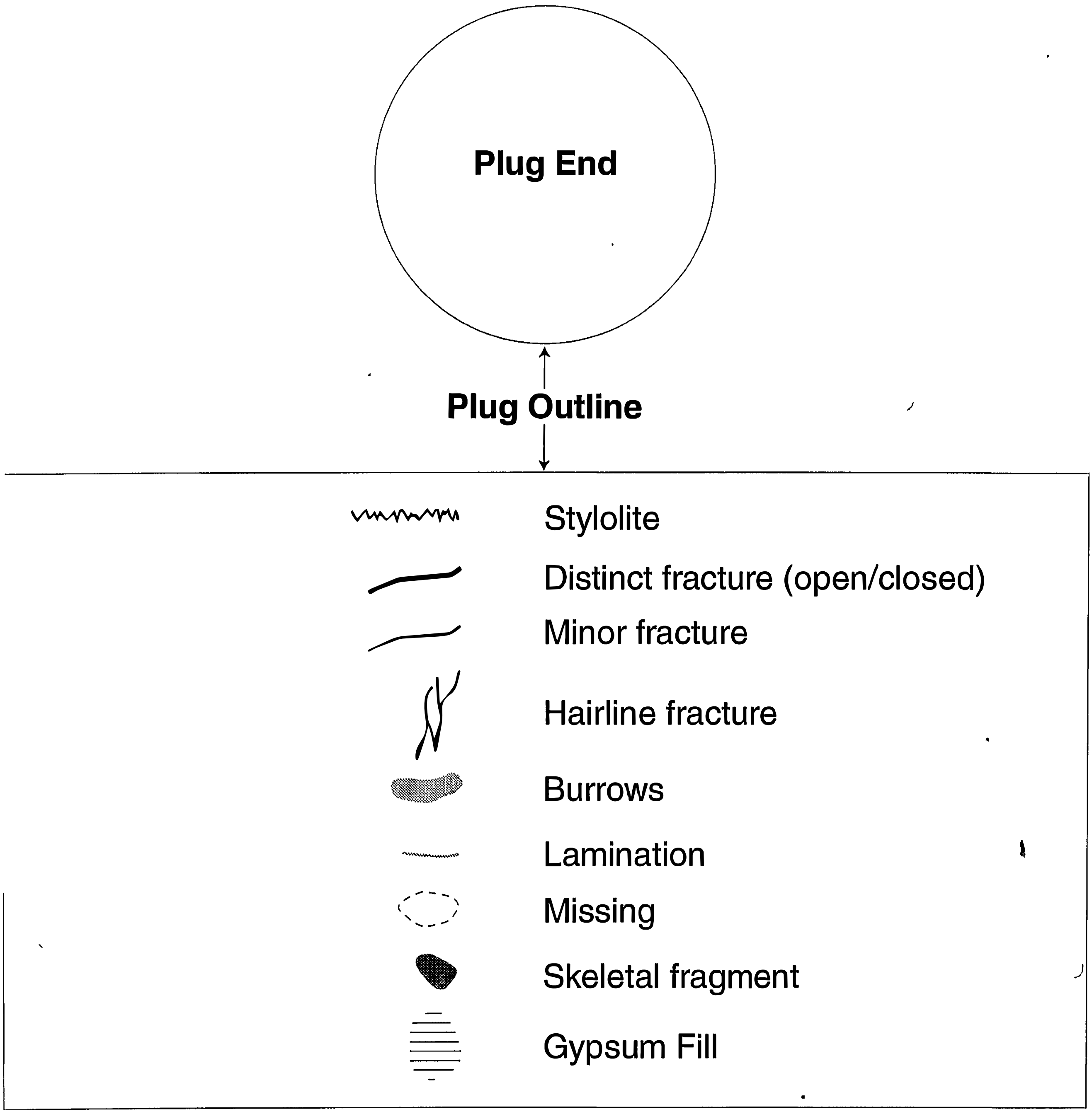
Plug End
Plug Outline
Stylolite
Distinct fracture (open/closed)
Minor fracture
Hairline fracture
Burrows
Lamination
Missing
Skeletal fragment
Gypsum Fill

STEVNS

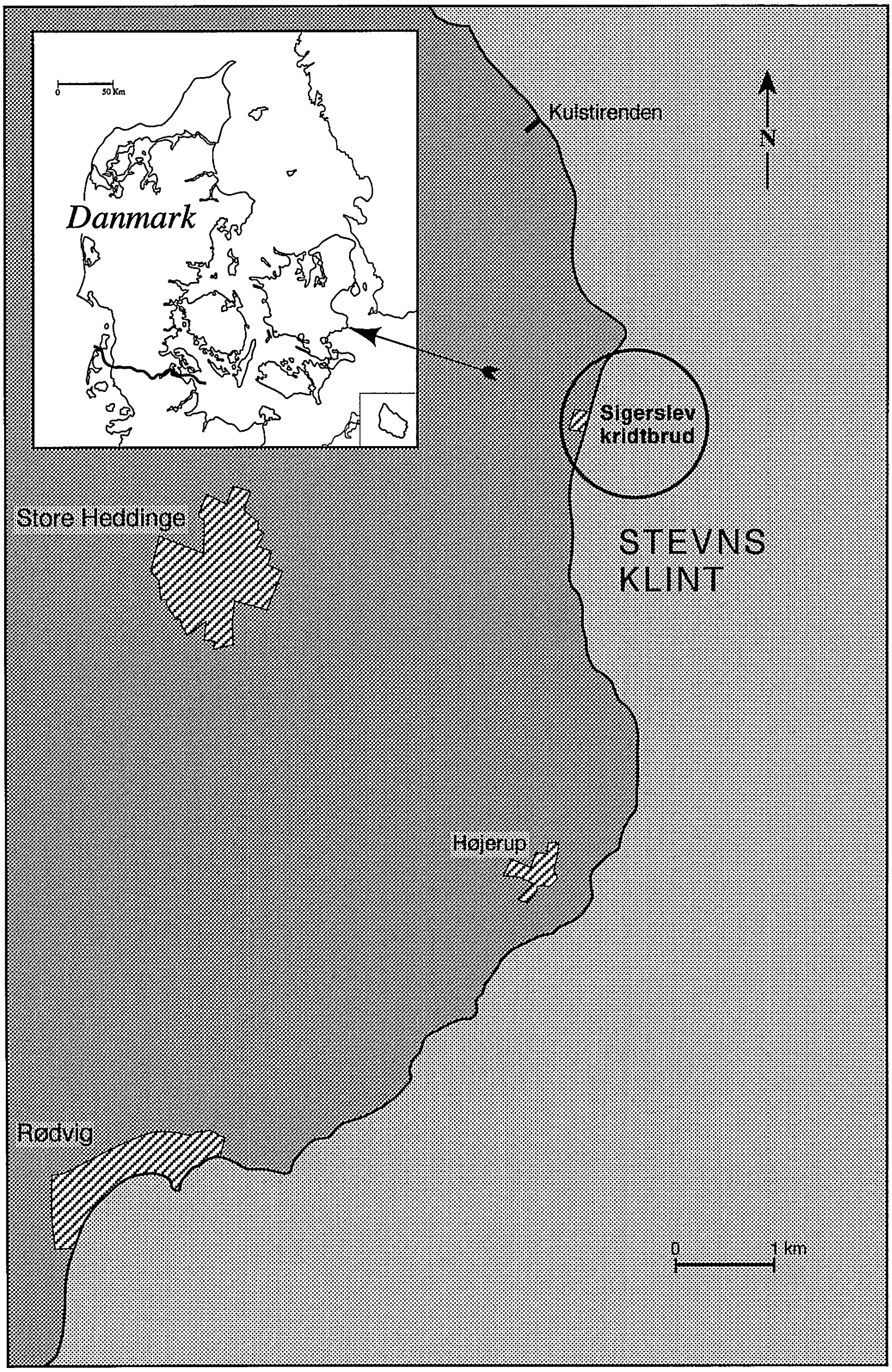

Figure ST-1: Locality map

Description:

The Maastrichtian chalk of Stevns (Sigerslev, fig. ST-1) is a soft, greyish white bioturbated chalk mudstone dominated by a coccolithic matrix with skeletal fragments, primarily bryozoans and foraminifera. The chalk is highly biomottled but exhibits only a medium density of trace fossils due to an overall pure chalk with low clay content. *Thalassinoides* is the most common ichnogeneous (fig. ST-2). *Planolites* and *Zoophycos* is less frequent. Bedding defined by horizontal fractures (corresponding to omission surfaces?) is in the order of 30-50 cm. Distinct horizons with flint nodules are found in intervals of approximately 2 m.

The chalk has a sparse biomicritic wackestone texture with foraminifera and bryozoan as the most common grain component (fig. ST-3). The chalk exhibits a highly intercrystalline porous matrix rich in well-preserved coccoliths. The average distribution of pore throat radius is ~0.6 μm (fig. ST- 5). The matrix is characterised by a high content of fine disintegrated material with scattered euhedral and subhedral calcite cement. The calcite cement crystals appear as poor sorted ranging in size < 1 μm to 5 μm (micrite cement). The shape of the crystals varies from cubic to elongated (fig. ST-4).

Syntaxial calcite overgrowth on coccolith platelets is normally scarce and the size of these crystals is normally less than 2 μm. Some overgrowth of coccolith platelets of specific coccolith species occurs.

Porosities and permeabilities are in the order of 44% and 8 mD, respectively. Open foraminifera chambers are common and their presence contributes to the high porosity.

Both the silica and clay content are low (less than 1%) and rarely seen in the SEM.

Analyses carried out on samples from Stevns.

From the Sigerslev quarry at Stevns three blocks were cut for triaxial model test on block size (Stevns block 50-1, 50-2 and 50-3). A geological description and description of fracturing after block test were carried out on the blocks. (NB! Stevns block 50-2 was damaged and is not described).

In addition chalk samples were taken for conventional geotechnical analysis. On the standard samples the geological description was carried out on both the plug trims to describe the initial stage of the sample and subsequent to the geotechnical test.

Figure ST-2.

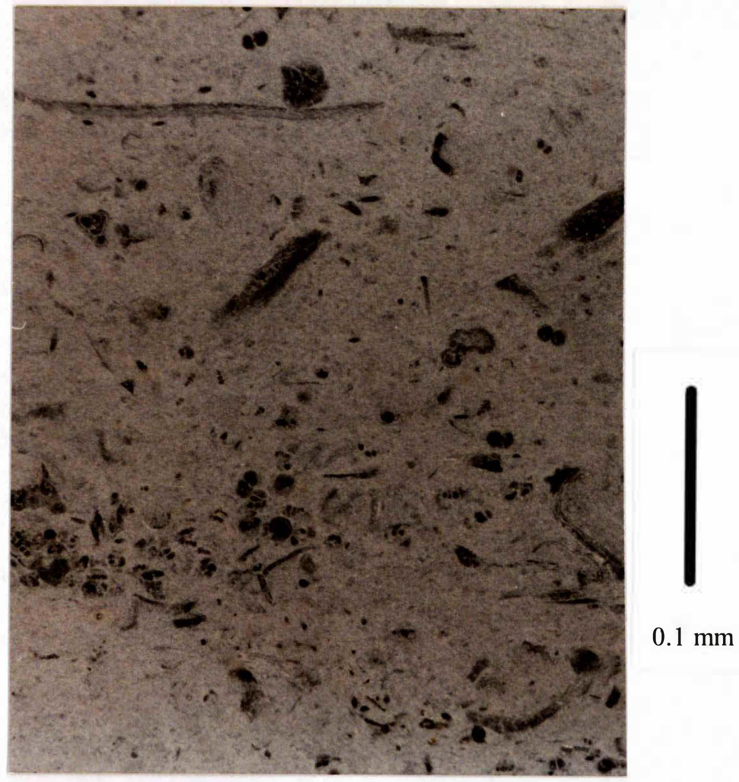

Figure ST-3

Figure ST-4 ↓

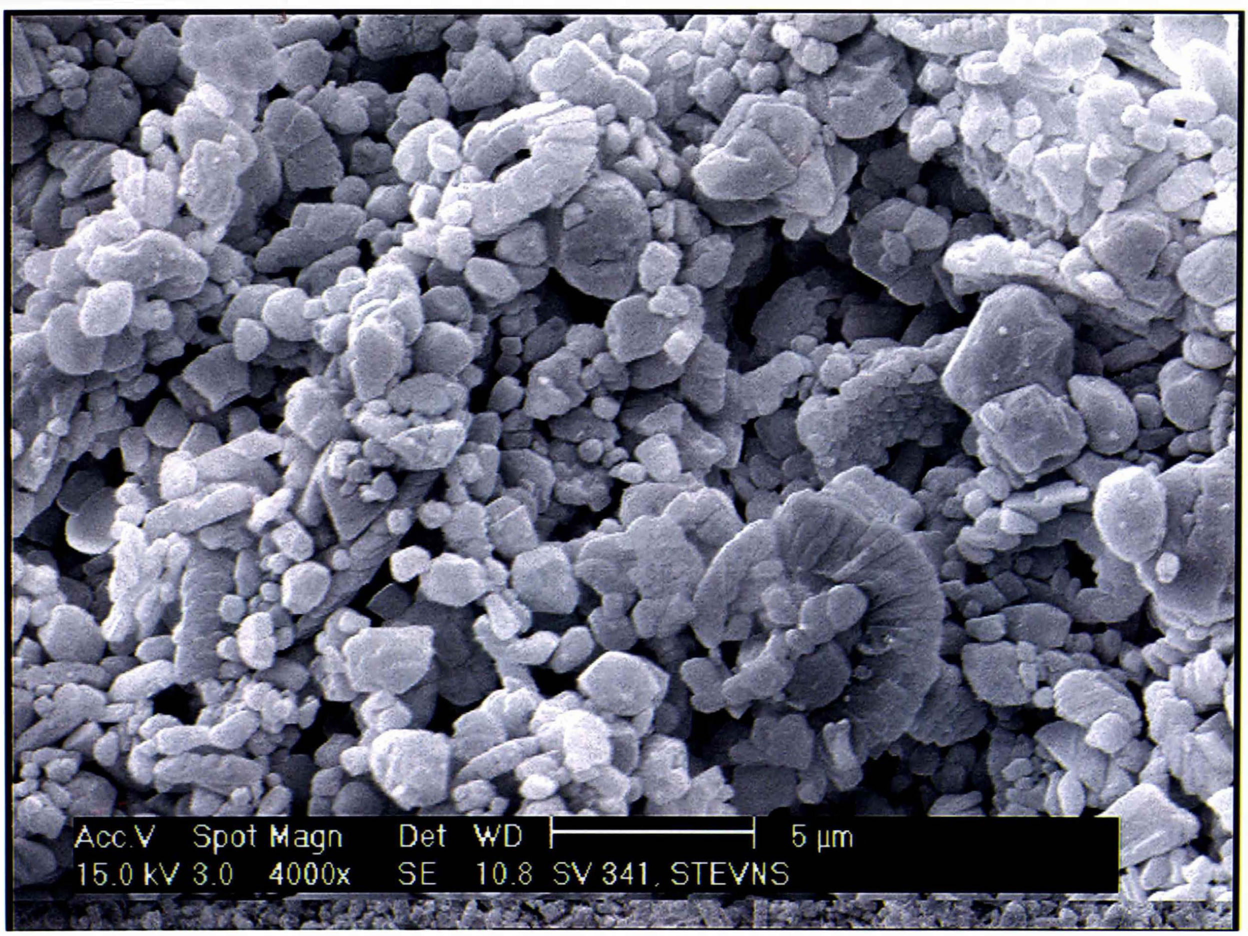

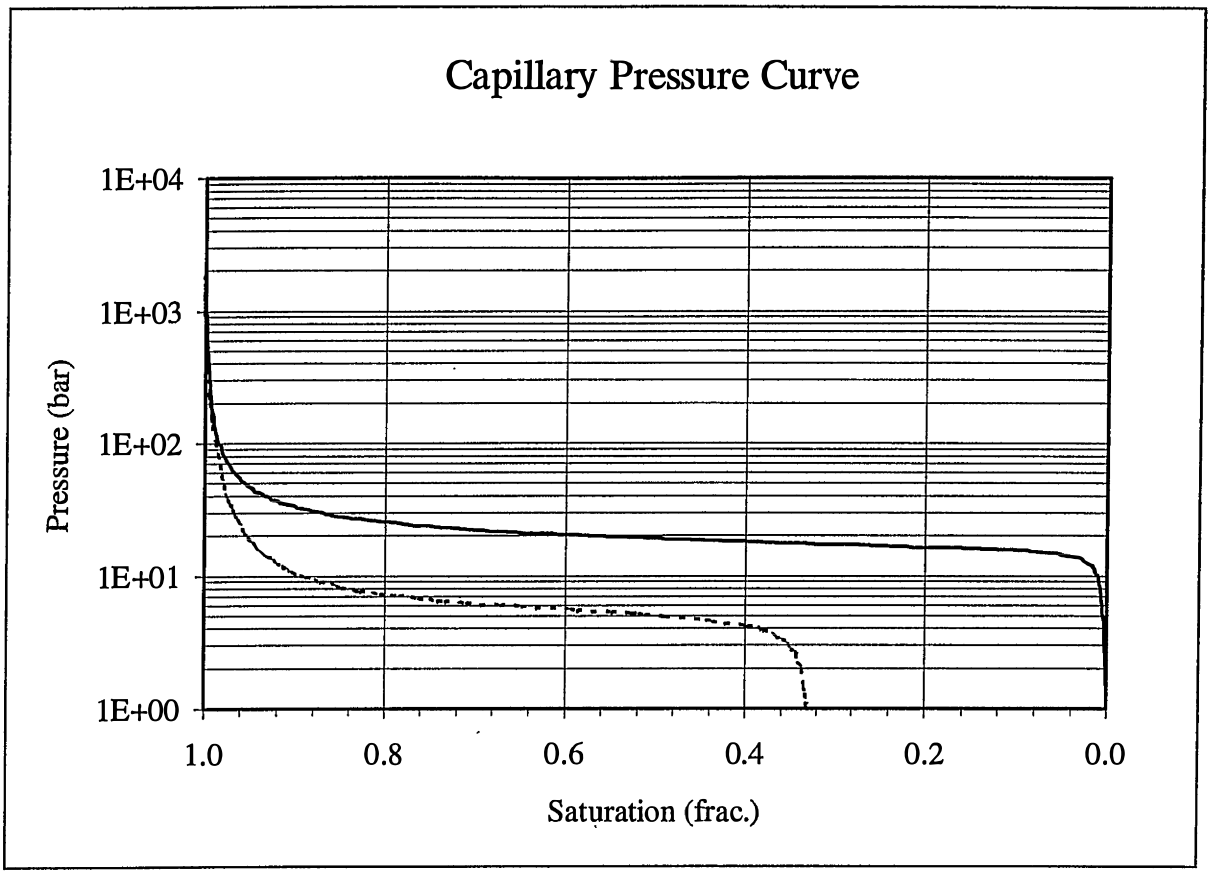

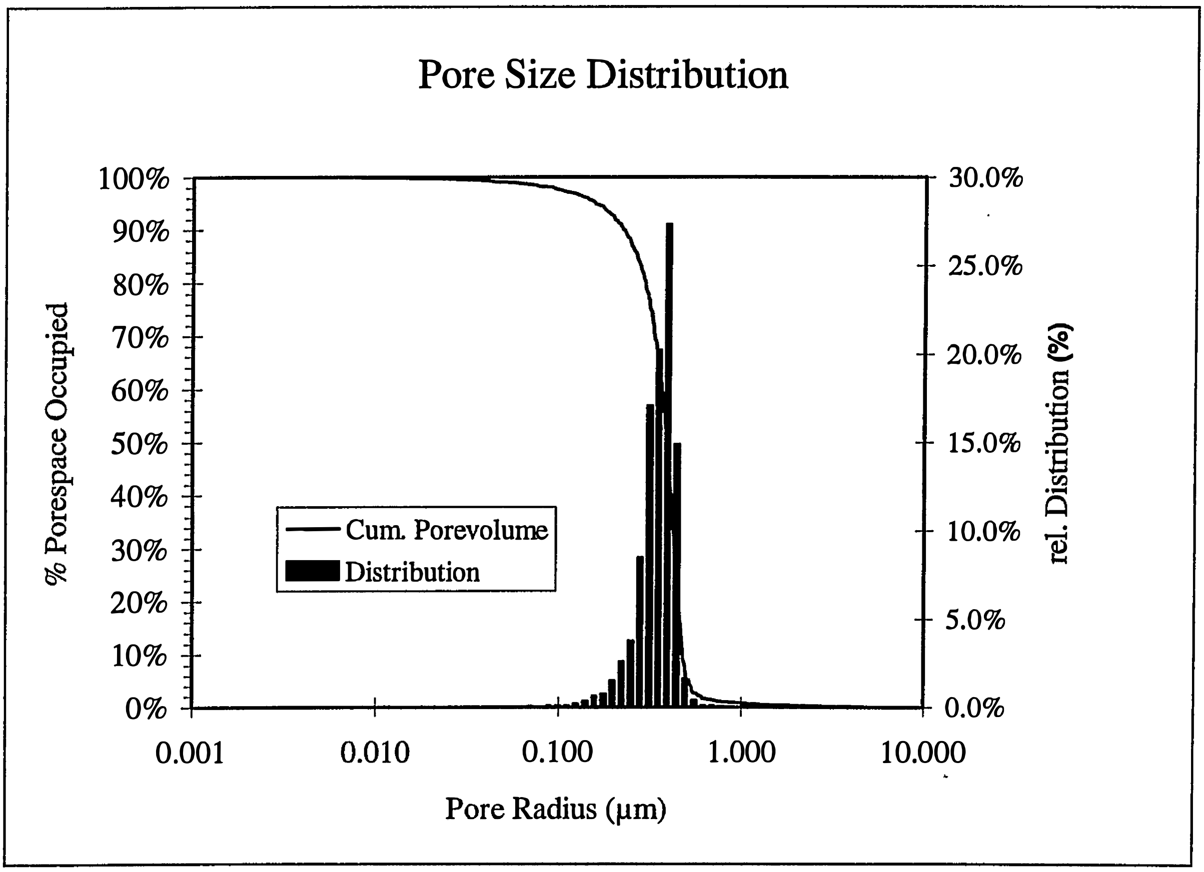

Figure ST-5. **Capillary pressure curves and pore size distribution for plug Maastricht outcrop SJ34**

Stevns, Block 3

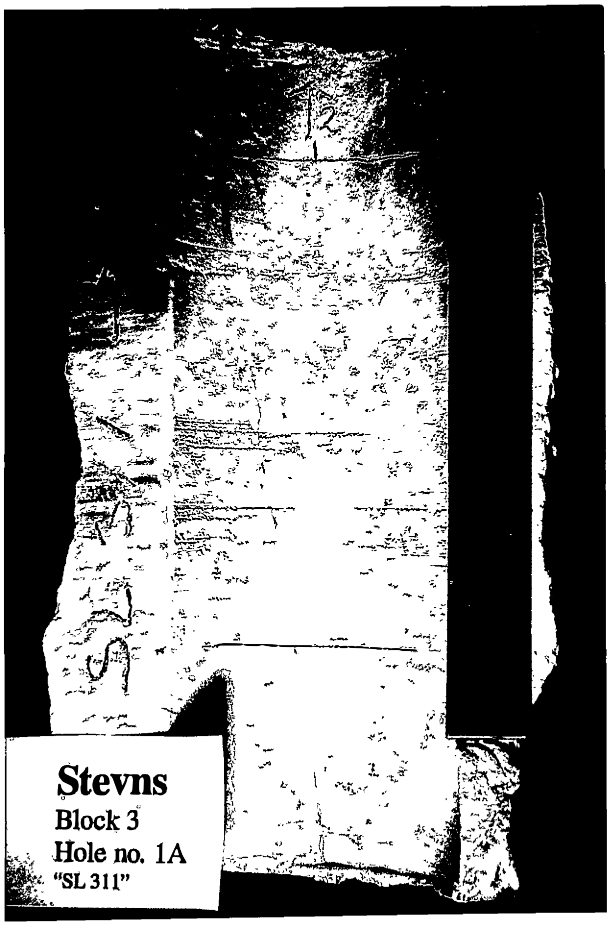

Figure ST-6.

Burrowed Massive
Chalk Mudstone

Well/location:	Stevns Sjælland, Denmark
Formation:	Tor (equivalent)
Depth:	Outcrop

M	mudstone
Ch	clean chalk
Gsk	skeleton grains (bryoz, foram)
Btn	thin bedded
Lpl	planar lamination (weak)
Dn	no visible deformation
Tm	medium density of trace fossils
Hs	soft
Cm	medium consolidation
Sn	no visible stylolites
Mn	no visible secondary minerals
Fhl	low density of hairline fractures

Description:

Block 3 is a highly biomottled chalk mudstone with a medium density of trace fossils (fig. ST-6). The burrows fill is hardly distinguishable from the surrounding matrix due to similarities in composition. A weak indication of lamination can be seen. Hairline fractures associated to water escaping cutting through burrows and causes offset ranging from 1 mm to 1 cm.

The chalk is a sparse biomicritic wackestone dominated by bryozoans and foraminifera. Skeletal fragments of echinoderms are rare. Open foraminifera chambers are common.

The chalk exhibits a poorly sorted, highly intercrystalline porous matrix rich in both well preserved and disintegrated coccoliths. The poor sorting most properly is due to disintegration of the chalk. Fine euhedral and subhedral cement crystals are found scattered in the pores. The calcite cement crystals do not generally exceed sizes above 2-3 μm.

Trace fossils:

Ichnogeneous: *Thalassinoides, Zoophycos* and *Planolites.*

Insoluble residue:

0.47 %
Quartz (13%) and clay.

Petrophysical properties:

Porosity:	43.69 %
Permeability (air):	8.275 mD
Density:	2.700 g/cm^3

Analyses carried out on block 3:

Sample	Porosity	Permea-bility	Thin section	Capillary pressure	Insoluble residue	SEM	Geotechnical test type
SL 311							**Multiple triaxial test**
SL 312							**Direct shear test**
SL 321							**Uniaxial strain compaction**
SL 33							**Multiple triaxial test**
SL 341	**X**	**AIR**	**X**	**X**	**X**	**X**	**Direct shear test**

Stevns, sample SL311
Multiple triaxial test

Pre-test description:

The sample is a vertical plug cut perpendicular to the bedding (identified from the weak indication of lamination). The plug comprises generally horizontal burrows related to *Thalassinoides, Zoophycos* and *Planolites.* The sample is cut through by a more than 1 cm wide hairline fracture zone (water escape structure), which gave rise to minor offset of the burrows. No open fractures are seen in the plug prior to test.

Post-test description:

During the test one set of parallel fractures has been developed, but the plug still appears as one coherent element after test (fig ST-7). The fractures are partly open and cutting through the plug, but no major displacement (offset) is seen. The fractures appear with a spacing of 2-3 cm.

The fractures seem to be controlled by the hairline fracture zone (fig. ST-8). “Fracture 1” is a 11 cm long, nearly vertical (75^o) and is parallel with the hairline fracture zone. The aperture of the fracture is less than 1 mm. “Fracture 2” is a 5 cm high angle fracture dipping 75^o, but do only cutting through the upper part of the plug. As “fracture 1” the fracture coincides with the hairline fracture zone. The aperture of the fracture is less than 1 mm.

Short (1- 3 cm) sub-horizontal fractures are found associated with the main fractures.

On the plug surface the fracture planes appear as planar to weakly undulating. Pulling apart the plug the fracture surface appears as an undulating plane with an amplitude less than 5 mm and a wavelength of 1 cm. Indications on slickensides are not seen.

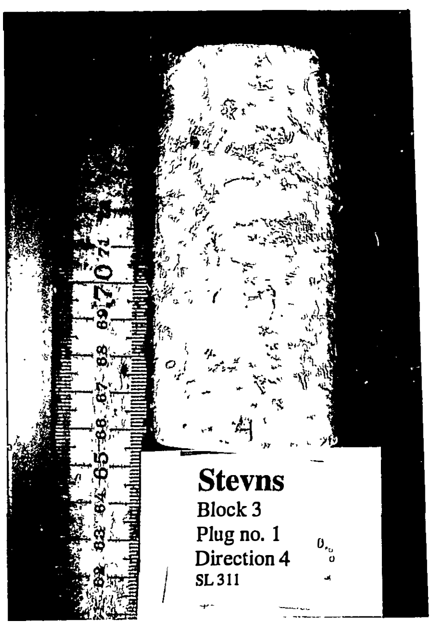

Figure ST-7.

ST-8

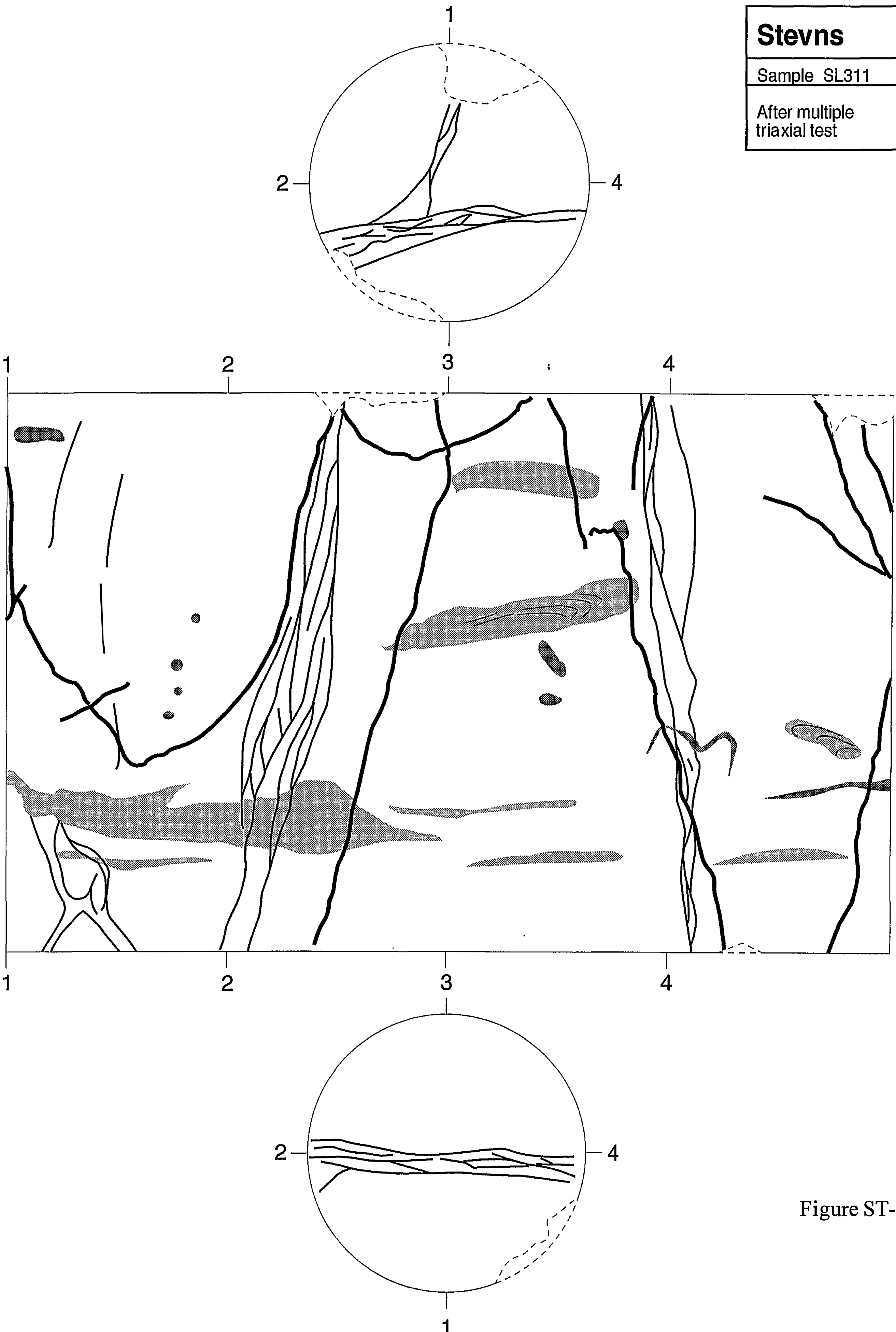
Stevns
Sample SL311
After multiple triaxial test
1
2
3
4
1
2
3
4
1
2
3
4
2
4
1

Figure ST-8

Stevns, sample SL312
Direct shear test

Pre-test description:

This sample is a continuation of plug SL 311. No separate description is made on the sample.

Post-test description:

The test was carried out with a pre-defined shear plane parallel to the bedding. After test the plug was in a poor condition. The upper part was broken into pieces in the order of 1 cm^3 and gave rise to a very rough "fracture plane" with a 1 cm relief (fig. ST-9).

The random fracturing was probably controlled by vertical zones of weakness and does not represent the real pre-defined shear plane. The shear plane most probably was developed as a zone of "chalk-paste" below the broken surface.

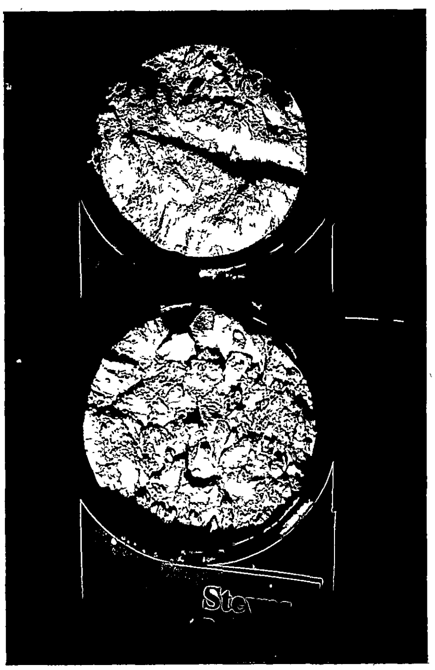

Figure ST-9

Stevns, sample SL321
Uniaxial strain compaction

Pre-test description:

The sample is a vertical plug. The weak indication of lamination is indicative of a plug perpendicular to the bedding.

The plug appears rather homogenous but comprises burrows related to weak discernible *Thalassinoides*, *Zoophycos* and *Planolites*. The sample is cut through by a narrow (~5 mm wide) vertical hairline fracture zone.

Post-test description:

During the test one set of fractures comprising three major open sub-horizontal fractures (~10^o) developed, dividing the sample into four nearly equally sized parts (fig. ST-10). The fractures cutting through the hairline zone and exhibit here an offset of 1 cm (fig. ST-11).

Short vertical fractures associated with the horizontal fractures are observed at the top and bottom of the plug. The vertical fractures may be a result of inappropriate destruction at the plug-ends during the test.

The fracture surfaces are planar and smooth grading to weakly undulating. Amplitude is less than 2 mm and wavelength approximately 1 cm.

Figure ST-10.

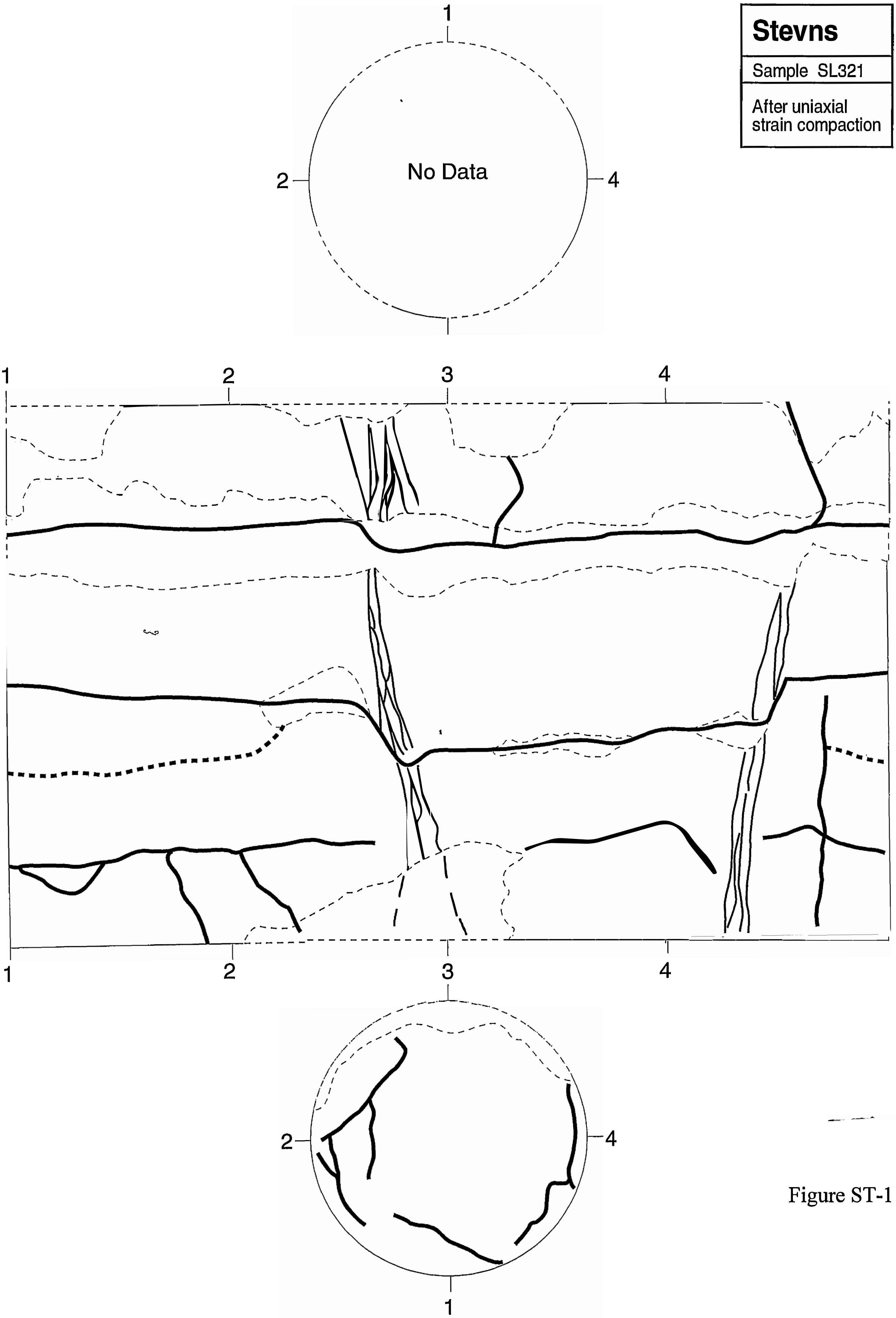

Stevns
Sample SL321
After uniaxial strain compaction
1
2
No Data
4
1
2
3
4
1
2
3
4
2
4
1

Figure ST-11.

Stevns, sample SL33
Multiple triaxial test

Pre-test description:

The sample is a vertical plug most probably perpendicular to the bedding.
The plug comprises *Thalassinoides* burrows. The sample appears as a homogeneous plug. No hairline fractures are seen.

Post-test description:

After test the plug only exhibits a weak fracturation (fig. ST-12). Two sub-parallel fractures with a spacing of 2-4 cm is developed.

At the base a gently dipping (25° from horizontal) fracture with an aperture of less than 1 mm is seen (fig. ST-13). In the middle of the plug a closed horizontal fracture is recorded. The weak appearance and lack of aperture are most probably due to "chalk paste" associated with the fracture zone.

No fracture surfaces have been described.

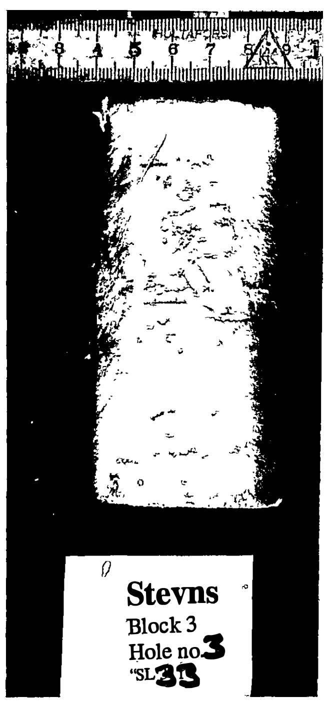

Figure ST-12.

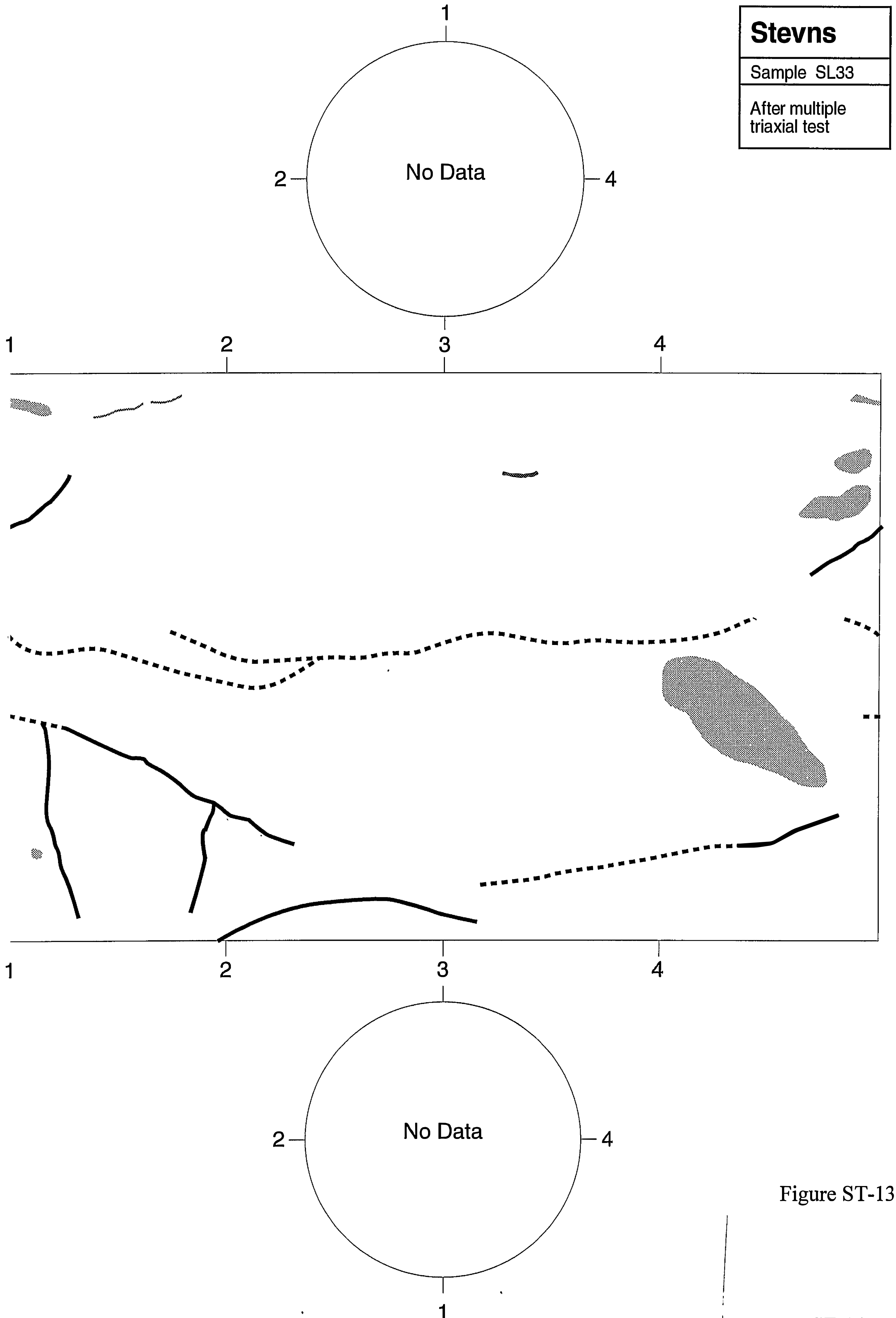
Stevns
Sample SL33
After multiple triaxial test
1
2
No Data
4
3
1
2
3
4
1
2
3
4
3
2
No Data
4
1

Figure ST-13.

Stevns, sample SV341
Direct shear test

Pre-test description:

The plug was cut as a horizontal plug parallel to the bedding. The plug appears as a homogeneous chalk without fractures and visible tracefossils.

Post-test description:

After test the plug still acted as one plug with no ruptures. However, along the shear plane a greyish colour is seen when moisturising the sample and a 1 mm offset can be identified. The colorchange along the shear zone is interpreted as a result of recrystallisation/reorganisation of the matrix particles.

Stevns, Block 50-1

Figure ST-14.

Burrowed Laminated Chalk Mudstone

Well/location:	Stevns Sjælland, Denmark
Formation:	Tor (equivalent)
Depth:	Outcrop

M	mudstone
Ch	clean chalk
Gsk	skeleton grains (bryoz, foram)
Bm	medium bedded
Lpl	planar lamination (weak)
Dn	no visible deformation
Tm	medium density of trace fossils
Hs	soft
Cm	medium consolidation
Sn	no visible stylolites
Mn	no visible secondary minerals
Fol	low density of open fractures

Description:

Block 50-1 is a highly biomottled chalk mudstone with a medium density of trace fossils (fig. ST-14). The chalk is rich in well preserved and disintegrated coccoliths. Bryozoans, foraminifera and skeletal fragments are present.

A few subhorizontal open fractures are seen in the block. Hairline fracture zones are rare.

The chalk exhibits a poorly sorted, highly intercrystalline porous chalk rich in both well preserved and disintegrated coccoliths. The poor sorting most properly is due to disintegration of the chalk. Fine euhedral and subhedral cement crystals are found scattered in the pores. The calcite cement crystals do not generally exceed sizes above 2-3 μm.

Trace fossils:

Ichnogeneous: *Thalassinoides, Planolites* and *Zoophycos.*

Insoluble residue:

0.97 %
Quartz (9 %) and clay (most likely detrital)

Petrophysical properties:

Porosity:	43.96 %
Permeability (air):	8.56 mD
Density:	2.705 g/cm^3

Analyses carried out on block 50-1:

Sample	Porosity	Permea-bility	Thin section	Capillary pressure	Insoluble residue	SEM	Geotechnical test type
50-1	X	**AIR**	X			X	**Block test**
50-1A	X	**LIQUID**			X	X	**(Cube test)**

A triaxial model test was carried on the Block 50-1. The geological description has focussed on the fracturing of the block.

Stevns, Block 50-1
Triaxial model test

Pre-test description:

Test made on the sample turned upside down. Diameter 48.9 cm. Height 51.3 cm. Weight 209.788 kg. Density 2.177 g/cm^3. Cell size: 20 x 20 mm

The block was cut as a vertical plug and was before test a "perfect" sample. One horizontal fracture zone is present in the middle of the block. A secondary horizontal fracture cut through the block 10 cm above the base of the block. Sign of weakness is seen at the base of the block along line 1 (orientation 0^o).

Prior to test holes and fractures were filled with gypsum. The gypsum does not fully act mechanically similar to the chalk during the test and does cover the surface after test. This obstructs the possibility for a detailed description of the original fractures.

Post-test description:

After test the sample was strongly fractured. The block was cut through by 3(+) sub-vertical fracture sets (fig. ST-15).

At orientation 0^o (fig. ST-15a) a listric fracture with a dip of 80^o is seen. A zone of weakness is found 20 cm above bottom where the fracture changes trace. Offset along the fracture zones is in the order of 1.5 cm. The fracture is open, planar and smooth in the upper part of the block grading into a closed anastomosing fracture zone at the base.

Movements along the fracture cause accumulation and swelling of the block at orientation 90^o (fig. ST-15b).

A listric fracture is developed at orientation 90^o. Less distinct fractures "growing from" the horizontal fractures are seen at 90^o.

At orientation 135^o a smooth, planar and open fracture with an aperture of 5 mm is seen. The fracture is grading into anastomosing fracture zones at the top of the block. The fracture is paired with the fracture at orientation 0^o and represents the main fracture of the block.

At orientation 180^o there is an open fracture with a dip of 70^o. The fracture is branching at the top of the block (fig. ST-15c).

At orientation 270^o there is a highly complex listric anastomosing fracture system. The overall dip is 90^o. Offset along the fracture is 3-5 cm (fig. ST-15d).

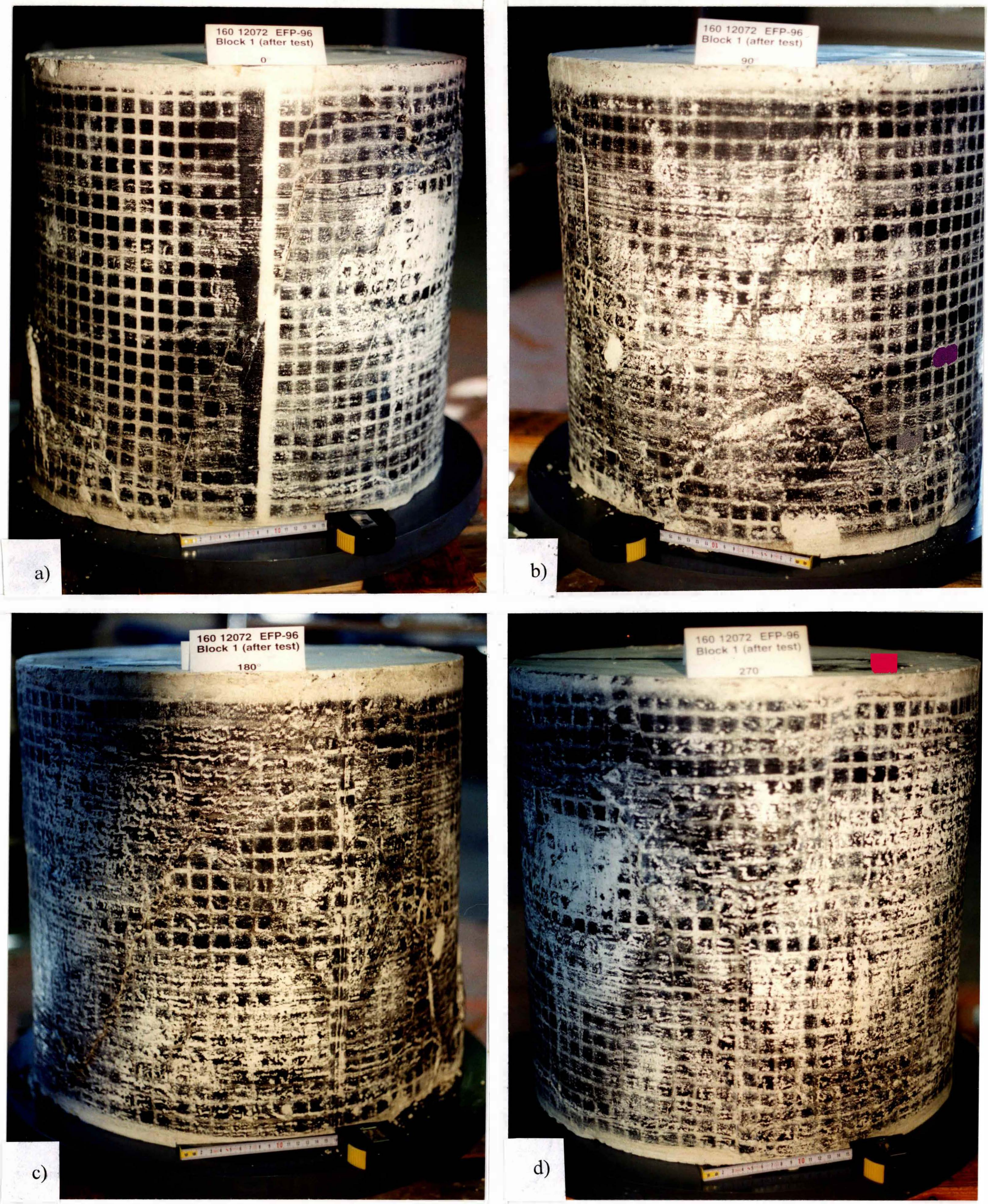
160 12072 EFP-96
Block 1 (after test)
0°
a)
160 12072 EFP-96
Block 1 (after test)
90°
b)
160 12072 EFP-96
Block 1 (after test)
180°
c)
160 12072 EFP-96
Block 1 (after test)
270°
d)

Figure ST-15.

The accumulation and swelling of the block during test is illustrated from the measurements of the circumference after test:

top	158.8 cm
middle	157.7 cm
bottom	160.8 cm

After test the upper part of the block was removed. During this process the block did break up at the middle along a supposed bedding plane exhibiting an irregular surface with a relative low relief (max 1 cm in amplitude). No striation or slickensides are associated with the surface (fig. ST-16).

The surface is cross cut by the main fracture. From the break up, the offset of the bedding plane is 2 cm. It is, however, questionable if the present surface on both sides of the fracture represents the same time-equivalent bedding plane or actually represents two different depositional surfaces (fig. ST-16).

The fracture surface itself is smooth with a weak indication of striation and slickensides. The amplitude is less than 2 mm and the wavelength is 2 - 3 cm (fig. ST-16).

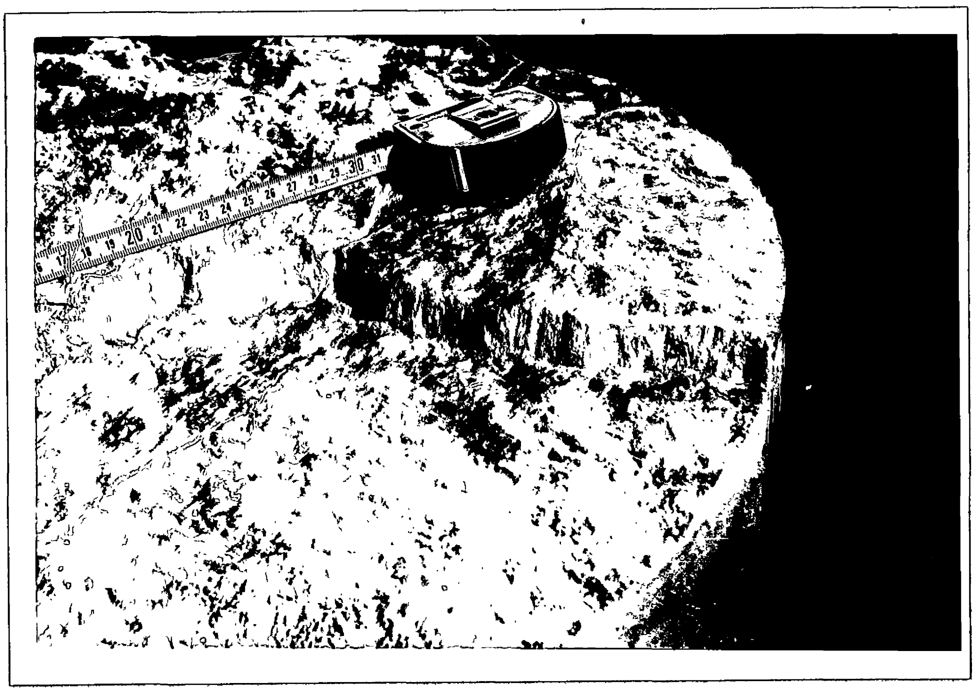

Figure ST-16.

The fracture observed in the block does not exhibit one narrow line of movement. Instead the movements have taken place along an up to 3-4 cm wide zone with a large number of microjoints. The fracture zone is widest at the block ends where anastomosing fracturing is observed.

Instead of straight continuous fracture plane the surface exhibits a rather uneven hummocky surface caused by a complex activation along the various microjoints (fig. ST-17).

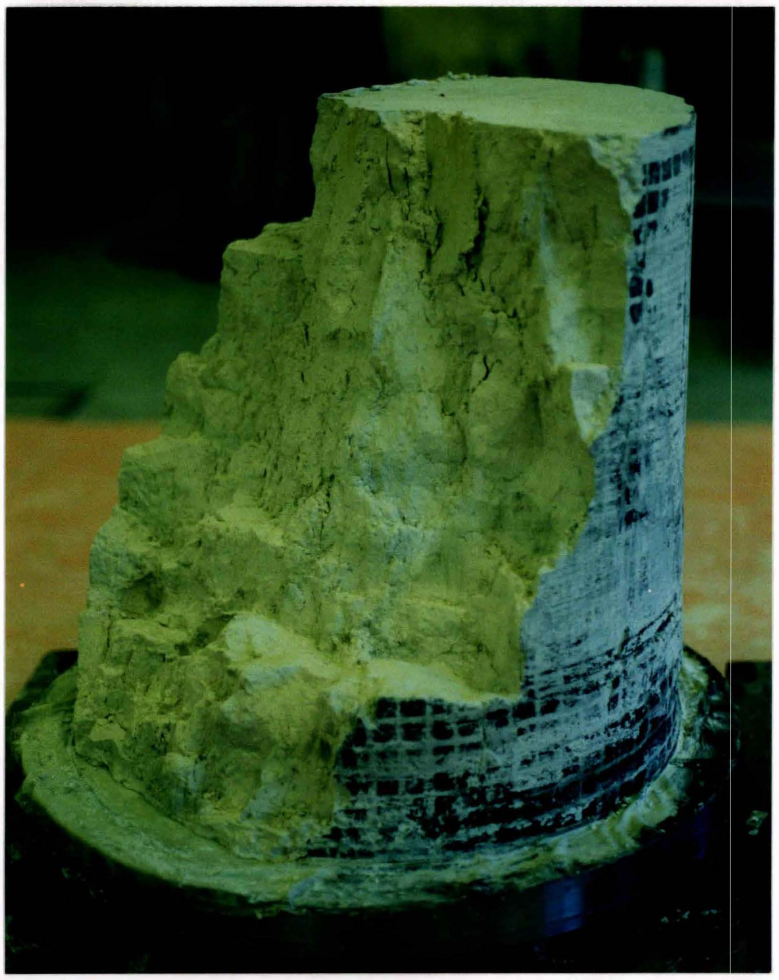

Figure ST-17.

The main fracture varies from an open fracture with chalk paste cover to a closed fracture. A reorientation of the texture is seen along the fracture zone and locally a destruction zone can be observed (fig. ST-18). From the present study there is no evidence of preferential location of the destruction zone related to dip angle and bend. In general the zone of destruction is found on both sides of the fracture.

Along well defined fractures there is evidence of change in the chalk texture (fig. ST-19). The movements along the fracture have caused a smearing of the chalk/reorientation of the chalk crystals giving rise to a narrow zone of a tight chalk matrix similar to the situation found in hairline fractures.

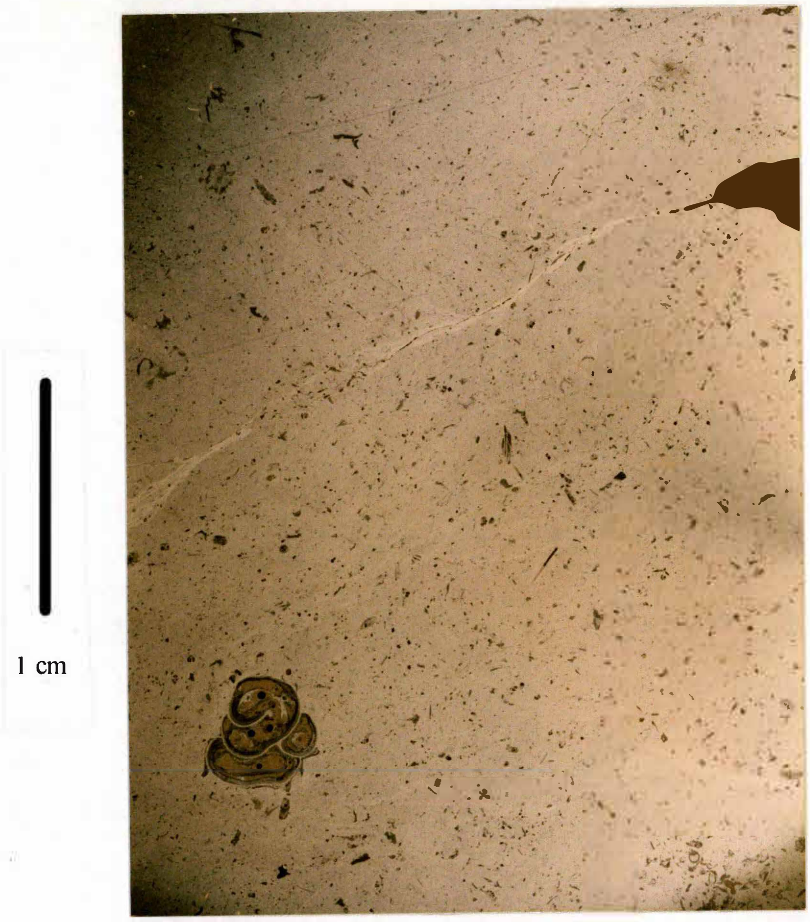

Figure ST-18.

Figure ST-19.

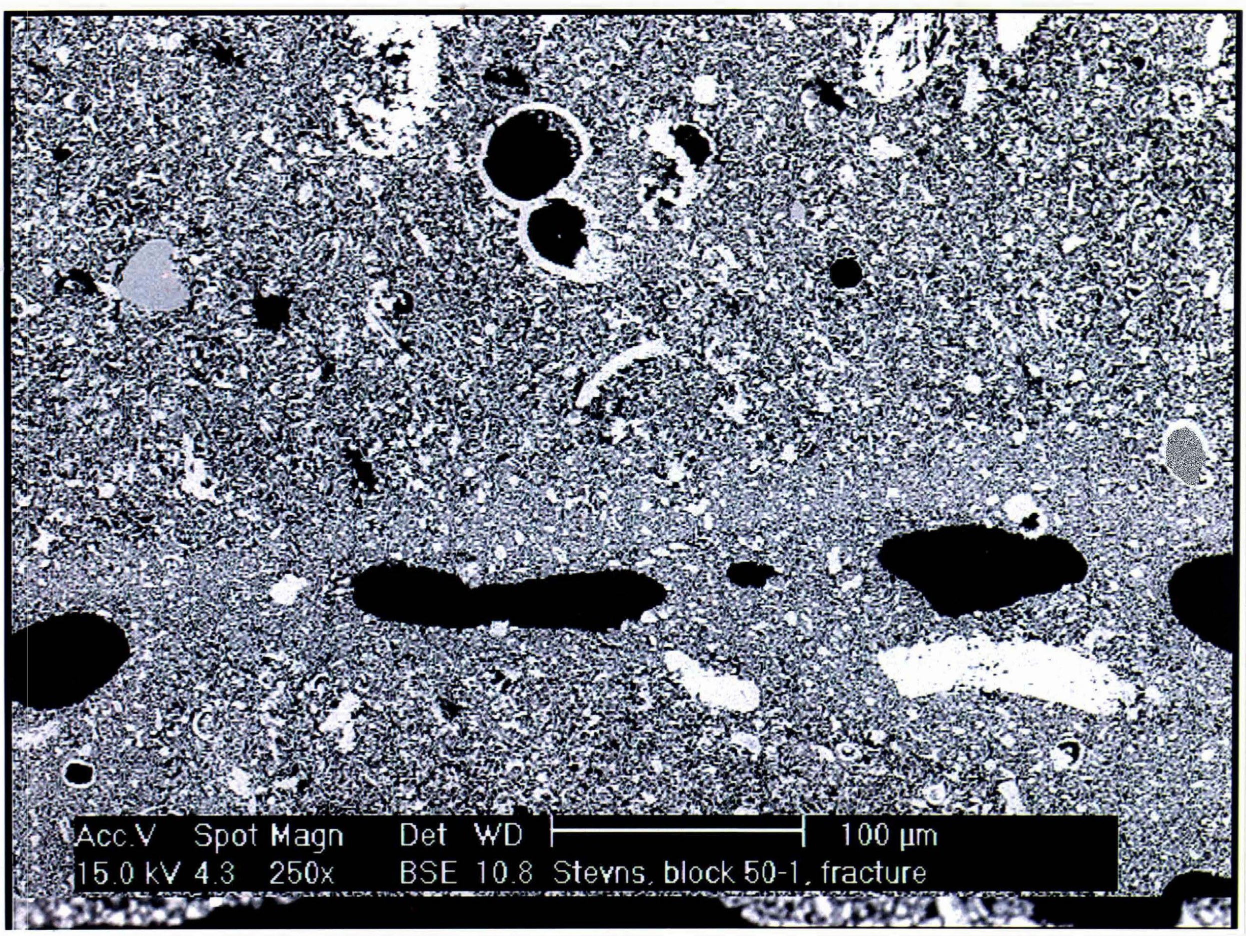

An attempt was made to test the impact of the fracture on permeability. A cube sized 4x4 cm was cut across the main fracture in the block. Permeability was measured in three directions (fig. ST-20):
A: parallel with fracture direction,
B: along the fracture strike
C: Perpendicular to the fracture zone.

The permeability was measured at two different sleeve pressures and two flow rates. No major differences in permeability related to the various directions are seen. A maximum in differences in the order of 0.75 mD is recorded. No preferential flow along the fracture is seen, which may be a result of similar flow in the heterogeneous chalk (porous burrows etc.) and in the fracture.

Stevns, Block 50-1A

Liquid permeability measurements on cube

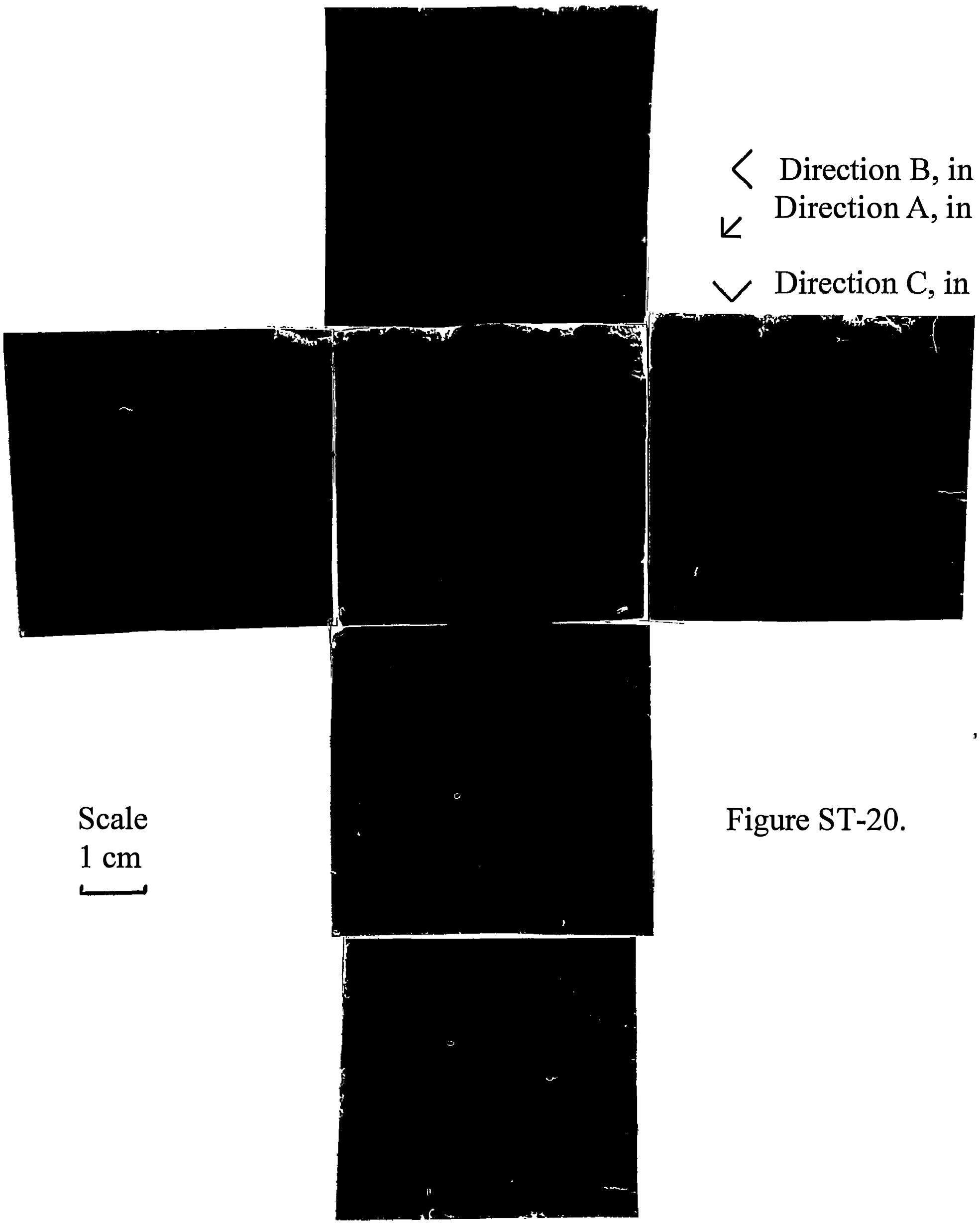

Figure ST-20.

Sleeve pressure	Direction A		Direction B		Direction C	
Bar	50 ml	100 ml	50 ml	100 ml	50 ml	100 ml
18	2.52 mD	2.28 mD		2.29 mD	3.00 mD	2.61 mD
25			2.39 mD	2.25 mD	2.54 mD	2.42 mD

Stevns, Plug 50-3

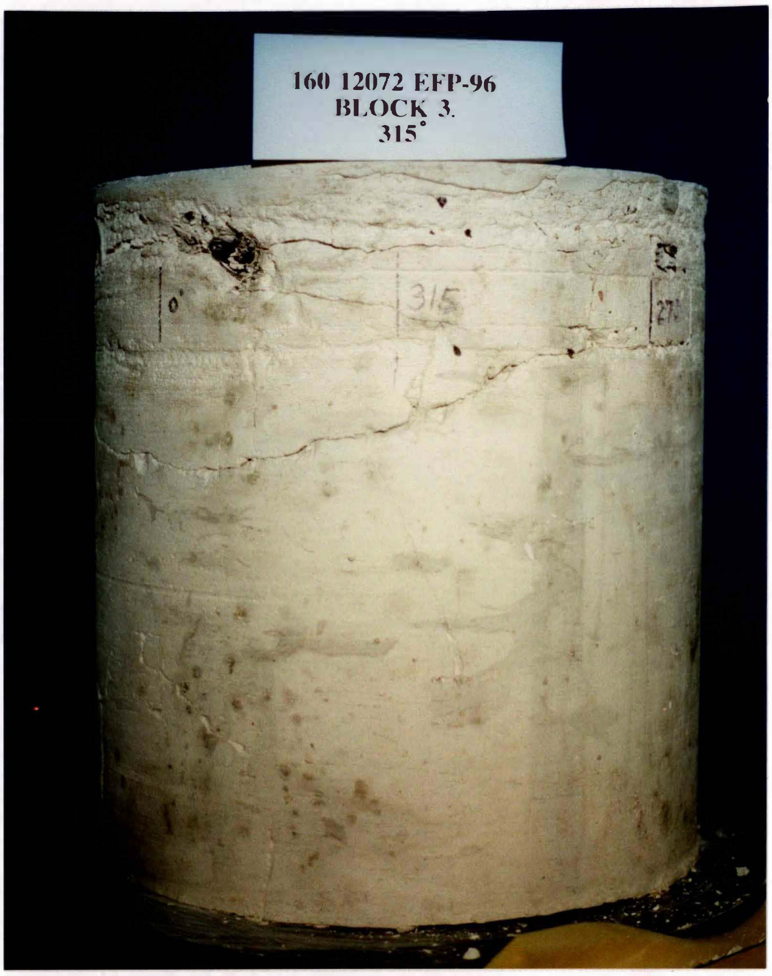

Figure ST-21.

Burrowed Laminated Chalk Mudstone

Well/location: Stevns
Sjælland, Denmark

Formation: Tor (equivalent)

Depth: Outcrop

M	mudstone
Ch	clean chalk
Gsk	skeleton grains (bryoz, foram)
Bm	medium bedded
Lpl	planar lamination (weak)
Dn	no visible deformation
Tm	medium density of trace fossils
Hs	soft
Cm	medium consolidation
Sn	no visible stylolites
Mn	no visible secondary minerals
Foh	high density of open fractures

Description:

Block 50-3 is a highly biomottled chalk mudstone with a medium density of trace fossils. The chalk is rich in both well preserved and disintegrated coccoliths. Bryozoans, foraminifera and skeletal fragments are present.

A large number of sub-horizontal open fractures are seen in the block. Hairline fracture zones are rare.

The chalk exhibits a poorly sorted, highly intercrystalline porous matrix. The poor sorting most properly is due to disintegration of the chalk. Fine euhedral and subhedral cement crystals are found scattered in the pores. The calcite cement crystals do not generally exceed sizes above 2-3 μm.

Trace fossils:

Ichnogeneous: *Thalassinoides, Planolites* and *Zoophycos.*

Insoluble residue:

0.97 %
Quartz (9 %) and clay (most likely detrital)

Petrophysical properties:

Porosity:	43.96 %
Permeability (air):	8.56 mD
Density:	2.705 g/cm^3

Analyses carried out on block 50-3:

Sample	Porosity	Permea-bility	Thin section	Capillary pressure	Insoluble residue	SEM	Geotechnical test type
50-3						**X**	**Block test**

A triaxial model test was carried on Block 50-3. The geological description has focussed on the fracturing of the block.

Stevns, block 50-3

Pre-test description:

The Stevns block 50-3 was before test heavily fractured with horizontal to sub-horizontal fractures.

3 first generation sub-horizontal and open fractures are seen in the upper part of the block. One fracture zone is associated with flint nodules.

Minor sub-vertical and horizontal second generation fractures are interconnecting the first generation fractures.

One major fracture is found in the base.

A sub-vertical fracture is seen at 110° paired with the fracture at 315°.

The first generation fractures are interpreted as pressure relaxation fractures and exhibit an undulating/irregular character. The undulation is in the range of 2-3 cm. Slickensides are absent on the fracture surface but locally a chalk paste cover is seen.

Before test the fractures were filled with gypsum and not all the original fractures can be identified after test.

After test description:

After test the block was cut through by a large number of conjugating fractures dipping 60-70°. The original horizontal fractures are only reactivated to some degree (hidden behind the gypsum cover).

The length of the fractures ranges from less than 10 cm to more than 50 cm. The spacing is from 5 cm to 10 cm.

The block broke apart along a rather uneven surface.

HILLERSLEV

HILLERSLEV

Hillerslev is located in the northern part of Jutland (Denmark)(fig. H-1).

The Hillerslev Quarry is an active quarry. It provides the only good exposure within the central portion of the Thisted Dome although it is located at some distance from the very centre.

The chalk in the quarry belongs to the *humboldtii-stevensis* Zone (Brachiopod zone 9, Upper Maastrichtian) (E. Håkansson, pers. com, 1996)

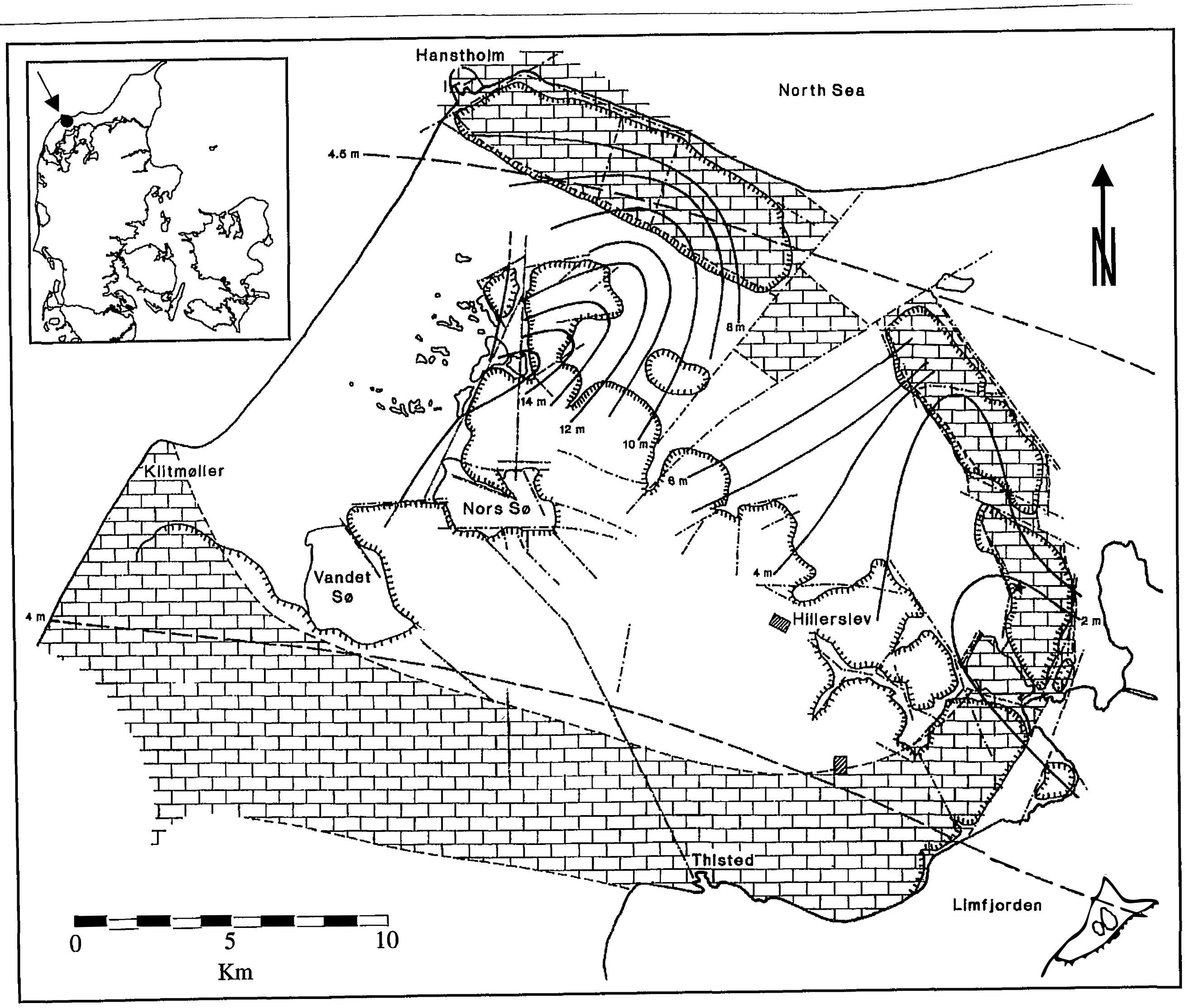

Figure H-1. Location map

HILLERSLEV

Figure H-2.

Burrowed Massive
Chalk Mudstone

Well/location: Hillerslev
North Jutland, Denmark

Formation: Tor (equivalent)

Depth: Outcrop

M	mudstone
Ch	clean chalk
Gn	no visible grains
Bm	medium bedded
Lpl	planar lamination (weak)
Dn	no visible deformation
Tl	low density of trace fossils
Hs	soft
Cm	medium consolidation
Sn	no visible stylolites
Mpy	pyrite minerals
Foh	high degree of open fractures

Description:

The chalk at Hillerslev is a soft, greyish white bioturbated chalk mudstone characterised by a weakly laminated structure partly destroyed by burrowing organisms (*Thalassinoides*, *Planolites*, *Zoophycos* and *Chondrites*). The bioturbation is weakly discernible due to similarities in lithology or coloration of burrow fills and matrix. The chalk sequence at Hillerslev is heavily cut through by horizontal and conjugated fractures (fig. H-2).

The chalk is a sparse biomicritic wackestone (fig. H-3). The microfossil content is dominated by calcispheres. Foraminifera and echinoderm fragments are rare.

The chalk of Hillerslev is dominated by a large amount of well preserved coccoliths (fig. H-4). Syntaxial calcite overgrowth on coccolith platelets is normally sparse and the size of these crystals is normally less than 1-2μm.

The chalk is porous with both intercrystalline and intrafossiliferous porosity. The calcisphere chambers are normally open. Fine euhedral and subhedral cement crystals are found scattered in the matrix. The size of the calcite cement crystals appears rather uniform with an average around 2 μm (micrite). Crystal sizes above 5 μm (microspar) are rare.

The average distribution of pore throat radius is ~0.6 μm (figs. H-11 and H-12).

The content of insoluble residue is approximately 4%. The clay content is low and rarely seen in the SEM. Silica (opal) is relatively common within the chalk and appears as cristobalite aggregates (fig. H-4).

Porosities and permeabilities are in the order of 46% and 8.5 mD, respectively.

Analyses carried out on samples from Hillerslev.

From the Hillerslev quarry three blocks (block 8, 9 and 10) were sampled. A number of plugs were drilled in the various blocks for geotechnical tests. A geological description was carried out on the plug trims to describe the initial stage of the sample. Subsequent to the geotechnical test a description of the plugs was made.

Sample	Porosity	Permea-bility	Thin section	Capillary pressure	Insoluble residue	SEM	Geotechnical test type
HL 81A	**X**	**AIR**	**X**	**X**	**X**	**X**	**Direct shear**
HL 81B							**Direct shear**
HL 82							**Unconfined uniaxial compression**
HL 91							**Direct shear**
HL 106	**X**	**AIR**					**Uniaxial strain compaction**
HL 107			**X**	**X**	**X**		**Multiple triaxial test**

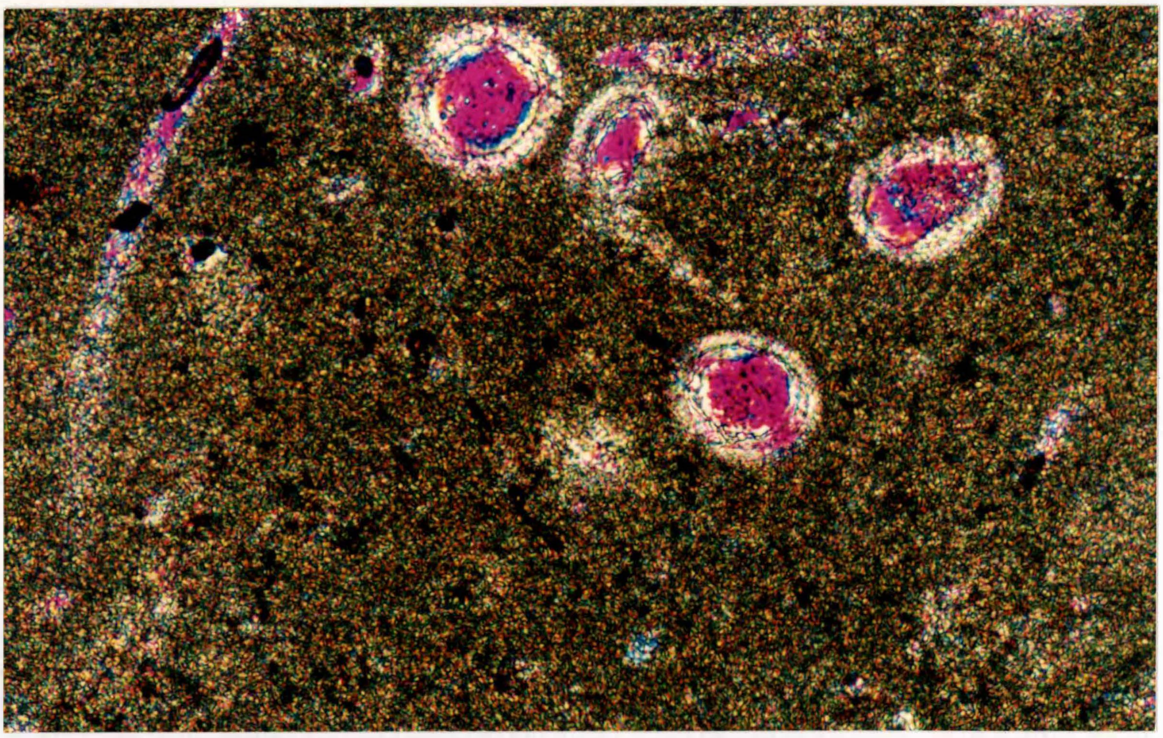

Figure H-3. Thin section. Scale: 100 μm

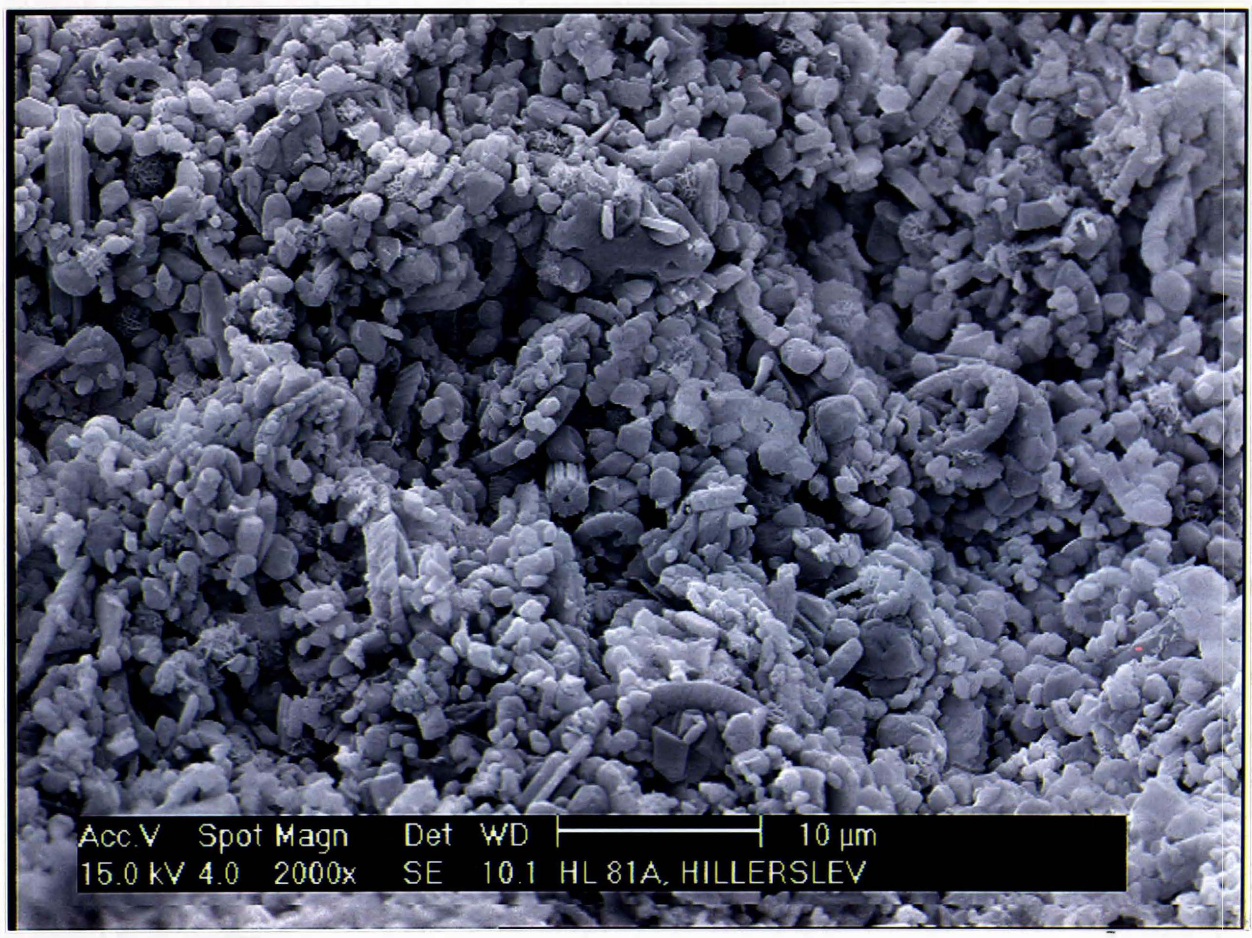

Figure H-4. SEM image.

Hillerslev, block 8

Description:

Block 8 is a highly biomottled chalk mudstone with a medium density of trace fossils. The burrow fills are hardly distinguishable from the surrounding matrix due to similarities in composition. A weak indication of lamination can be seen.

The chalk is a sparse biomicritic wackestone dominated by calcispheres and foraminifera. Skeletal fragments of echinoderms are rare. Open calcispheres and foraminifera chambers are common.

The matrix comprises a poorly sorted, highly intercrystalline porous chalk rich in both well preserved and disintegrated coccoliths. Fine euhedral and subhedral cement crystals are found scattered in the pores. The calcite cement crystals do not generally exceed sizes above 2-3 μm.

Trace fossils:

Ichnogeneous: *Zoophycos* and *Planolites.*

Insoluble residue:

3.72 %
Quartz (9%, primarily opal) and clay.

Petrophysical properties:

Porosity:	46.11 %
Permeability (air):	8.308 mD
Density:	2.696 g/cm^3

Hillerslev, samples 81A and 81B
Direct shear test

Pre-test description:

From hole 1 in block 8 there is a weak indication of bedding which partly is emphasised by the presence of *Planolites*. The plug is not drilled fully perpendicular to the bedding. A dip of approximately 20^{o} is seen in plug HL 81A and HL 81B.

No fracture or offset within the chalk is seen.

Post-test description:

After test both plugs still acted as intact plugs without ruptures. However, the plugs exhibit somewhat broken upper and lower ends.

No rupture is seen along the pre-defined shear plane but a greyish colour is seen when moisturising the sample and a minor (<1 mm) offset can be identified. The colorchange along the shear zone is interpreted as a result of recrystallisation/reorganisation of the matrix particles.

Hillerslev, sample 82
Unconfined uniaxial compression

Pre-test description:

From hole 1 in block 8 there is a weak indication of bedding which partly is emphasised by the presence of *Planolites* and *Zoophycos*. The plug is not drilled fully perpendicular to the bedding. A dip of approximately 25° is seen.

No fracture or offset within the chalk is seen.

Post-test description:

After test the samples comprise 3 short, closed vertical-subvertical fractures. The fracture planes appear smooth to gently rough (figs. H-5 and H-6).

No direct relationship between fractures and sedimentological features are seen.

Figure H-5.

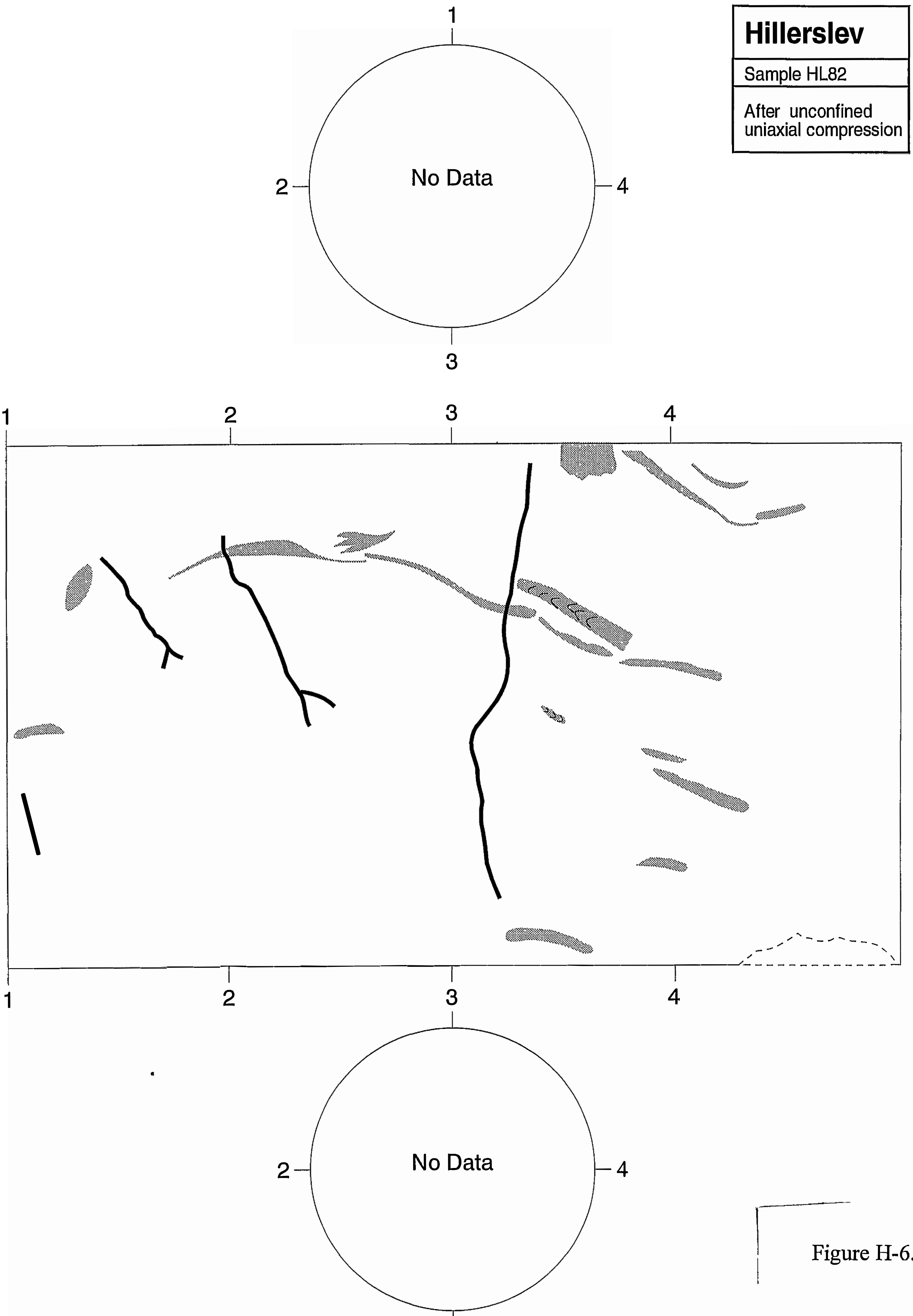
Hillerslev
Sample HL82
After unconfined uniaxial compression
1
2
3
4
No Data
1
2
3
4
1
2
3
4
3
2
4
1
No Data

Figure H-6.

Hillerslev, sample 91
Direct shear test

Pre-test description:

Block 9 comprises the same chalk as block 8, but was taken around a slightly inclined horizontal fracture. The fracture appears as a clean relatively smooth plane fracture with indistinct slickensides.

The sample was processed so the fracture came out parallel to the pre-defined shear plane. Therefore the lamination and hairline fractures are dipping 20-30^0 in the plug.

Post-test description:

The test was carried out with a predefined shear plane parallel to the fracture. After test the plug was in a poor condition. The upper part was broken into pieces in the order of 1 cm^3 and gave rise to a very rough "fracture plane" with a 1-2 cm relief (fig. H-7).

The random fracturing was probably controlled by vertical zones of weakness (hairline fractures?) and do not represent the real predefined shear plane. The shear plane most probably was developed as a zone of "chalk-paste" below the broken surface.

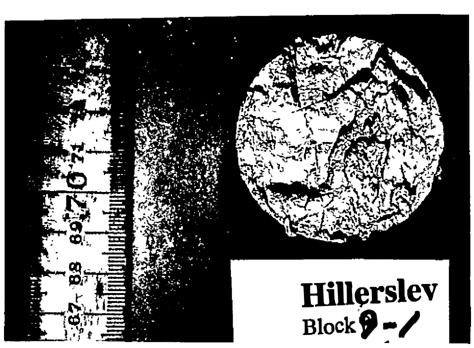

Figure H-7.

Hillerslev, sample 106
Uniaxial strain compaction

Pre-test description:

Block 10 comprises the same chalk as block 8. Trace fossils in this block also include *Thalassinoides* and *Chondrites*.

The plug is drilled perpendicular to the bedding.

No fractures are seen in the plug, and the plug appears as a homogeneous sample. However, a zone of weakness is seen in the upper part (at direction "3").

Post-test description:

After test the plug could be divided into two parts separated by an open, slightly inclined fracture (~15^{o}) in the middle of the plug (fig. H-8).

The upper part of the plug is broken and comprises a few vertical and horizontal fractures. The fracturing in this part of the plug most probably is related to the zone of weakness observed prior to test.

In the lower part of the plug only weakly developed fractures (vertical and 45^{o}) are seen. The direction of the fractures does not correspond to sedimentological features.

The surface of the main fracture is smooth to gently rough. Slickensides are not developed, but the surface is indicative of a 1-2 mm offset.

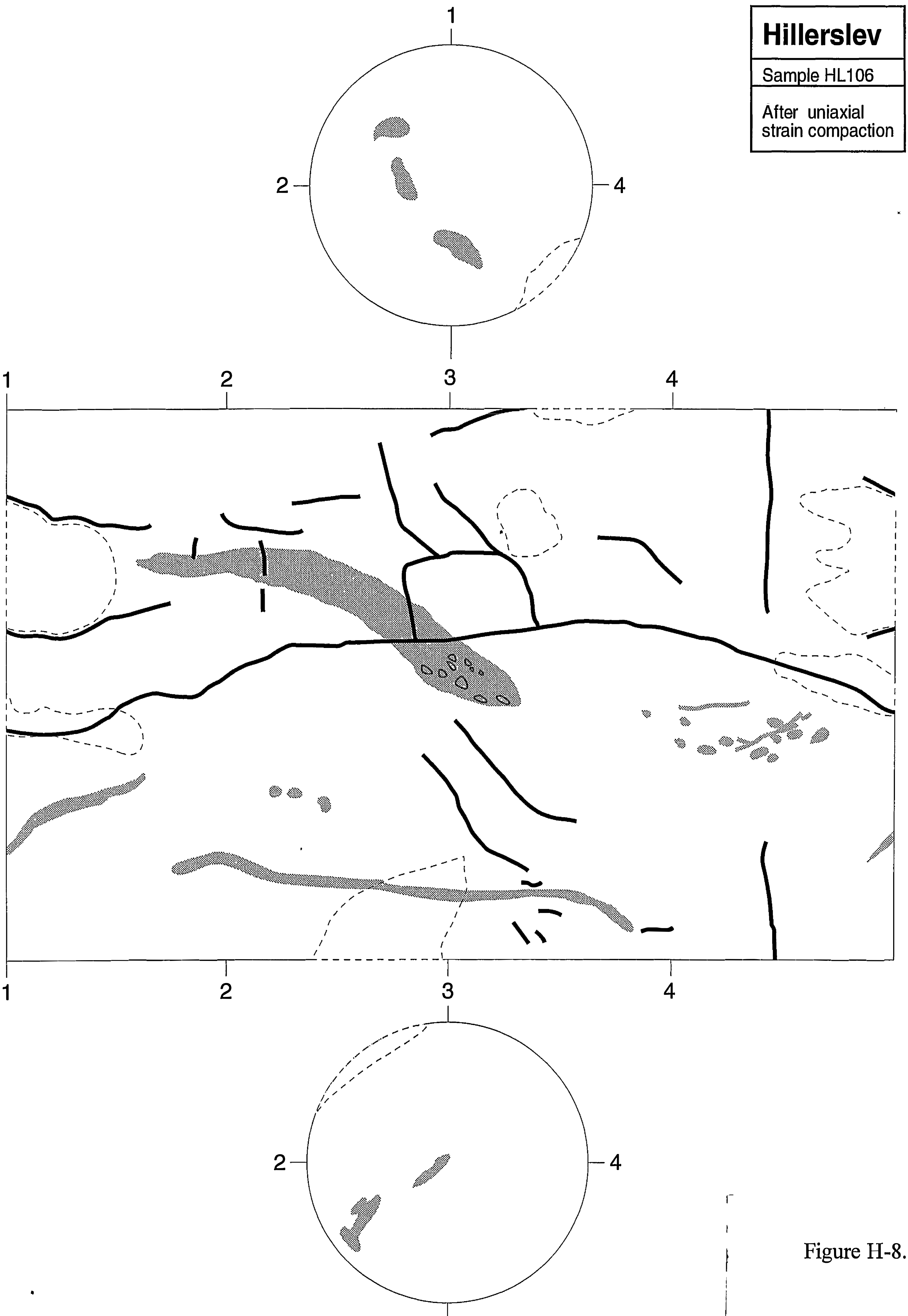
Hillerslev
Sample HL106
After uniaxial strain compaction
1
2
3
4

Figure H-8.

Hillerslev, sample 107
Multiple triaxial test

Pre-test description:

Sample 107 is lithologically similar to sample 106. The sample is a homogeneous chalk with a few burrows related to *Planolites, Thalassinoides* and *Chondrites?*.

No fractures are observed prior to test.

Post-test description:

After test the plug appears as an intact sample (fig. H-9). At direction 2 one distinct, partly open fracture is observed, but the fracture does not penetrate the whole plug (fig. H-10). The fracture dips 70° and exhibits a rough highly irregular fracture plane.

The fracture cross-cuts trace fossils without offset. No evidence of sedimentological control of fractures is seen.

The fracture surface has not been described.

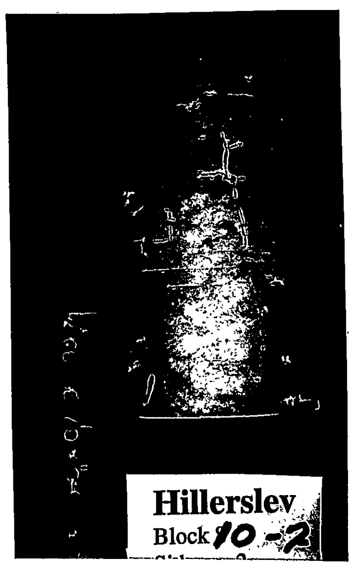

Figure H-9.

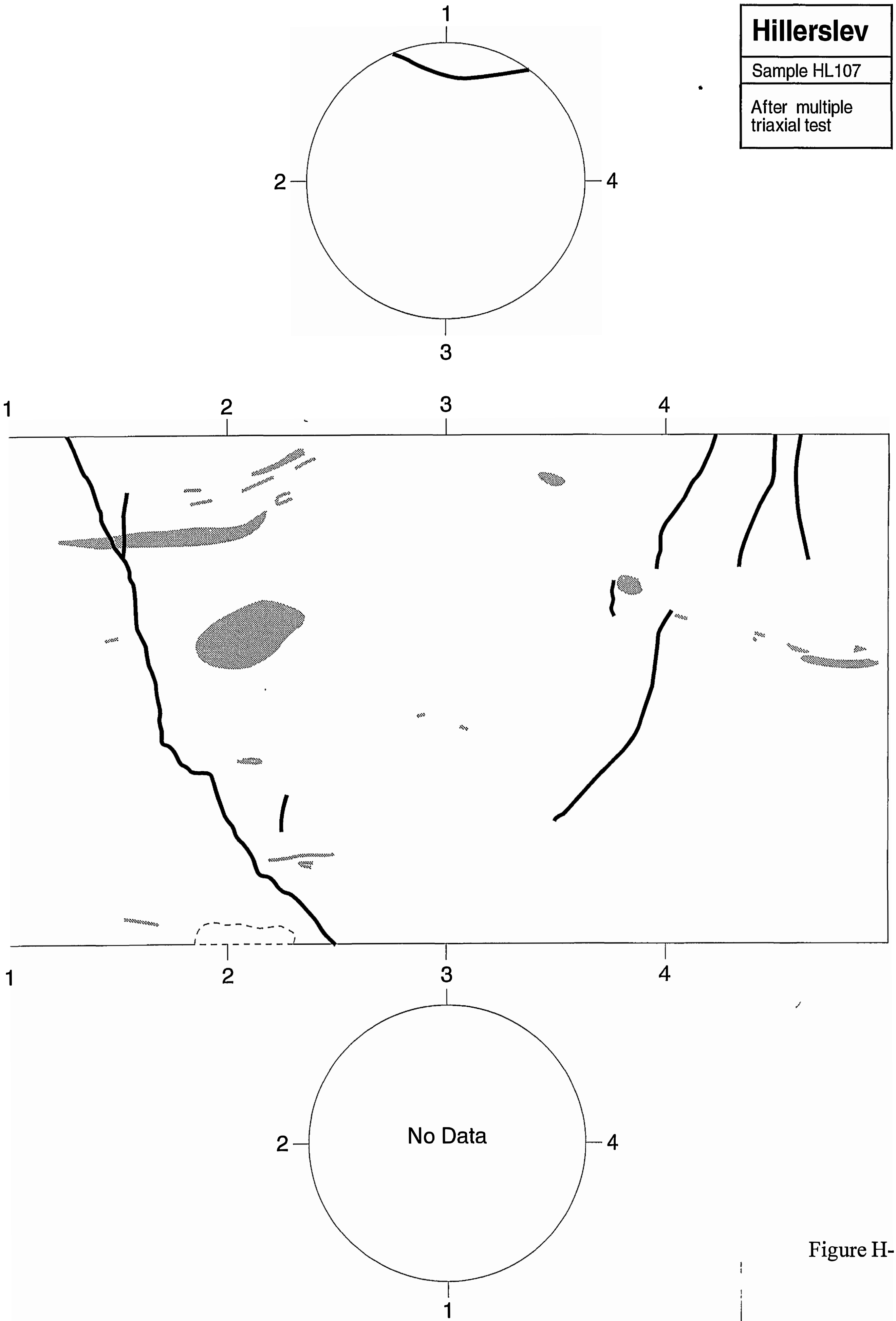
Hillerslev
Sample HL107
After multiple triaxial test
1
2
3
4
No Data

Figure H-10.

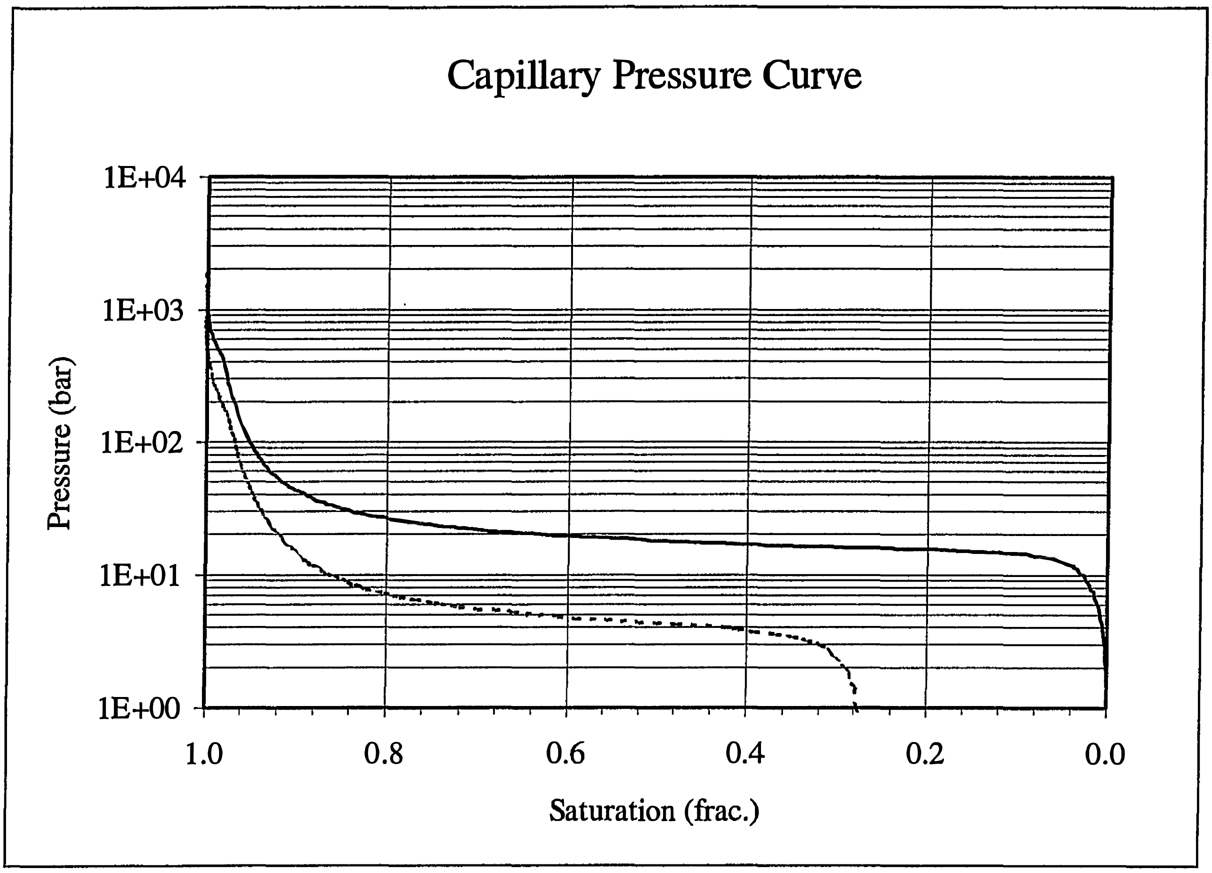

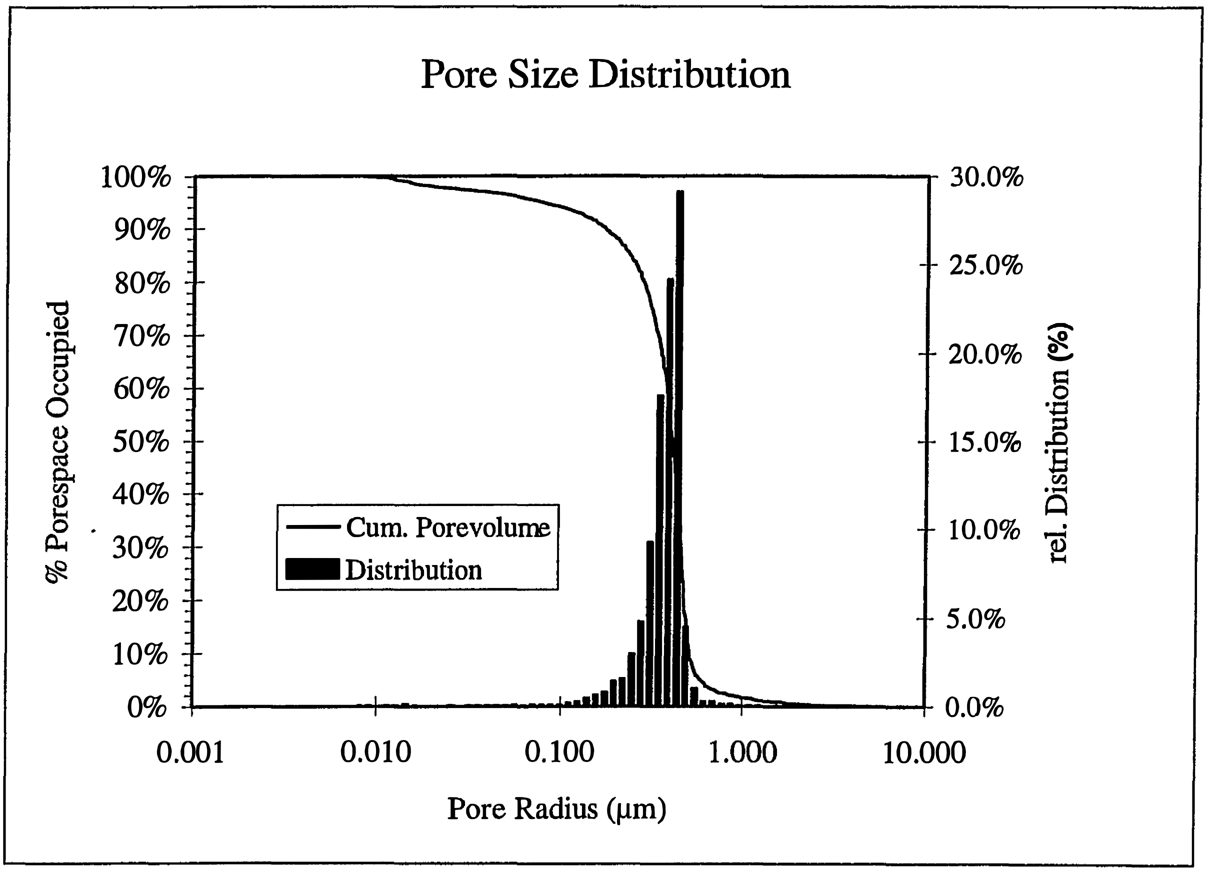

Figure H-11. **Capillary pressure curves and pore size distribution for plug Maastricht outcrop NJ107**

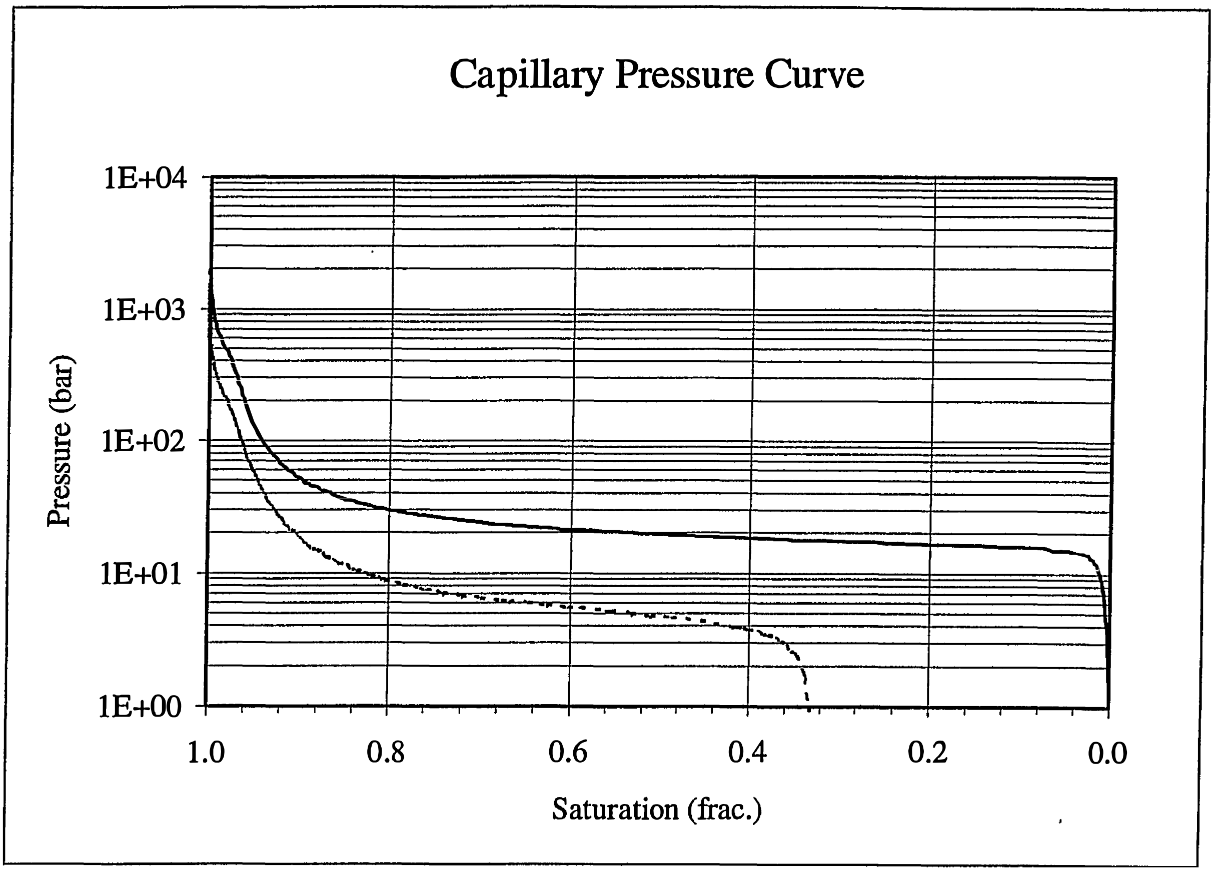

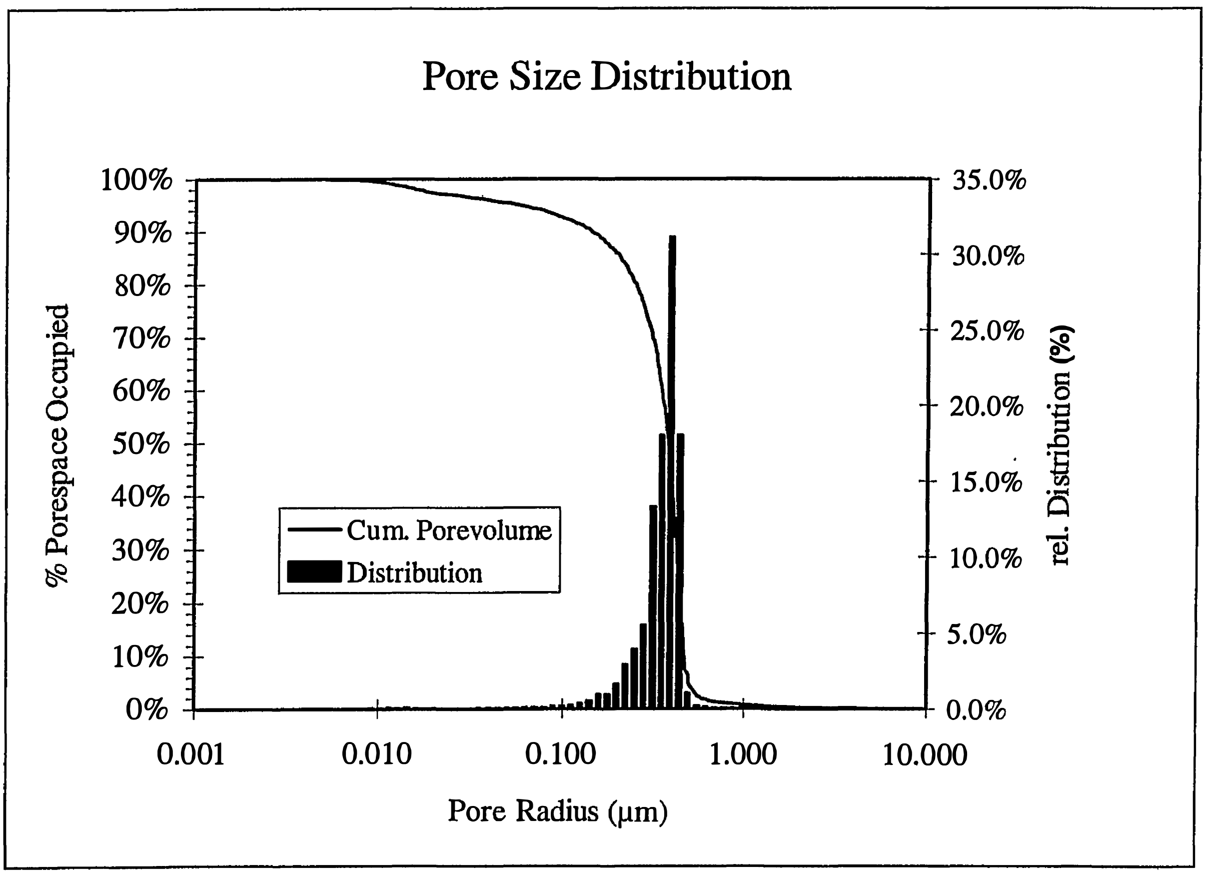

Figure H-12. **Capillary pressure curves and pore size distribution for plug Maastricht outcrop NJ81**

TYRA FIELD

In September 1996 a 150 ft core interval from a Tyra well was inspected at Mærsk core laboratory. The core interval was described in some detail and a number of samples were taken for rock mechanical analyses.

A summary of the core description is shown on figure T-1. Sample intervals are indicated with arrows.

The examined interval is bioturbated but in varying intensity. In the upper 10' of the interval the chalk is relatively clayish indicated by lamination, primary as well as secondary (pressure dissolution seams). Downward the chalk becomes massive with a high density of hairline fractures prevails. The pressure dissolution seams grades slightly into thin, low amplitude stylolites.

The interval from 80' to 100' is characterised by a rather homogeneous chalk. Burrows of *Thalassinoides* are seen but no stylolites or dissolution seams are observed. The interval is heavily affected by shearing and up to 1 cm wide shear fractures are seen. The shear fractures are often filled with brecciated clasts in a fine grained matrix.

From 100' to 170' the massive chalk is dominated by high amplitude stylolites.

The presence of stylolites and dissolution seams is indicative of severe dissolution of the chalk with subsequent recrystallisation giving rise to hard well cemented chalk. Due to some variation in the diagenesis in the core interval some variation in the cementation is seen and the samples are described separately.

The chalk in the examined core interval is characterised by a biogenic wackestone texture. The chalk is highly cemented. In the upper part calcite cement crystals are in the order of 1-2 μm. Microspar crystals (> 5 μm) are rare in the matrix but common in the foraminifera chambers. In the lower part microspar crystals are more common in the matrix which may be a result of a higher intensity of stylolitization.

Analyses carried out on Tyra core samples

Sample	Porosity	Permea-bility	Thin section	Capillary pressure	Insoluble residue	SEM	Geotechnical test type
10	**X**	**-**	**X**		**X**	**X**	**Direct shear test**
11A	**X**	**AIR**	**X**		**X**	**X**	**Direct shear test**
11B						**X**	**Direct shear test**
13A	**X**	**AIR**	**X**		**X**	**X**	**Multiple triaxial test**
13B						**X**	**Multiple triaxial test**
14A	**X**	**AIR**					**Multiple triaxial test**
16	**X**	**AIR**				**X**	**Multiple triaxial test**
16B	**X**	**AIR**	**X**		**X**	**X**	**Uniaxial strain compaction**
20A						**X**	**Direct shear test**
20B	**X**	**-**	**X**		**X**	**X**	**Direct shear test**

Tyra well

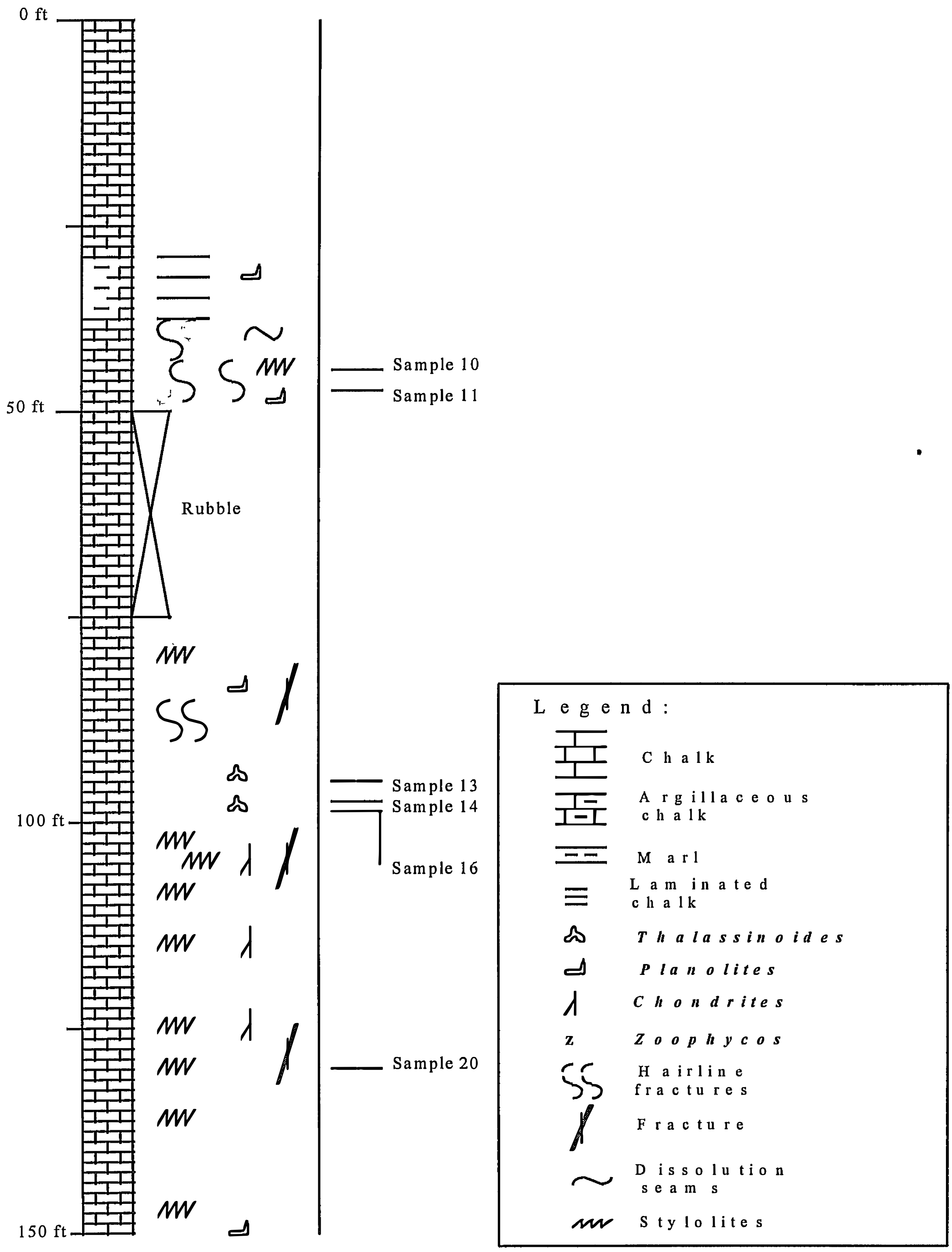

0 ft
50 ft
100 ft
150 ft
Rubble
Sample 10
Sample 11
Sample 13
Sample 14
Sample 16
Sample 20
Legend:
Chalk
Argillaceous chalk
Marl
Laminated chalk
Thalassinoides
Planolites
Chondrites
Zoophycos
Hairline fractures
Fracture
Dissolution seams
Stylolites

Tyra, sample 10

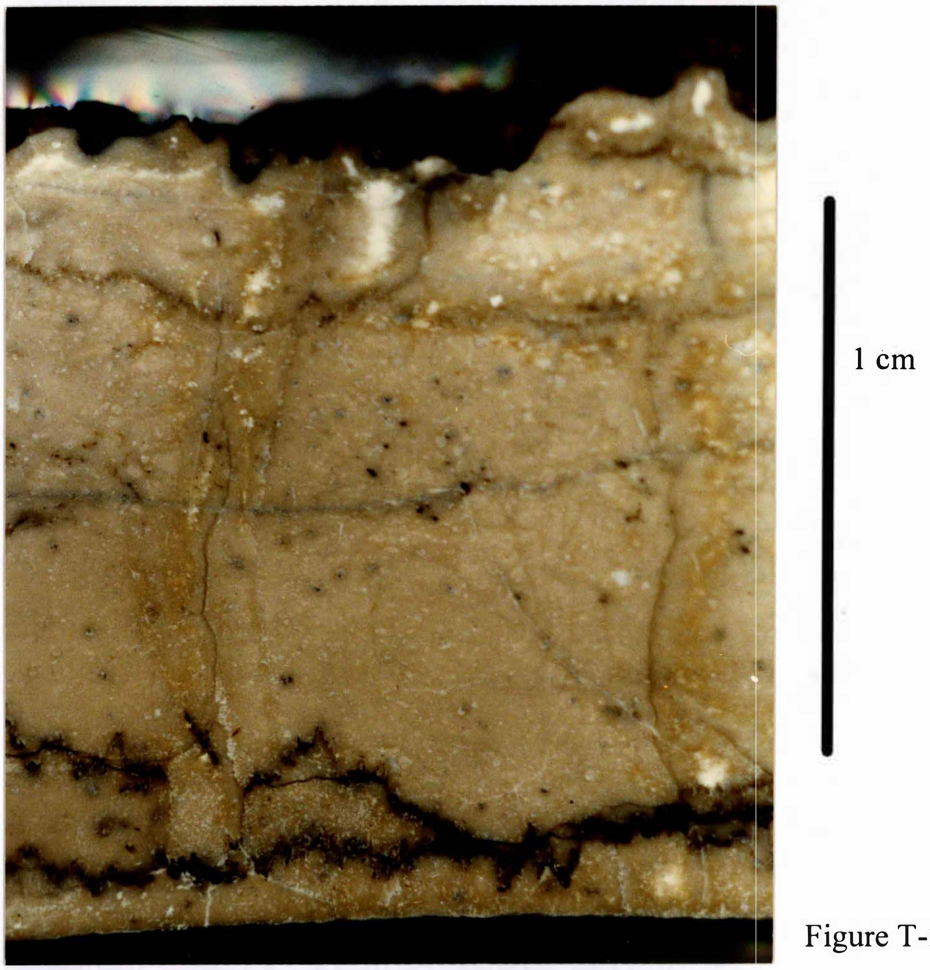

Figure T-2

Burrowed Massive Chalk Mudstone

Well/location: Tyra, Denmark

Formation: Tor

Depth:

M	mudstone
Ch	clean chalk
Gn	no visible grains
Bn	no visible bedding
Lpl	planar lamination (weak)
Dn	no visible deformation
Tl	low density of trace fossils
Hh	hard
Chi	high degree of consolidation
Sh	high degree of stylolites
Mp	pyritic minerals
Fsh	high degree of stylolite fractures

Description:

Hard, massive chalk mudstone. A few weak clayish laminae are seen in the chalk. Relatively thick, medium amplitude (2 mm) stylolites dominates the sample. Associated with the stylolites healed fractures can be seen. A few indistinct hairline fractures are present (fig. T-2).

The chalk has a sparse biomicritic wackestone texture where the predominant grain component is foraminifera (fig. T-3). The foraminifera chambers are often filled with microspar crystals (> 5 μm). The foraminifera tests are recrystallised (fig. T-4).

Differential cementation of the matrix associated with stylolitisation is seen (see thin section, fig. T-3; White area = cemented, Blue area = porous).

The matrix is rather uniform and is dominated by euhedral calcite crystals (1-3 μm). Well preserved coccoliths are rare.

Trace fossils:

Ichnogeneous: *Not observed.*

Insoluble residue:

3.22 %
Quartz (27 %) and clay

Petrophysical properties:

Porosity:	35.81 %
Permeability:	- mD
Density:	2.696 g/cm^3

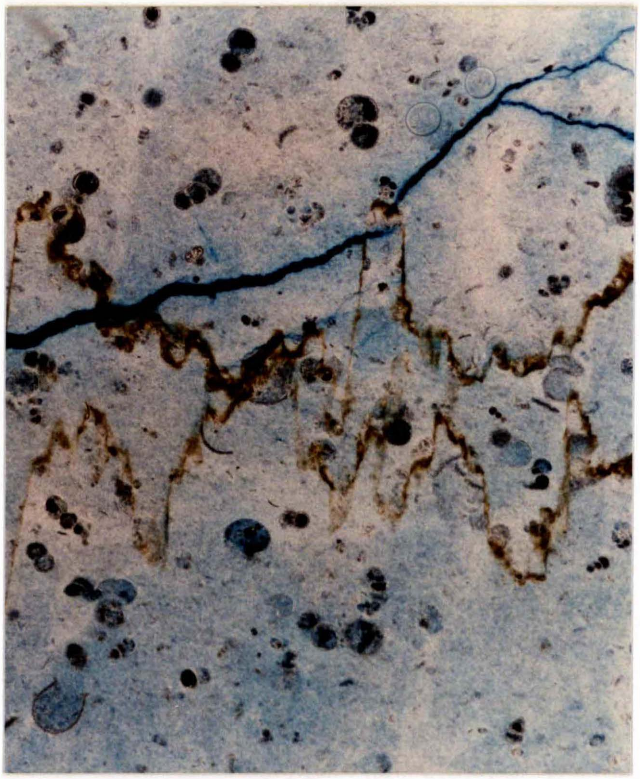

Figure T-3. Scale: 5 mm

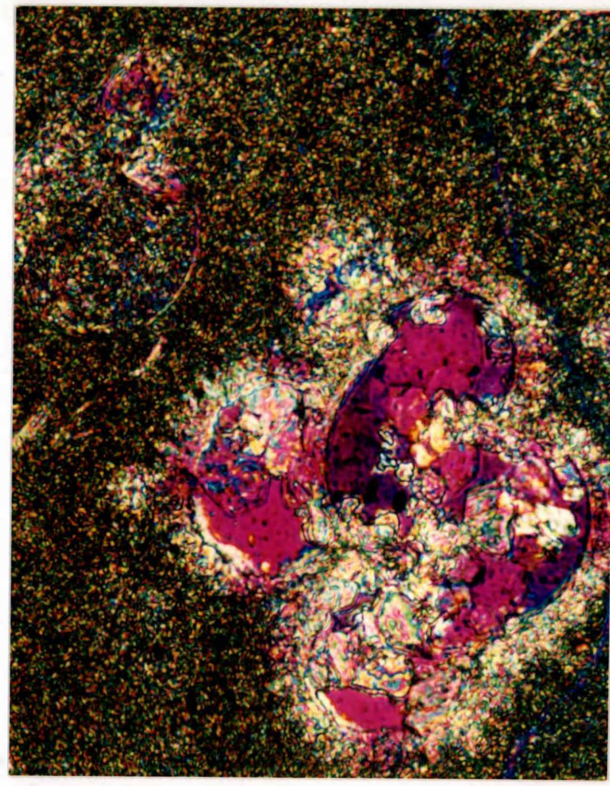

Figure T-4. Scale: 0.1 mm

↓ Figure T-5.

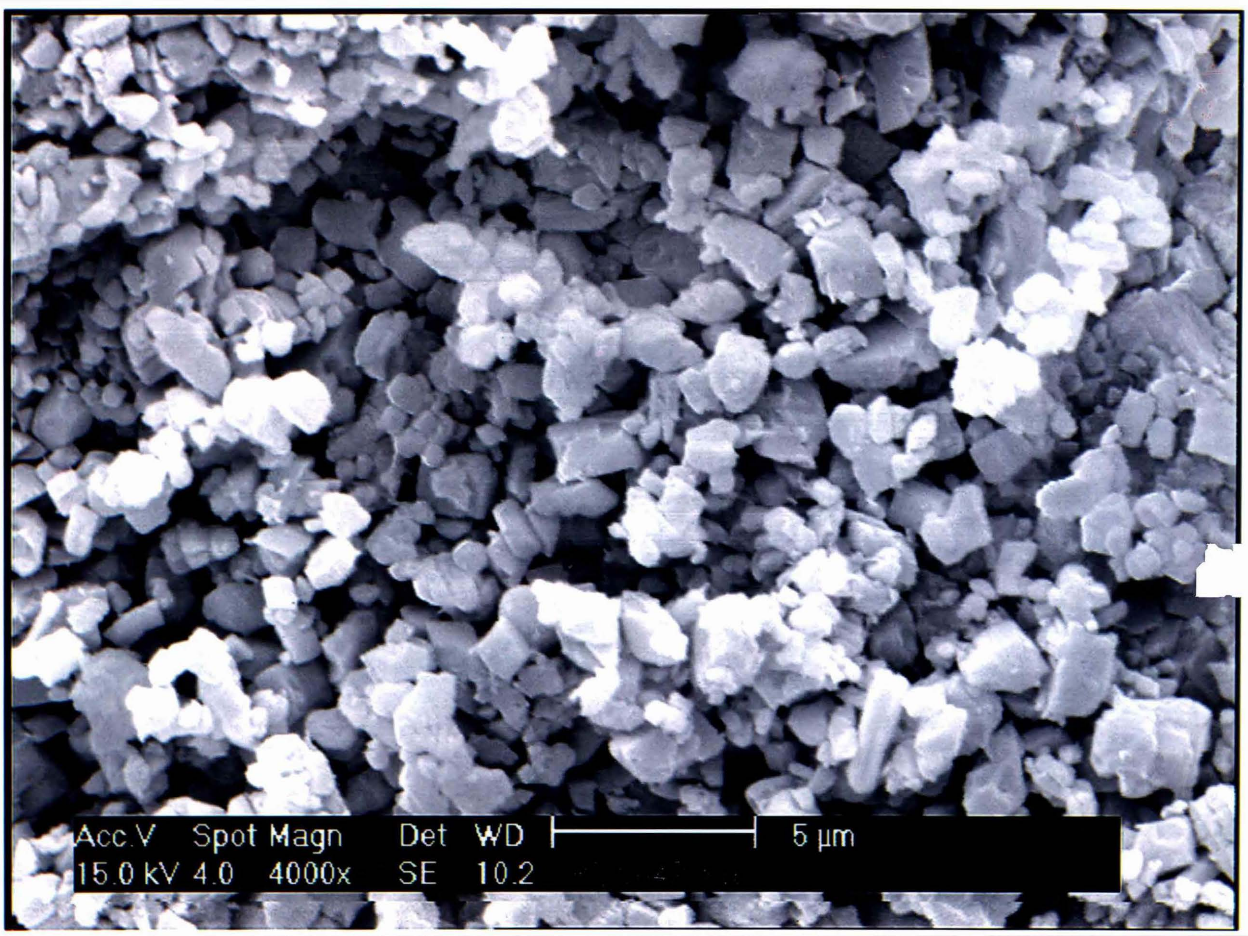

Tyra, sample 10
Direct shear test

Pre-test description:

The plug was cut parallel to the stylolites. The pre-defined shear direction was selected to be perpendicular to the stylolite surface.

The amplitude of the stylolites is in the order of 2 mm.

No stylolite associated fractures are seen.

Post-test description:

After test the plug was broken along the stylolite surface. The shear plane was very smooth to gentle wavy. The surface is weakly slickensided.

Tyra, sample 11

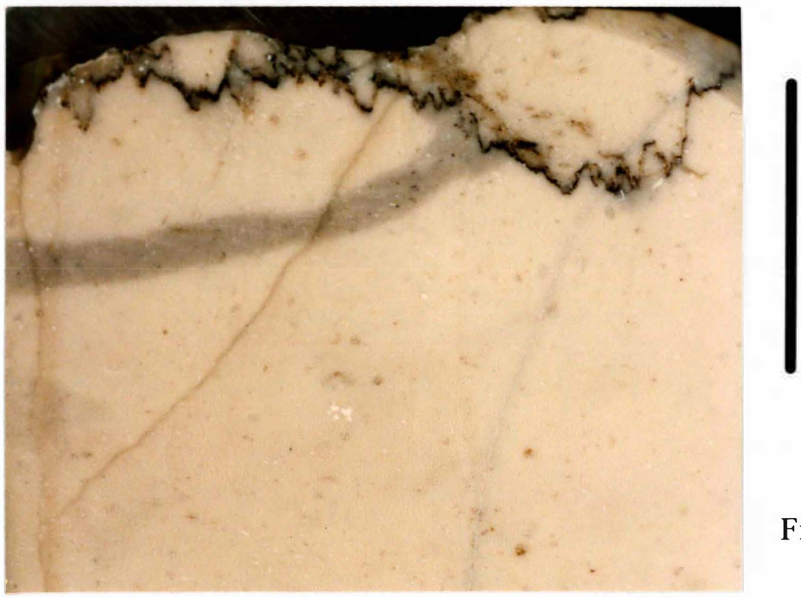

5 mm

Figure T-6.

Burrowed Massive Chalk Mudstone

Well/location: Tyra, Denmark

Formation: Tor

Depth:

M	mudstone
Ch	clean chalk
Gn	no visible grains
Bn	no visible bedding
Lpl	planar lamination
Dn	no visible deformation
Tm	medium density of trace fossils
Hh	hard
Chi	high degree of consolidation
Sl	low degree of stylolitization
Mp	pyrite minerals
Fhh	high degree of hairline fractures

Description:

The sample is taken next to sample 10.

The chalk is a hard, massive chalk mudstone with a high density of hairline fractures. Contrary to sample 10, the matrix is less affected by dissolution and recrystallisation. Foraminifera chambers are filled with spar crystals but the tests are not recrystallised to the same degree as in sample 10.
Well preserved coccoliths are seen in the matrix. Large euhedral calcite cement crystals ~5 μm are common in the pores.

Clay flakes (single flakes) are found uniformly distributed in the matrix.

Trace fossils:

Ichnogeneous: *Planolites* and *Zoophycos.*

Insoluble residue:

2.92 %
Quartz (12 %), clay and feldspar.

Petrophysical properties:

Porosity:	34.14 %
Permeability:	12.822 mD (fractured)
Density:	2.688 g/cm^3

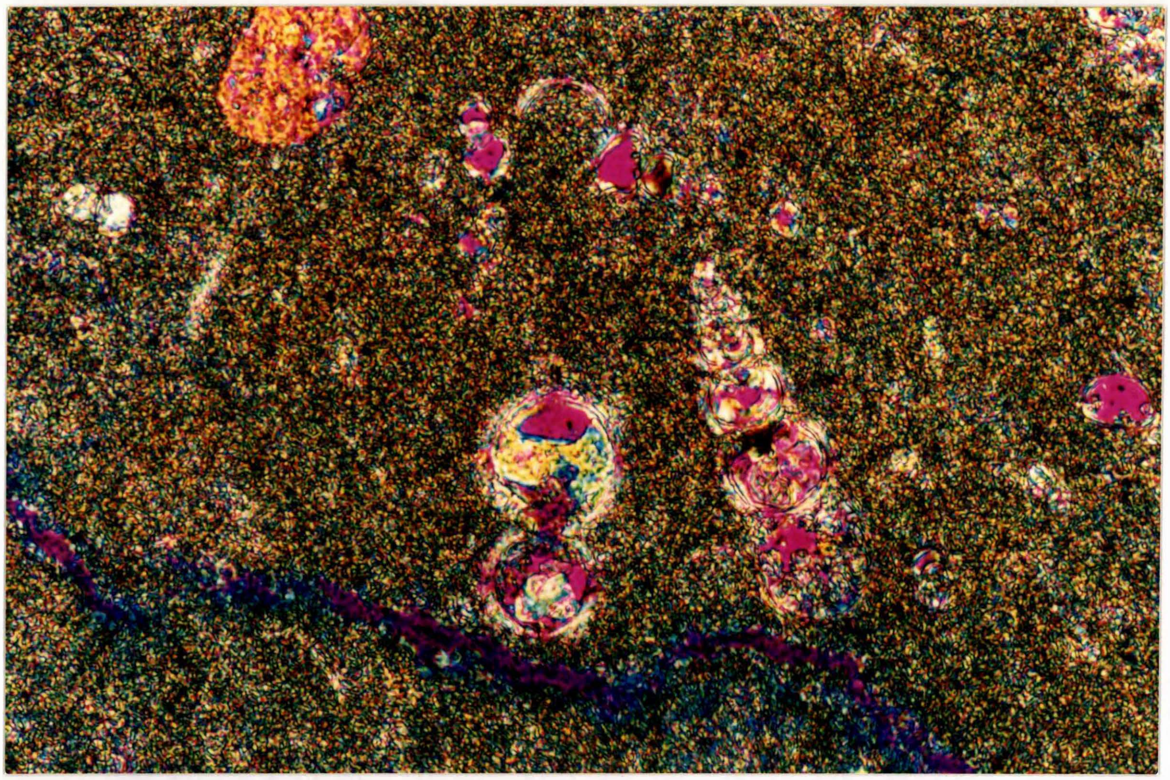

Figure T-7. Scale: 0.1 mm

Figure T-8.

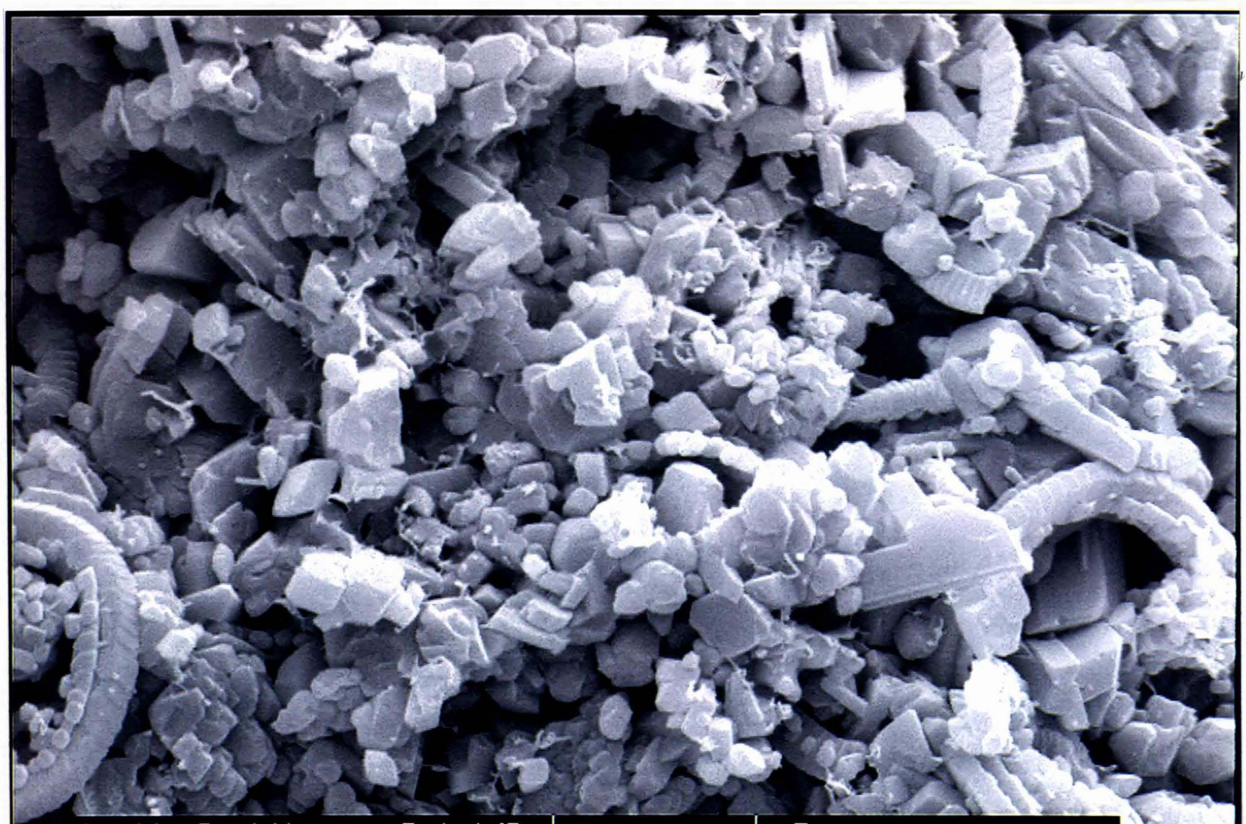

Tyra, sample 11A
Direct shear test

Pre-test description:

An attempt was made to cut the plug perpendicular to the bedding. However, the stylolites incline 10°. The pre-defined shear movements were performed along the dip direction of the dipping stylolite surface.

Stylolite amplitude 2 mm

Post-test description:

The developed shear plane was smooth with slickensides. Half of the plug end was broken at the upper part of the plug. Most probably the destruction was due to weakness along stylolite associated fractures.

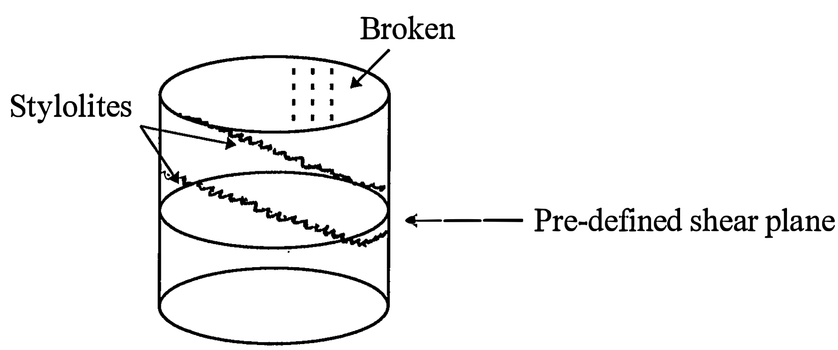

Tyra, sample 11B
Direct shear test

Pre-test description:

Sample 11B is a continuation of plug 11A. The stylolites incline 10°.

The stylolites cross-cut subvertical hairline fractures. Dissolution along the stylolites offsets the hairline fractures. Restoring of the hairline fractures into a straight line indicates a dissolution along the stylolite zone in the order of 5 mm.

The amplitudes of the stylolites are ~2 mm.

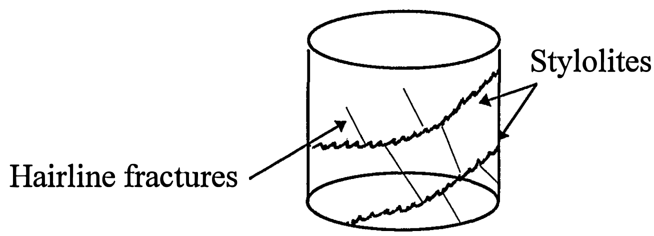

Post-test description:

The pre-defined shear movement was performed along the strike direction of the stylolite surface. (The test was stopped very early due to insufficient shearing capacity, and may not be comparable to sample 11A).

The shear fracture surface was controlled by the stylolite surface (approximately 1/2 of the fracture follow the stylolite surface). The surface is gently wavy with indication of slickensides.

Tyra, sample 13

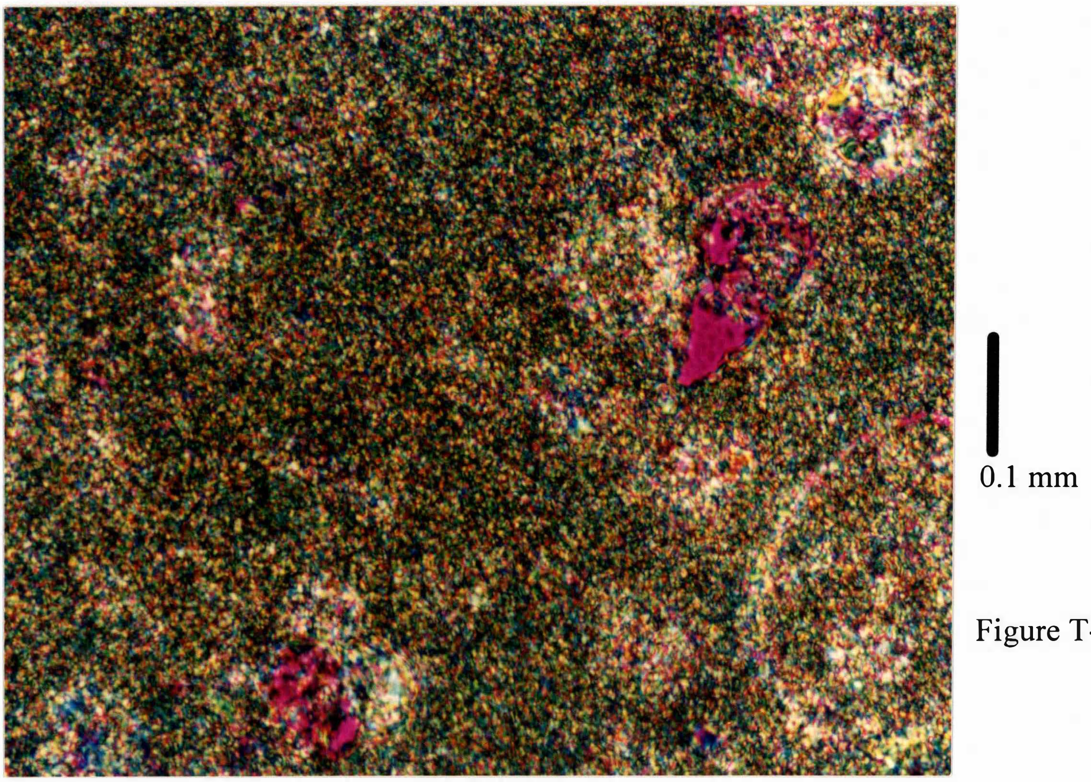

Figure T-9.

Burrowed Massive Chalk Mudstone

Well/location: Tyra, Denmark

Formation: Tor

Depth:

M	mudstone
Ch	clean chalk
Gn	no visible grains
Bn	no visible bedding
Lpl	planar lamination
Ds	shear deformation
Tl	low density of trace fossils
Hh	hard
Chi	high degree of consolidation
Sn	no visible stylolites
Mn	no visible secondary minerals
Fhh	high degree of hairline fractures

Description:

Hard, massive chalk mudstone with a high degree of conjugated shear fractures. Traces of *Chondrites* are seen. Brecciation is seen associated with the shear fractures. The width of the shear fractures are up to 5 mm. The shear fractures are filled with fine grained gray mud. The shear fractures branch off and exhibits healed fractures.

The chalk has a biomicritic mudstone texture, where the original grain components (primarily foraminifera) are recrystallised (to micrite) and appears as matrix (fig. T-9).

Within the original fossil chambers micrite prevail - microspar and spar crystals are less frequent.

The matrix has a relatively high content of well preserved coccolith with some overgrowth and is characterised by a high content of euhedral calcite crystals in the size range from 1 to > 5 μm reducing the overall intercrystalline porosity.

Trace fossils:

Ichnogeneous: *Thalassinoides, Planolites* and *Chondrites.*

Insoluble residue:

0.97 %
Quartz (22 %), clay and felspar.

Petrophysical properties:

Porosity:	34.65 %
Permeability:	4.130 mD
Density:	2.705 g/cm^3

Tyra, sample 13A
Multiple triaxial test

Pre-test description:

The plug appears as a homogeneous plug with a 1-2 cm wide zone of healed fractures (fig. T-10). A burrow cross-cut by the fractures is offset 3 mm.

Post-test description:

After test the lower part of the plug was broken. On the remaining part 2 sets of fractures are seen.

The main fracture is dipping 55°. The dip of the fracture does not show any relationship to the sedimentology. However, the fracture comprises a rough surface with a high relief caused by a heterogenetic breaking up when cross cut by hairline fractures. The surface appears with a wavelength of 1-1½ cm and an amplitude of 2 mm. The surface is weakly slickensided.

The second fracture set consists of vertical fractures partly associated with hairline fractures. The vertical fractures seem to be cut by the main fracture.

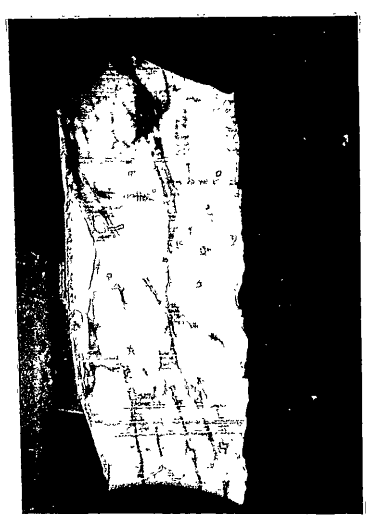

Figure T-10.

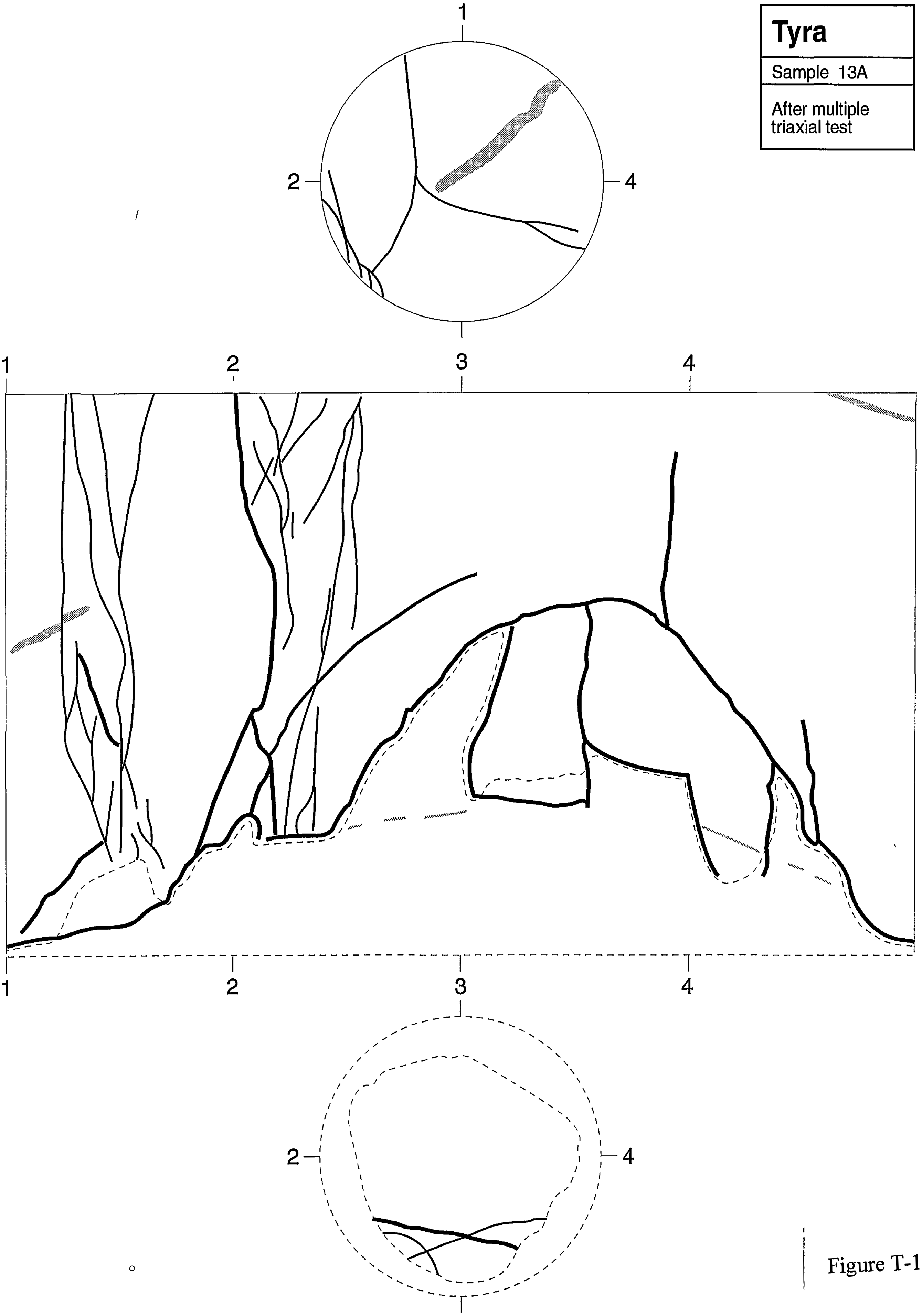

Figure T-11.

Tyra, sample 13B
Multiple triaxial test

Pre-test description:

The plug comprises bioturbated chalk with a high degree of vertical hairline fractures. Trace fossils (*Thalassinoides* and *Planolites*) are concentrated in the lower part of the plug. The hairline fractures offset the burrows up to 5 mm.

A conjugated set of subvertical open fractures is present (fig. T-12).

Post-test description:

After test some destruction is seen at the lower end.

3 sets of fractures are seen. The original open fractures (dip 80^{o}) are acting as the main fractures.

These fractures are parallel with the hairline fractures, but no connection between fractures and hairlines is seen. The surface plane is smooth and brittle .

A second fracture set is dipping 70-75^{o}. At the top of the plug the fracture zone might be affected by the directions of hairlines.

The third fracture set is sub-horizontal and is cutting perpendicular to the hairline fracture zone.

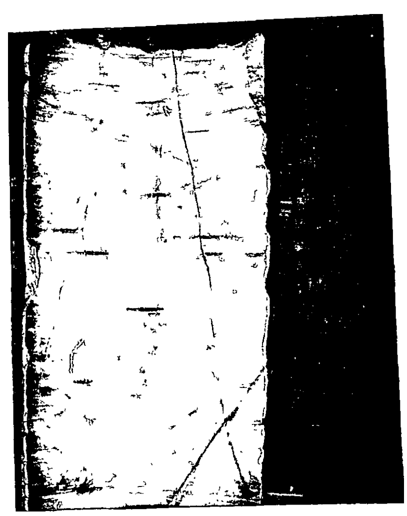

Figure T-12.

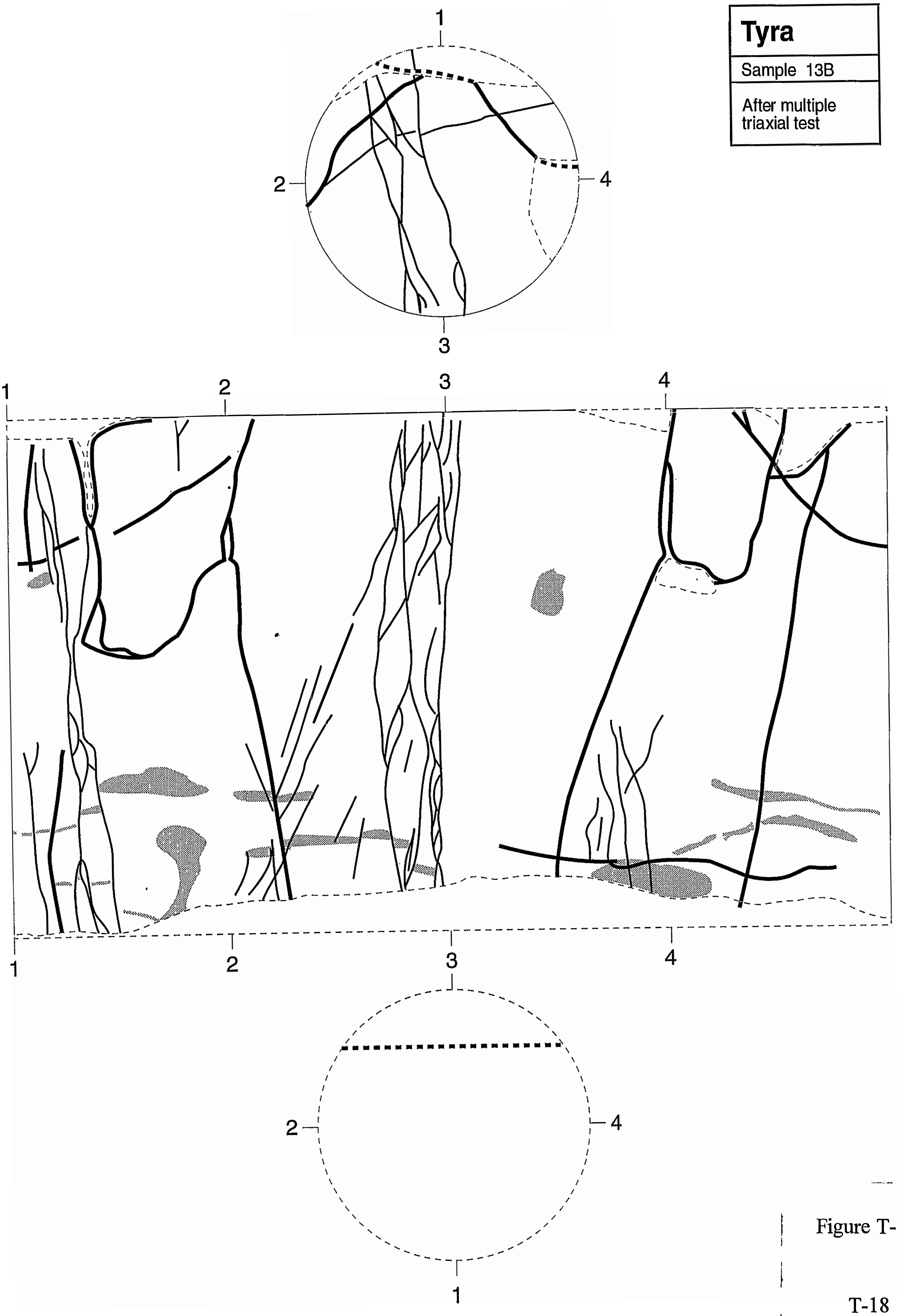
Tyra
Sample 13B
After multiple triaxial test
1
2
3
4
1
2
3
4
1
2
3
4
3
2
4
1

Figure T-13.

Tyra, sample 14

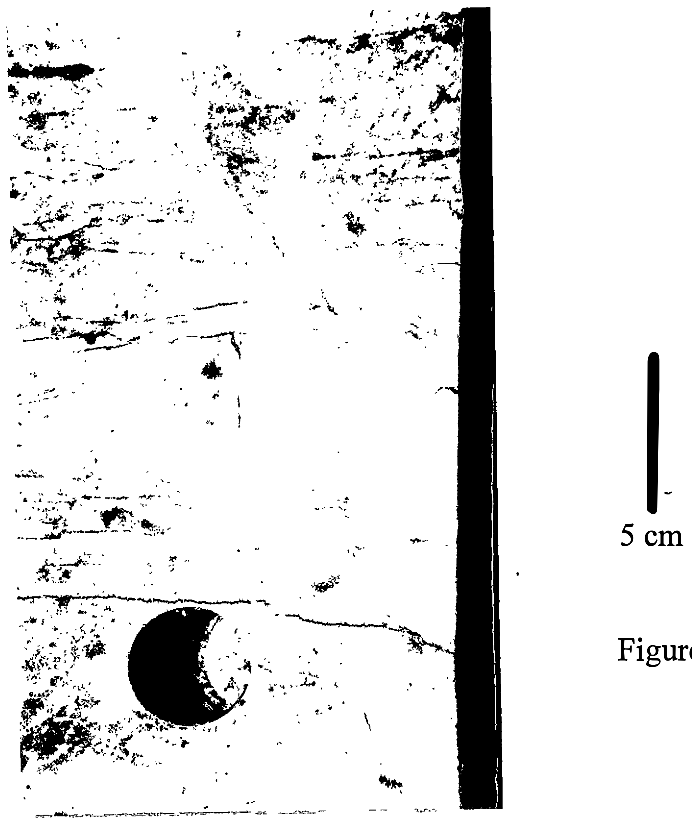

Figure T-14.

Burrowed Massive Chalk Mudstone

Well/location: Tyra, Denmark

Formation: Tor

Depth:

M	mudstone
Ch	clean chalk
Gn	no visible grains
Bn	no visible bedding
Lpl	planar lamination
Ds	shear deformation
Tl	low density of trace fossils
Hh	hard
Chi	high degree of consolidation
Sh	high degree of stylolites
Mn	no visible secondary minerals
Fhl	low degree of healed fractures

Description:

Hard, laminated chalk mudstone with conjugated shear fractures. The lamination is reinforced by a large number of sub-parallel stylolites (fig. T-14). Traces of *Chondrites* are seen.

The chalk has a biomicritic mudstone texture, where the predominant grain component is foraminifera. The foraminifera tests are often recrystallised.

Within the fossils chambers micrite prevail - microspar and spar crystals are less frequent.

The matrix comprises a relatively high content of well preserved coccolith with some overgrowth and is characterised by a high content of euhedral calcite crystals in the size range from 1 to > 5 μm reducing the overall intercrystalline porosity.

Trace fossils:

Ichnogeneous: *Thalassinoides*, *Zoophycos, Planolites* and *Chondrites.*

Insoluble residue:

no data

Petrophysical properties:

Porosity:	27.98 %
Permeability:	3.070 mD
Density:	2.704 g/cm^3

Tyra, sample 14
Multiple triaxial test

Pre-test description:

The plug is bioturbated, with dark, grey burrows. *Thalassinoides* burrows comprise several generations of fill.

The plug has a high density of stylolites with amplitudes less than 2 mm. The stylolite planes are becoming disorientated when crossing burrows.

2 sets of open fractures are seen (50^{o} and 80^{o}). There is no relation between the fractures and sedimentary structures.

Figure T-15. Scale: ▬▬ 1 cm

Post-test description:

After test the upper part of the sample was broken apart. Only the lower part was possible to describe (fig. T-16).

The remaining plug appears with a characteristic shape following the pre-existing fracture zones. No new fractures seem to have been induced during test. The fracture surface has been grated during transport and storage. Therefore no description has been made on the fracture surface.

Plug shape after test

Angles

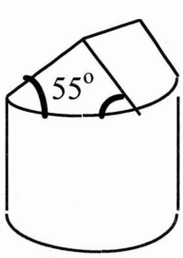

Tyra
Sample 14A
After multiple triaxial test

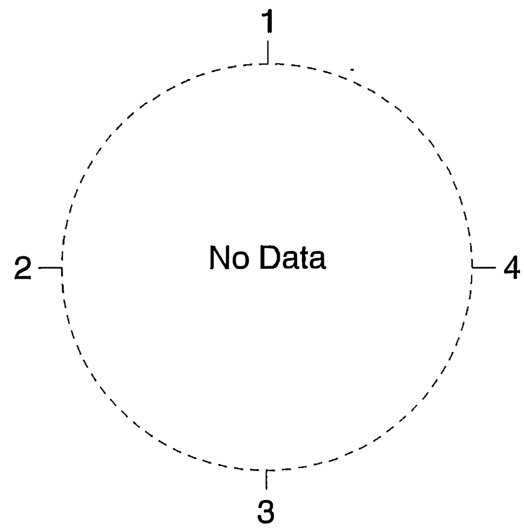

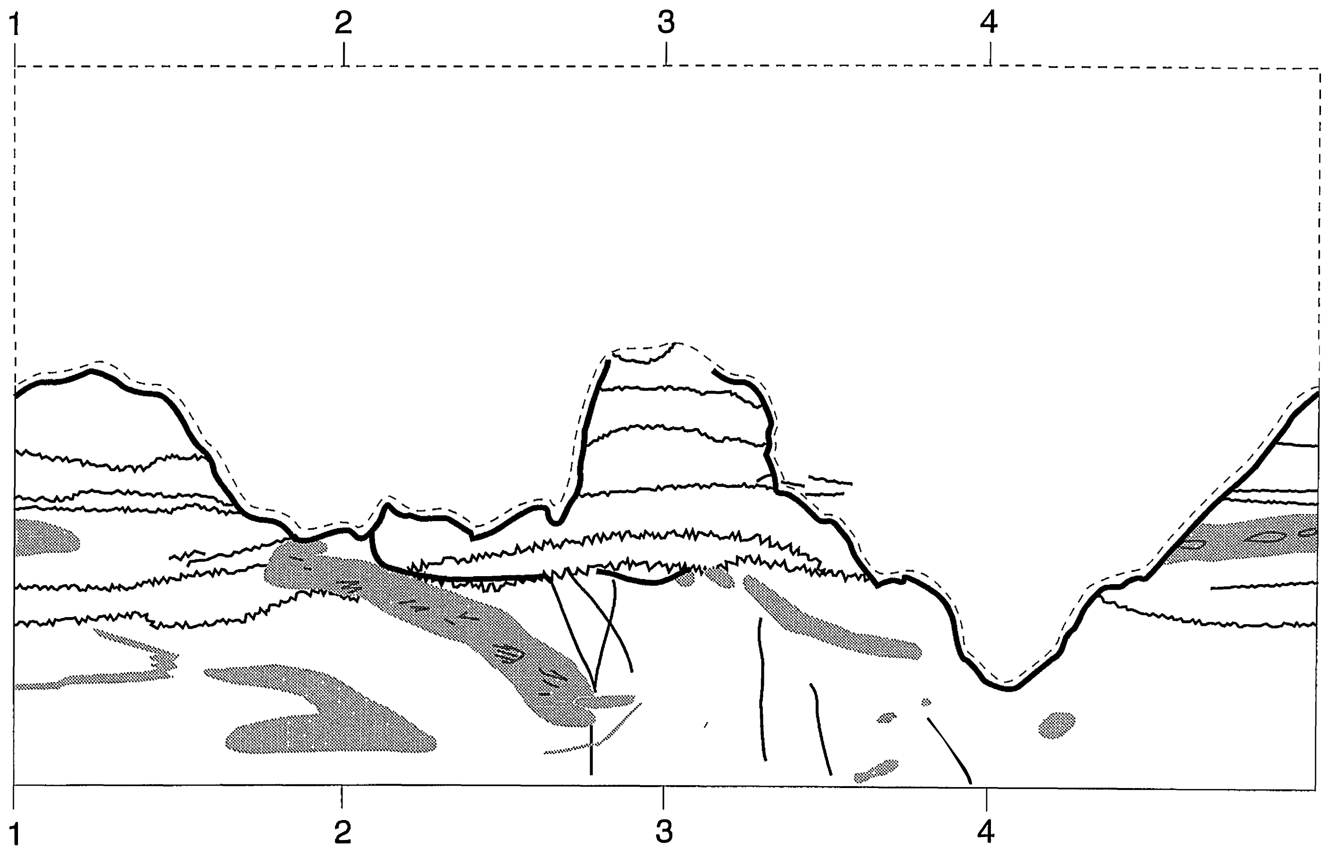

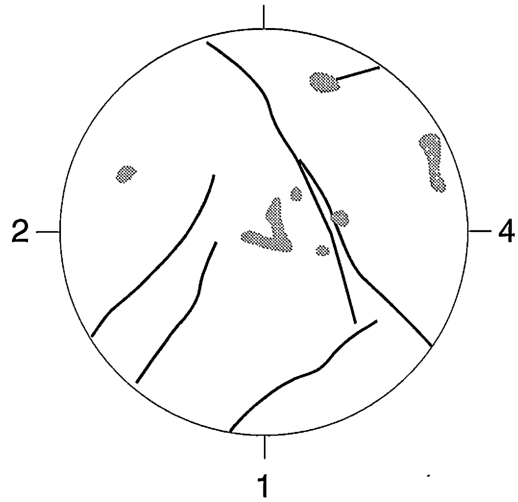

Figure T-16.

Tyra, sample 16

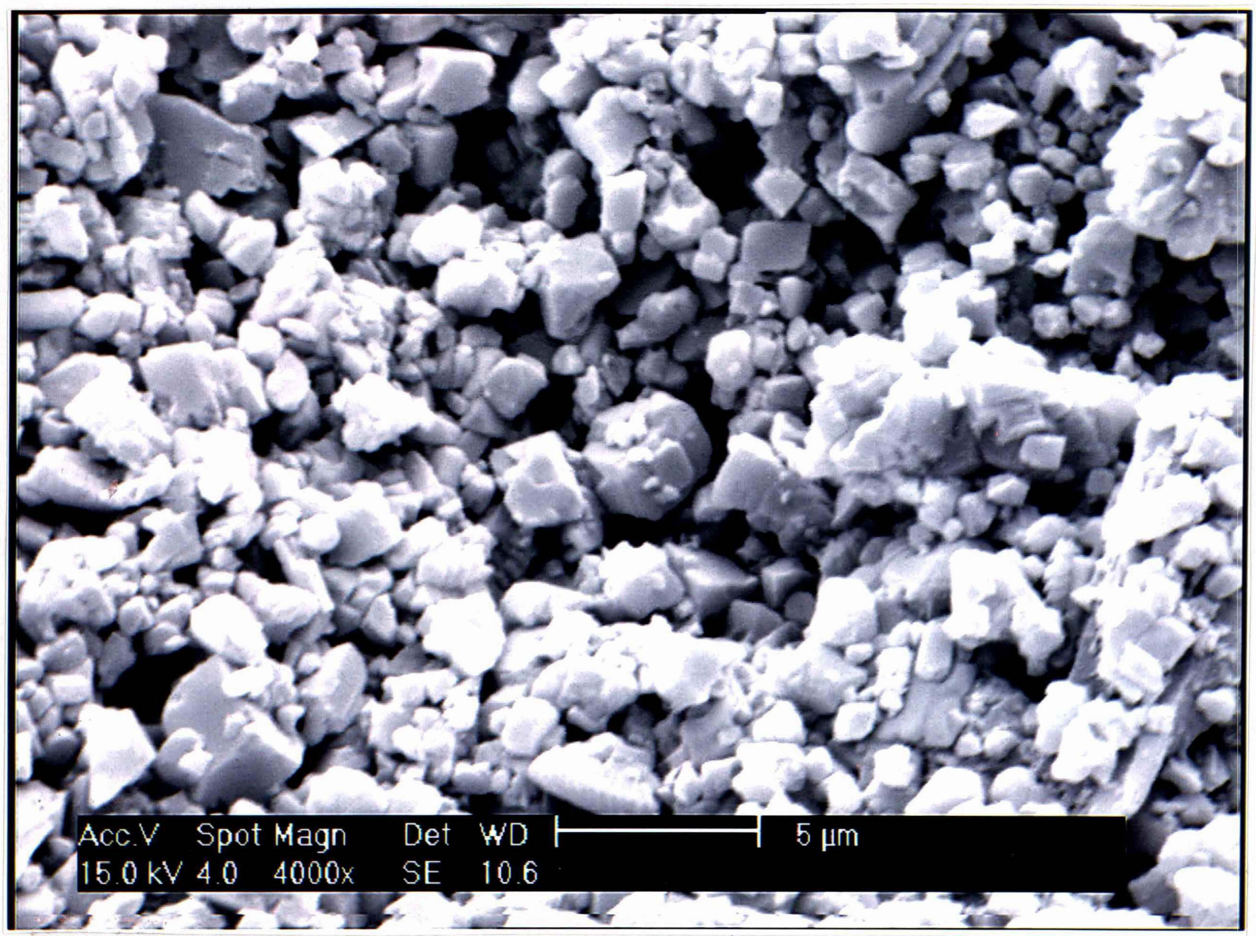

Figure T-17.

(Burrowed) Massive Chalk Mudstone

Well/location: Tyra, Denmark

Formation: Tor

Depth:

M	mudstone
Ch	clean chalk
Gn	no visible grains
Bn	no visible bedding
Ln	no lamination
Dn	no visible deformation
Tl	low density of trace fossils
Hh	hard
Chi	high degree of consolidation
Sn	no visible stylolites
Mn	no visible secondary minerals
Fhl	low degree of hairline fractures

Description:

Hard, massive chalk mudstone with hairline fractures. Traces of *Chondrites* is seen.

The chalk has a sparse biomicritic mudstone texture where the predominant grain component is foraminifera. The foraminifera tests are recrystallised (to micrite) and appears locally as relicts within the matrix.

The matrix is rather uniform and characterised by a high content of euhedral calcite cement crystals (1-3 μm) and a low content of well preserved coccoliths (fig. T-17). A characteristic cubic shape dominates the calcite crystals

Trace fossils:

Ichnogeneous: *Chondrites.*

Insoluble residue:

0.95 %
Quartz (19 %), clay and feldspar.

Petrophysical properties:

Porosity:	33.33 %
Permeability:	3.07 mD
Density:	2.699 g/cm^3

Tyra, sample 16A
Multiple triaxial test

Pre-test description:

The plug appears as a homogeneous massive chalk with fine conjugated (65-70^{o}) hairline fractures.

A few *Chondrites* burrows are seen.

Post-test description:

2 conjugated open fracture sets are seen after test (fig. T-18). Both sets dip 65-75^{o} similar to the direction of the hairline fractures, but the fractures do not follow the zone of weakness defined by hairline fractures.

The fracture planes are hummocky with offset. The fracture surface is rough-wavy and slickensided.

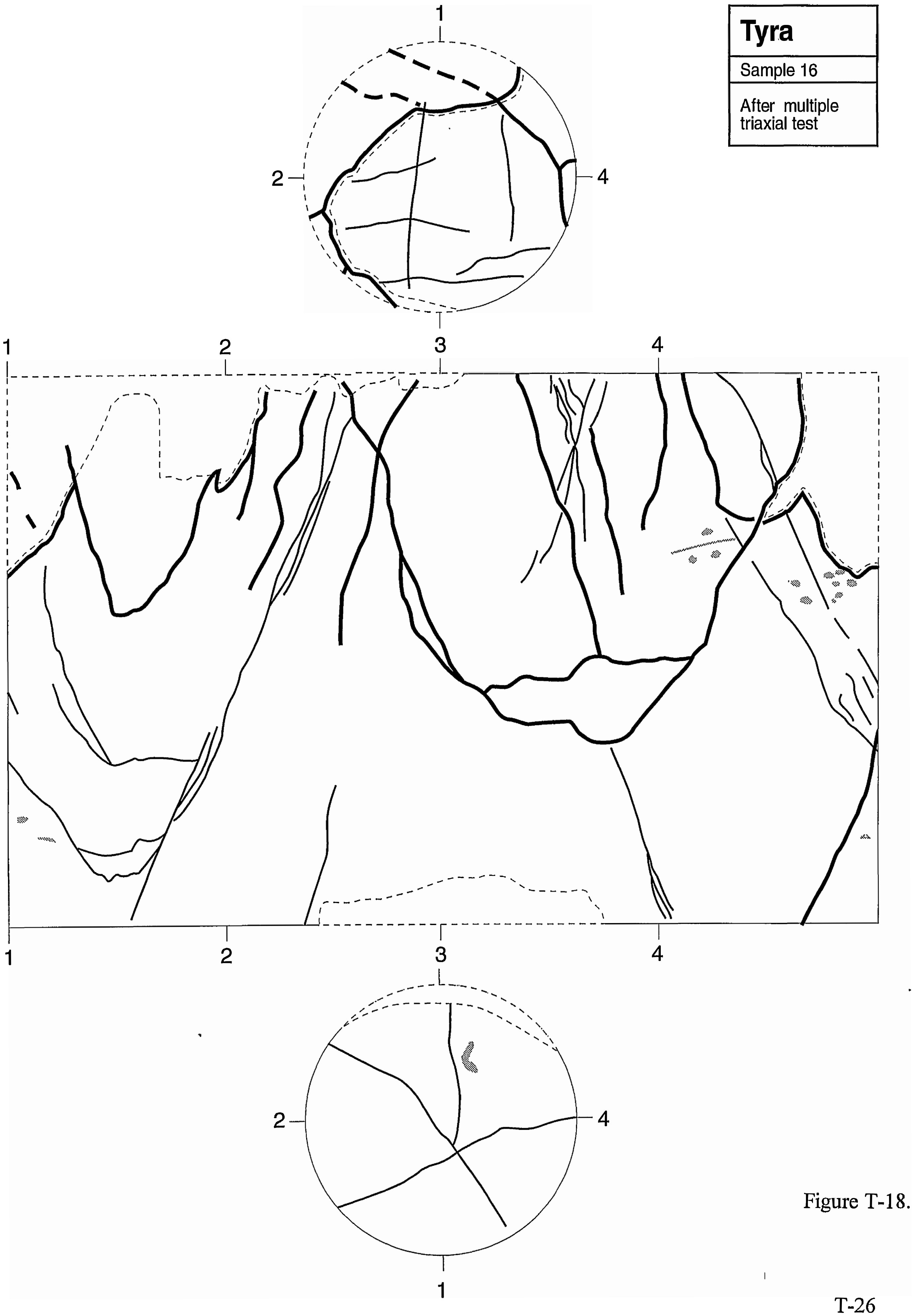

Figure T-18.

Tyra, sample 16B
Uniaxial strain compaction

Pre-test description:

No description.

Post-test description:

Poor sample, not described.

Tyra, sample 20

Figure T-19.

Burrowed Massive Chalk Mudstone

Well/location: Tyra, Denmark

Formation: Tor

Depth:

M	mudstone
Ch	clean chalk
Gsk	skeleton grains
Bn	no visible bedding
Lpl	planar lamination
Dn	no visible deformation
Tl	low density of trace fossils
Hh	hard
Chi	high degree of consolidation
Sh	high degree of stylolites
Mn	no visible secondary minerals
Fn	no visible fractures

Description:

Hard, bioturbated massive chalk wackestone with a high density of stylolites. Trace fossils as *Planolites* and *Chondrites* is common. The stylolites are partly controlled by *Planolites* burrows (fig. T-19).

The texture is a sparse micritic wackestone with a high content of shell fragments (echinoderms and foraminifera). Open foraminifera chambers are seen, but generally the chambers are filled with microspar crystals.

The matrix is highly cemented with crystals larger than 5 μm. A few well preserved coccoliths are seen.

Trace fossils:

Ichnogeneous: *Chondrites* and *Planolites.*

Insoluble residue:

1,65 %
Quartz (16 %), clay and feldspar.

Petrophysical properties:

Porosity:	30.71 %
Permeability:	- mD
Density:	2.698 g/cm^3

Tyra, sample 20A
Direct shear test

Pre-test description:

This plug is characterised by high amplitude (up to 5 mm) stylolites with associated fractures. Burrows (*Planolites*) are seen above and between the stylolites.

This plug was cut perpendicular to the stylolite surfaces. The pre-defined shear direction was parallel with the stylolite planes.

Post-test description:

Part of the predefined shear plane coincides with the stylolite surface and the movements within this plug may be controlled by the pre-existing features.

The shear plane is a low amplitude, wavy, slickensided surface.

Tyra, sample 20B
Direct shear test

Pre-test description:

This sample and sample 20A was taken next to each other. However, this time the plug was cut parallel to the stylolite surfaces. The pre-defined shear direction was perpendicular to the stylolite planes (parallel to the associated fractures).

Post-test description:

The induced shear plane can be described as a wavy surface with a medium relief (amplitude max. 2 mm). Wave length of the ripples is 1 cm.

VALHALL FIELD

Valhall Field

The Valhall Field is located within the chalk province of the North Sea Central Trough (fig. V-1).

The Valhall Field is a northwest-southeast asymmetrical anticline (fig. V-2) comprising Late Cretaceous to Early Tertiary chalk of the Hod and Tor formations of Turonian to Danian age. The development of the anticline is related to the tectonic activities of the Lindesnes ridge - in special the inversion phase in Late Cretaceous and Early Tertiary (Leonard & Munns, 1987).

The chalk reservoir is found at a depth of about 2400 - 2700 meters. The distribution of hydrocarbons is controlled partly by the structural development of the field, partly by the reservoir quality of the chalk related to stratigraphy (fig. V-3).

Sedimentary structures indicate that the chalk of the Tor formation and the Hod-4 unit is composed by a variety of allochthonous deposits, deposited from slumps, debris flows, mud flows, turbiditic currents and mud clouds. The rest of the Hod formation is interpreted as autochthonous pelagic chalk (Leonard & Munns, 1987).

The porosity in the Valhall Field reservoir unit range from > 50 % in the crestal parts of the Tor formation unit to < 20 % in the most deeply buried parts of the reservoir units. The very high porosities in the Tor formation are believed to be caused by initial high porosities being preserved by fluid overpressuring (Ali & Alcock, 1994, Andersen, 1995).

The reservoir units of the Valhall Field are apparent from figure V-4 where the subdivision of the chalk section is illustrated on the log from the 2/8A-8 (Ali & Alcock, 1994). The chalk section is subdivided into two units belonging to the Tor formation and 6 units belonging to the Hod formation. A dense zone is separating the Hod-1 unit and the Tor-2 unit.

Amoco Norway has made two sets of data available for this study. One set is samples from the Tor 1 formation. The second set comprises samples from the Hod 3 formation.

No core description or core photos have been available for this study. Only core pieces were sent to the DGI.

Both wells have been drilled as horizontal wells, which was taken into consideration when orientating the samples prior to plugging for geotechnical tests.

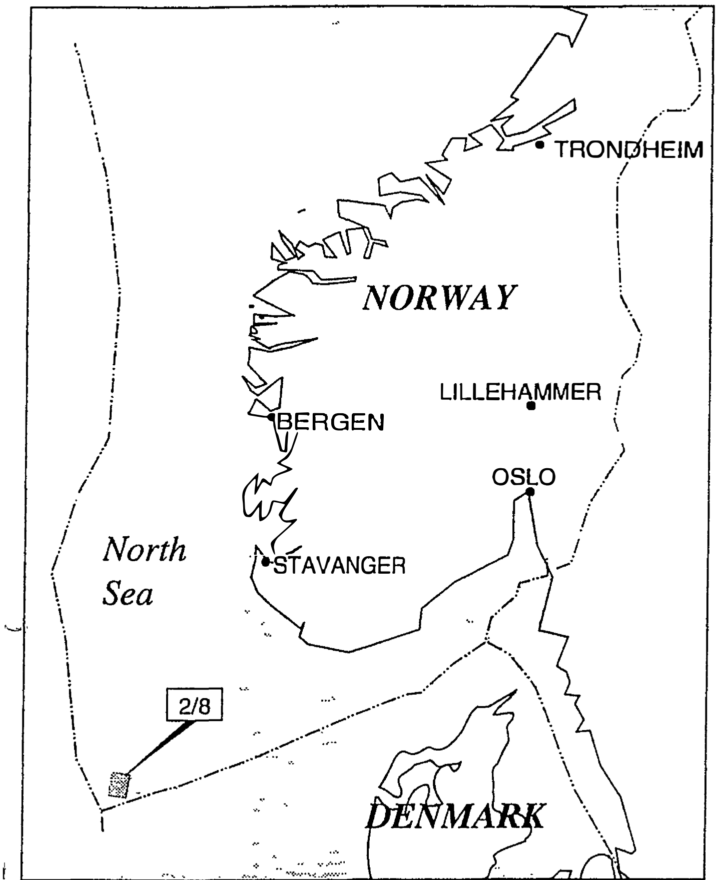

Figure V-1.

Valhall Field Location Map (Block 2/8)

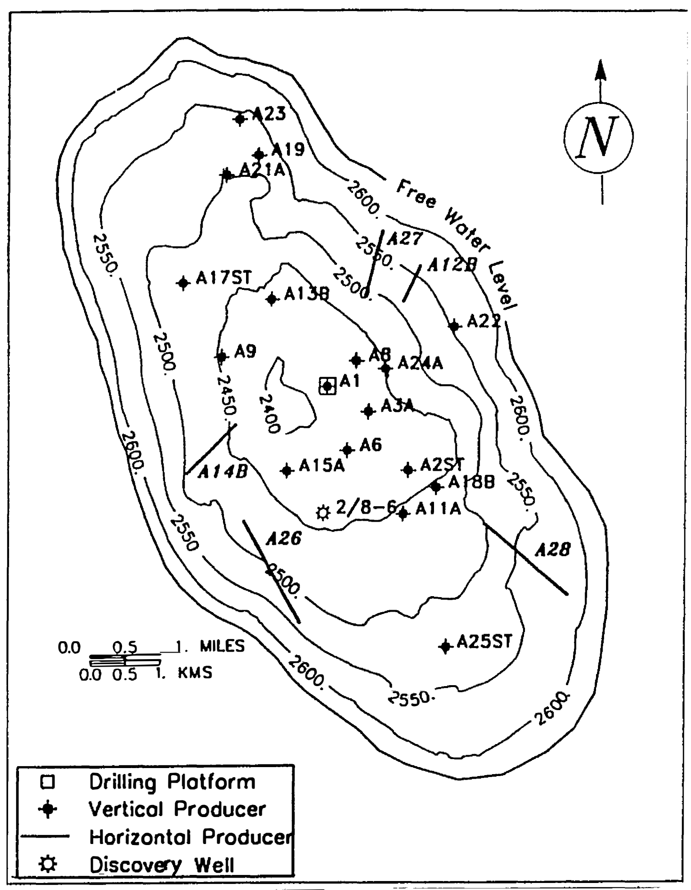

Figure V-2.

Valhall Field Depth to Top of Chalk (meter subsea)

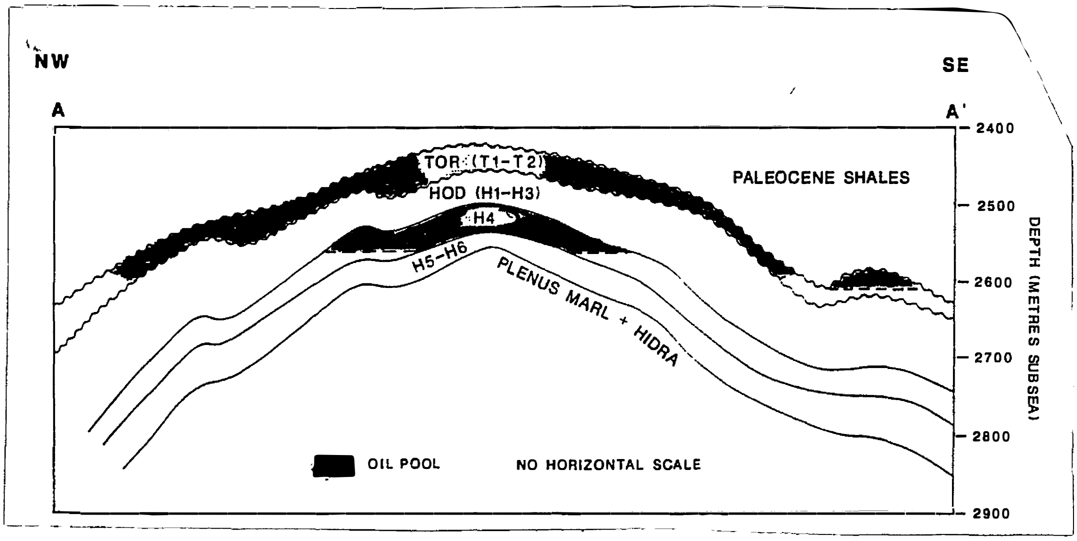

Figure V-3. Schematic cross-section showing major reservoir zones with 80% S_w.

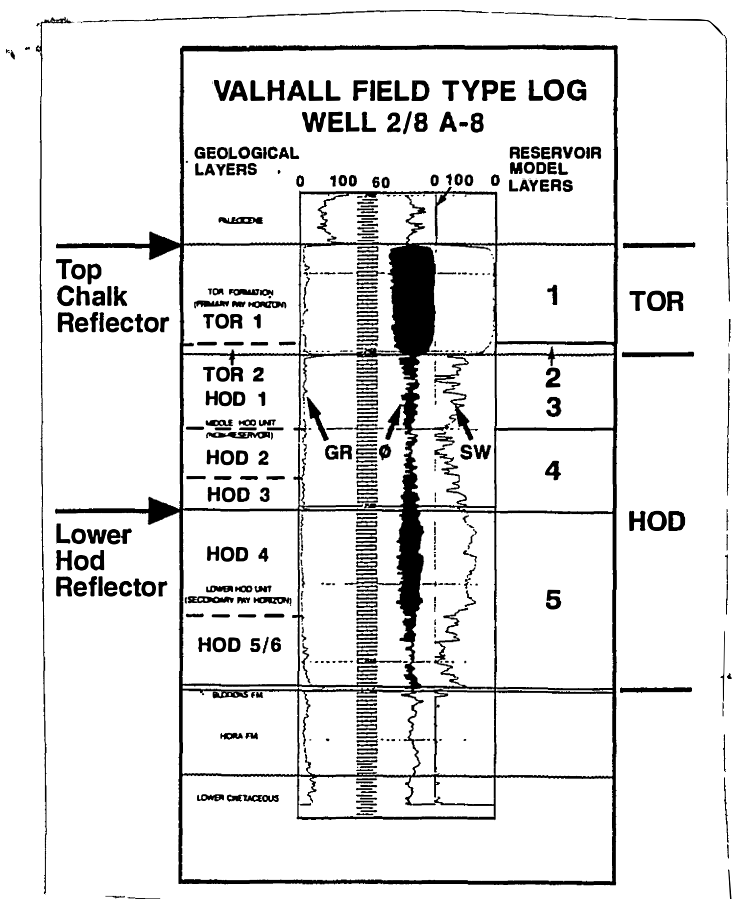

Figure V-4. Reservoir unit in the Valhall Field.

Tor Formation:

The examined samples from the Tor formation in the Valhall Field comprise the same chalk type: predominantly massive chalk mudstone with a dense network of hairline and shear fractures. A rather complex multidirectional fracture pattern characterises the Tor Formation samples. A few low amplitude stylolites/pressure dissolution seams are present.

Both the intensive hairline fracturing and the shear fracturing are indicative of reworking. High density of hairline fractures (related to water escape) is indicative of rapid deposited mud flows. Shear fracture zones locally comprising conglomeratic chalk indicate slump.

Hod Formation:

The Campanian to Turonian Valhall Hod samples comprise a large content of planktonic foraminifera indicative of predominantly autochthonous pelagic origin. The samples have a high content of clay (kaolinite) and quartz, indicative of a high detrital supply from a nearby source area. A high density in bioturbation indicates that oxic conditions have prevailed.

Pressure dissolution seams grading into low amplitude stylolites are seen. The consolidation of the Hod samples is primarily due to compaction and only secondary related to calcite cementation. The degree of cementation is most likely a result of the content of insoluble residue. From foraminifera chambers with a high clay content there is evidences of very little cementation and in general the crystals are less than 5 μm.

Analyses carried out on Valhall core samples

Sample	Porosity	Permea-bility	Thin section	Capillary pressure	Insoluble residue	SEM	Geotechnical test type
21	**X**	**AIR**	**X**	**X**	**X**	**X**	**Multiple triaxial test**
22	**X**	**-**	**X**		**X**		**Direct shear test**
23			**X**		**X**		**Multiple triaxial test**
24	**X**		**X**		**X**		**Direct shear test**
25	**X**	**-**	**X**		**X**		**Uniaxial strain compaction**
26	**X**	**-**	**X**		**X**		**Direct shear test**
31	**X**	**-**	**X**		**X**		**Multiple triaxial test**
32	**X**	**AIR**	**X**		**X**		**Uniaxial strain compaction**
33	**X**	**AIR**	**X**		**X**		**Direct shear test**
34	**X**	**AIR**	**X**	**X**	**X**		**Direct shear test**

Valhall Field, Tor Formation

1 cm

Figure V-5.

Massive Chalk Mudstone

Well/location: Valhall, Norway

Formation: Tor

Depth:

M	mudstone
Ch	clean chalk
Gch	chalk clasts
Btn	thin bedded
Lpl	planar lamination
Ds	shear deformation
Tn/Tl	no /low density of trace fossils
Hs	soft
Cm	medium consolidation
Sn/Sl	no visible/low degree of stylolites
Mn	no visible secondary minerals
Fhh	high density of hairline fractures

Description (for all Valhall Tor samples):

The Valhall Tor samples are soft, (burrowed) massive chalk mudstone comprising a large number of multidirectional hairline fractures. Shear fracture zones are common.

The chalk has a sparse biomicritic wackestone texture with planktonic foraminifera as the dominant grain component. Fragments of foraminifera tests filled with matrix are common.

The matrix is dominated by both a large amount of well preserved and disintegrated coccoliths. There is very little indication of overgrowth.

The chalk is highly porous, predominantly intercrystalline. The pores are dominated by angular euhedral cubic to elongated shaped calcite cement crystals. The size of the calcite cement crystals is in the range < 1 μm to 5 μm of which the crystals < 1 μm are the most common.

The clay content is low and rarely seen in the SEM.

Trace fossils:

Ichnogeneous: *Chondrites* and indistinct *Planolites.*

Insoluble residue:

1.91 - 2,16 %
Quartz (13-19 %) and clay (traces of feldspar).

Petrophysical properties:

Porosity:	42.77 - 44.41 %
Permeability (air):	6.894 mD
Density:	2.687 - 2.705 g/cm^3

Valhall, sample 21
Multiple triaxial test

Pre-test description:

The sample is a soft and weakly consolidated, (burrowed) massive chalk mudstone with horizontal laminae. The plug appears with high density of converging hairline fractures cutting through burrows without offset.

Porosity:	44.41 %
Permeability:	6.89 mD
Density:	2.705 g/cm^3
Insoluble residue:	2.16 % (Quartz (19%), clay and traces of feldspar)

The sample is plugged perpendicular to the bedding. One set sub-horizontal fractures comprising 3 open fractures were present before test (fig. V-6a). The uppermost fracture has the widest aperture. The fractures are parallel to the *Planolites* burrows and cross cut the hairline fractures. The dip of the fractures is 15^o for the upper and lower fractures, and 5^o for the middle fracture.

Post-test description:

After test small indistinct subvertical fractures have been developed in addition to the horizontal fractures (fig. V-6b). The vertical fractures follow the hairline directions (fig. V-7).

The fracture planes are smooth. However, the middle fracture exhibits an offset of 2-5 mm. The surfaces are smooth with chalk paste cover.

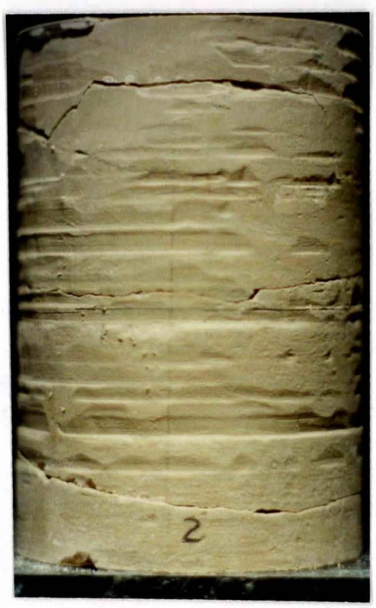

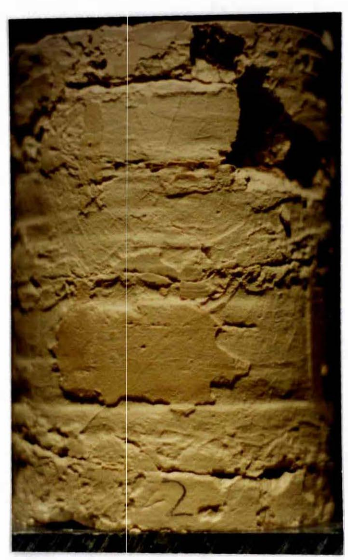

Figure V-6

a) before test b) after test

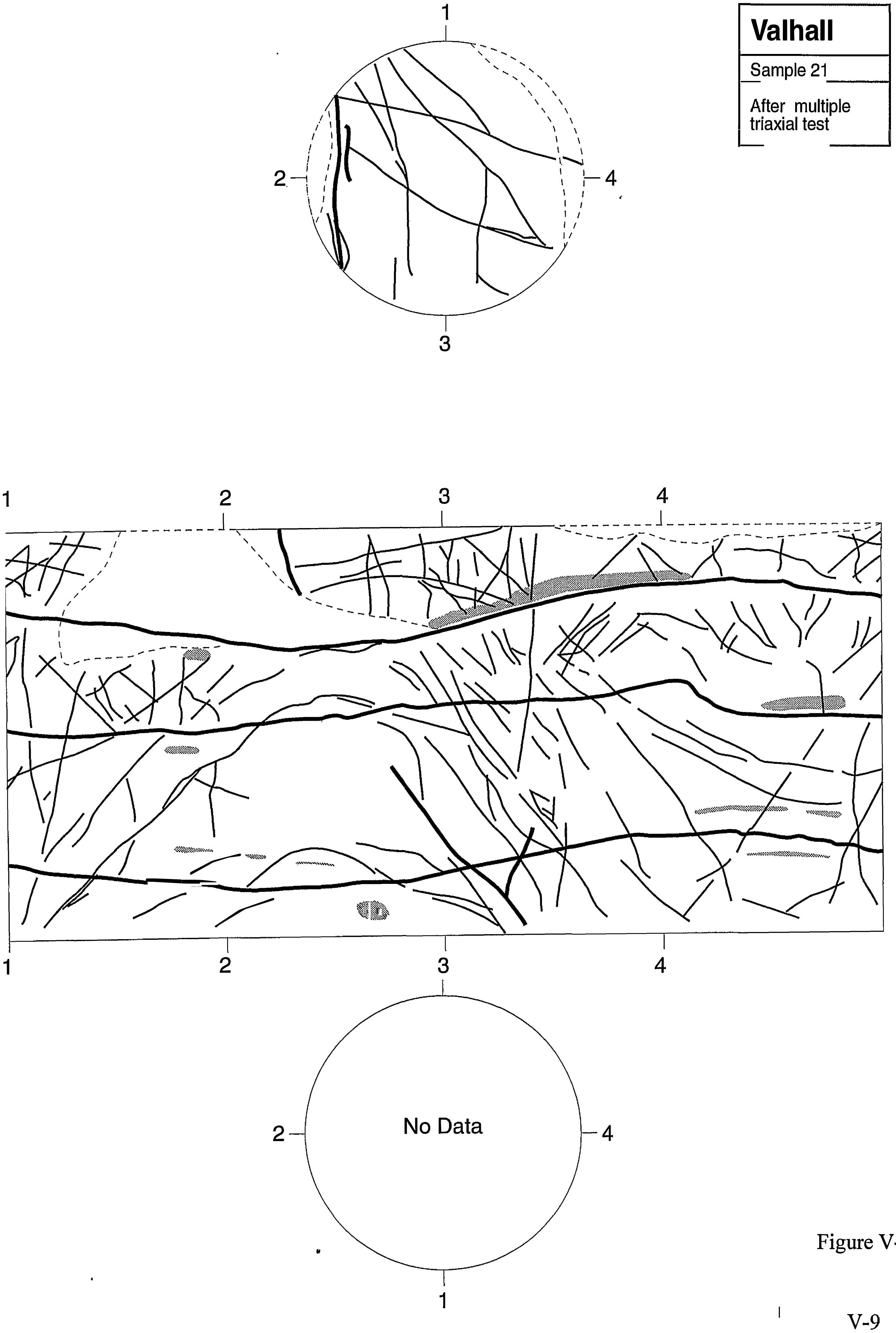
Valhall
Sample 21
After multiple triaxial test
1
2
3
4
1
2
3
4
1
2
3
4
No Data
2
4
1

Figure V-7

Valhall, sample 22
Direct shear test

Pre-test description:

Weakly laminated chalk mudstone, oil stained. Lamination is caused by/amplified by pressure dissolution. The sample is highly affected by converging hairline fractures, but no offset of the lamination is seen.

Conjugated shear zones (with a density of 0.5/cm) cut through the sample and give rise to offset of the laminae in the order of 2-3 mm.

One 5 mm thick shear fracture with deformed chalk clasts cut through the core sample.

Burrows of *Planolites* and *Chondrites* are seen.

Porosity:	44.42 %
Permeability (air):	- mD
Density:	2.703 g/cm^3
Insoluble residue:	1.91 % (Quartz (13 %) and clay (traces of feldspar))

The test plug was taken around the shear zone and it was attempted to cut parallel with the shear zone, but the sample was cut in a way that the shear zone appears with a dip of 45^o in the plug. The predefined shear direction was carried out along the dip direction and cross cut the shear zone.

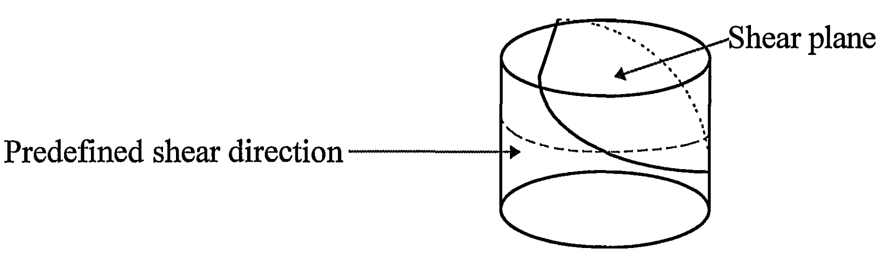

Post-test description:

No sample material.

Valhall, sample 23
Multiple triaxial test

Pre-test description:

Weakly laminated chalk mudstone, oil stained. Lamination is caused by/amplified by pressure dissolution. The sample is highly affected by converging hairline fractures, but no offset of the lamination is seen. Burrows of *Chondrites* are seen.

Conjugated shear zones (with a density of 0.5/cm) cut through the sample and give rise to offset of the laminae in the order of 2-3 mm.

Porosity:	- %
Permeability (air):	- mD
Density:	- g/cm^3
Insoluble residue:	2.97 % (Quartz (18 %) and clay) (traces of feldspar))

Prior to test 2 sets of open fractures are seen (subhorizontal, 15-20^o and subvertical, 60^o) in addition to the conjugated sets of hairline fractures (ca. 60^o)(Fig. V-8).

Missing parts of the plug was fill with gypsum which limited the possibility for description of the test induced fracturing.

↑ Figure V-8.
↓ Figure V-9.

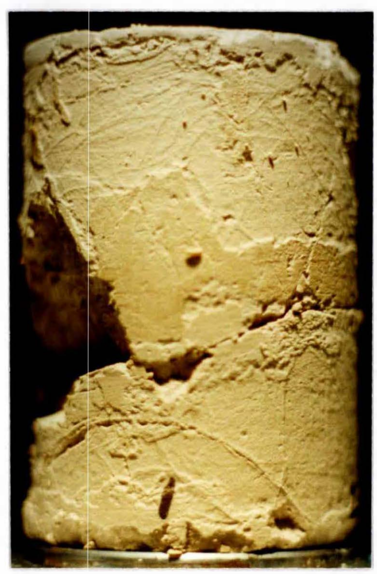

Post-test description:

After test two new open fractures were developed in the top of the sample (fig. V-9).
The fractures were subhorizontal and steep dipping. A sub-vertical fracture was developed between the new in the top and the original fracture in the middle (fig. V-10).

The middle original fracture is planar - weak undulating and the surface is smooth to gentle rough. No slickensides are developed

The fractures cut through the hairline fractures but without offset.

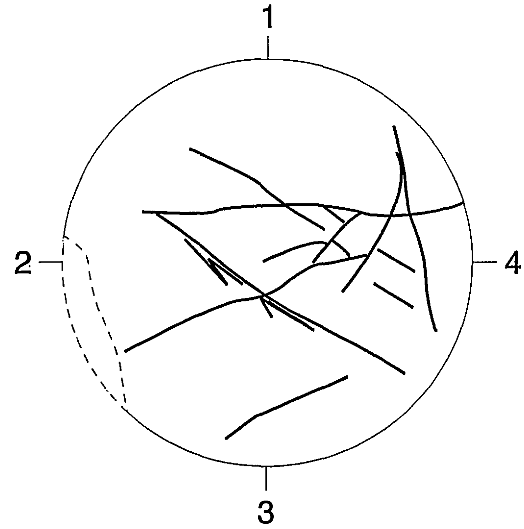

Valhall
Sample 23
After multiple triaxial test

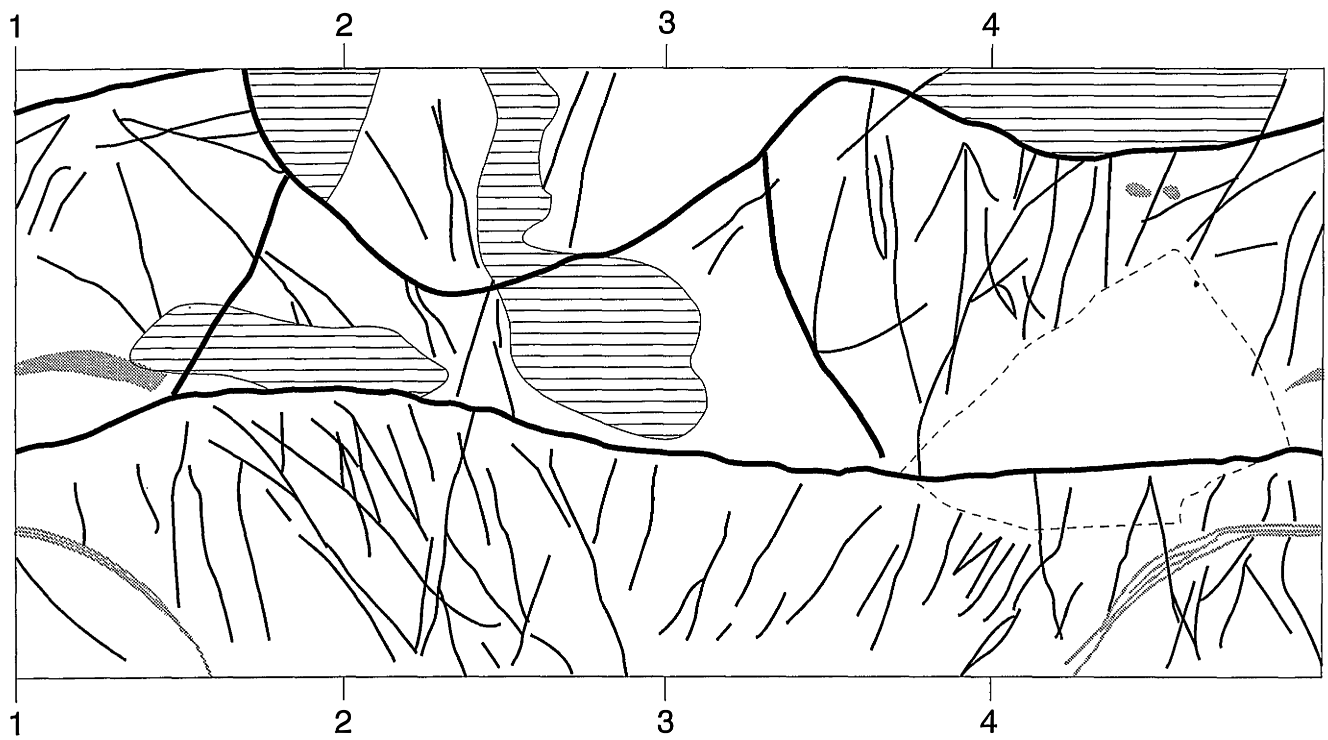

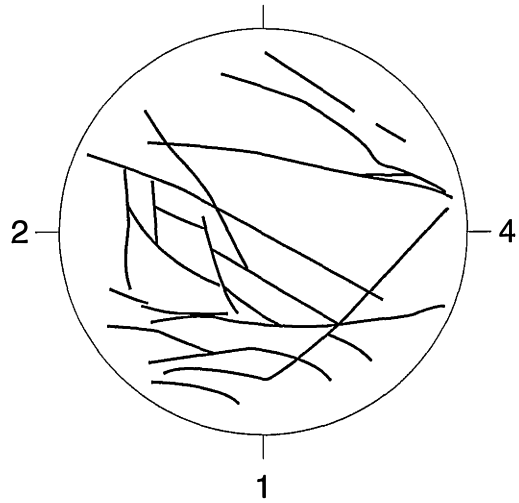

Figure V-10

Valhall, sample 24
Direct shear test

Pre-test description:

Soft, weakly laminated chalk mudstone, oil stained. Lamination is caused by/amplified by pressure dissolution. The dissolution seams grades into thin low amplitude stylolites. A dendroid fan of dissolution seams is found in connection with shear fractures. Brecciated pebbles associated with conjugated shear fractures are seen. Original lamination is offset up to 1 cm by the shear fractures. Locally open fractures with an aperture of 2 mm are present.

The sample comprises a high density of converging hairline fractures affecting the direction of the shear fractures.

Burrows are not seen in the sample.

Porosity:	42.79 %
Permeability (air):	- mD
Density:	2.699 g/cm^3
Insoluble residue:	2.59 % (Quartz (10 %) and clay)

The test plug was parallel with an open fracture.

Post-test description:

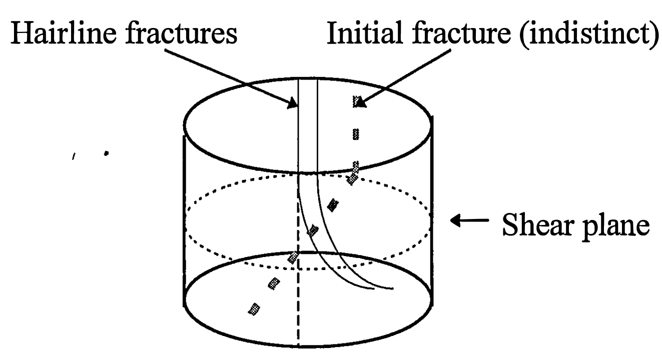

After test the plug still acted as one plug with no ruptures. However, along the shear plane a greyish colour is seen when moisturising the sample. The change in colour along the shear zone is interpreted as a result of recrystallisation/reorganisation of the matrix particles.

Valhall, sample 25
Uniaxial strain compaction

Pre-test description:

Soft, weakly laminated chalk mudstone with conjugated shear fractures and high intensity of converging hairline fractures. The sample is highly affected by hairline fractures, but no offset of the lamination is seen. Lamination is caused by/amplified by pressure dissolution.

Burrows are not seen in the sample.

Porosity:	44.45	%
Permeability (air):	-	mD
Density:	2.706	g/cm^3
Insoluble residue:	2.21	% (Quartz (16 %) and clay (feldspar))

Post-test description:

The sample was impossible to describe after test but appeared as an undisturbed sample with initial fracturing.

Valhall Tor, sample 26
Direct shear test

Pre-test description:

Soft, massive chalk mudstone, oil stained. The sample is highly affected by converging hairline fractures.

One open fracture (core handling?) cross-cut the core piece.

Pressure dissolution may give some indication of a lamination.

The plug is cut perpendicular to the “lamination”.

Porosity:	42.77	%
Permeability (air):	-	mD
Density:	2.706	g/cm^3
Insoluble residue:	2.28	% (Quartz (31 %) and clay).

Post-test description:

Not available.

Valhall Hod, sample 31

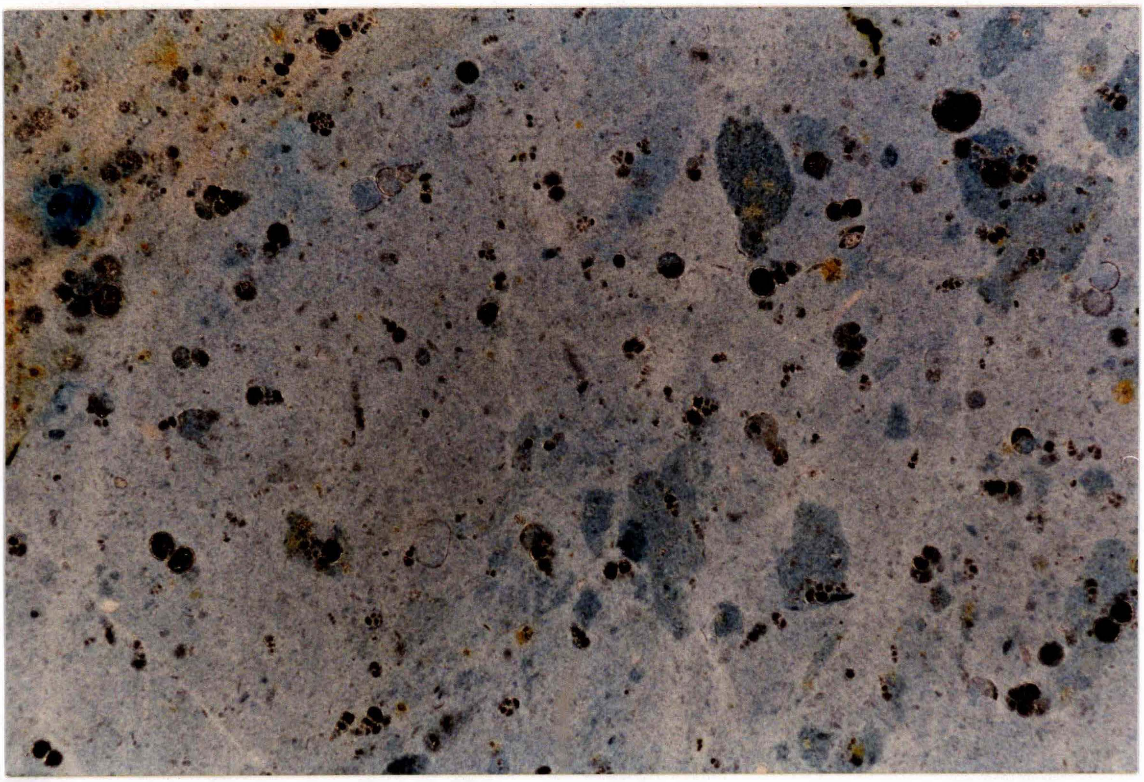

Figure V-11. Scale: 1 mm

Burrowed Laminated Chalk Mudstone

Well/location: Valhall, Norway

Formation: Hod

Depth:

M	mudstone
Arl	low argillaceous
Gn	no visible chalk grain
Bn	no bedding
Lpl	planar lamination
Dn	no deformation
Th	high density of trace fossils
Hm	medium hard
Cm	medium consolidation
Sn	no visible stylolites
Mn	no visible secondary minerals
Fn	no visible fractures (original rock)

Description:

Medium hard, highly bioturbated argillaceous mudstone with weak lamination.

The chalk has a sparse biomicritic wackestone texture with foraminifera as the most dominant grain component (fig. V-11). The chambers are open or filled with micrite.

The chalk is dominated by well preserved coccoliths interceded with clay flakes (fig. V-12). An open porous framework formed by "grainbridging of coccoliths" is characteristic for this sample. The clay content is relatively high and there seems to be a relationship between clay content and the cementation. Overgrowth is rare and relatively few euhedral calcite cement crystals are present.

Trace fossils:

Ichnogeneous: *Planolites*, *Zoophycos, Chondrites* and *Thalassinoides.*

Insoluble residue:

16.07 %
Quartz (40 %), kaolinite and feldspar.

Petrophysical properties:

Porosity:	39.83 %
Permeability (air):	- mD
Density:	2.702 g/cm^3

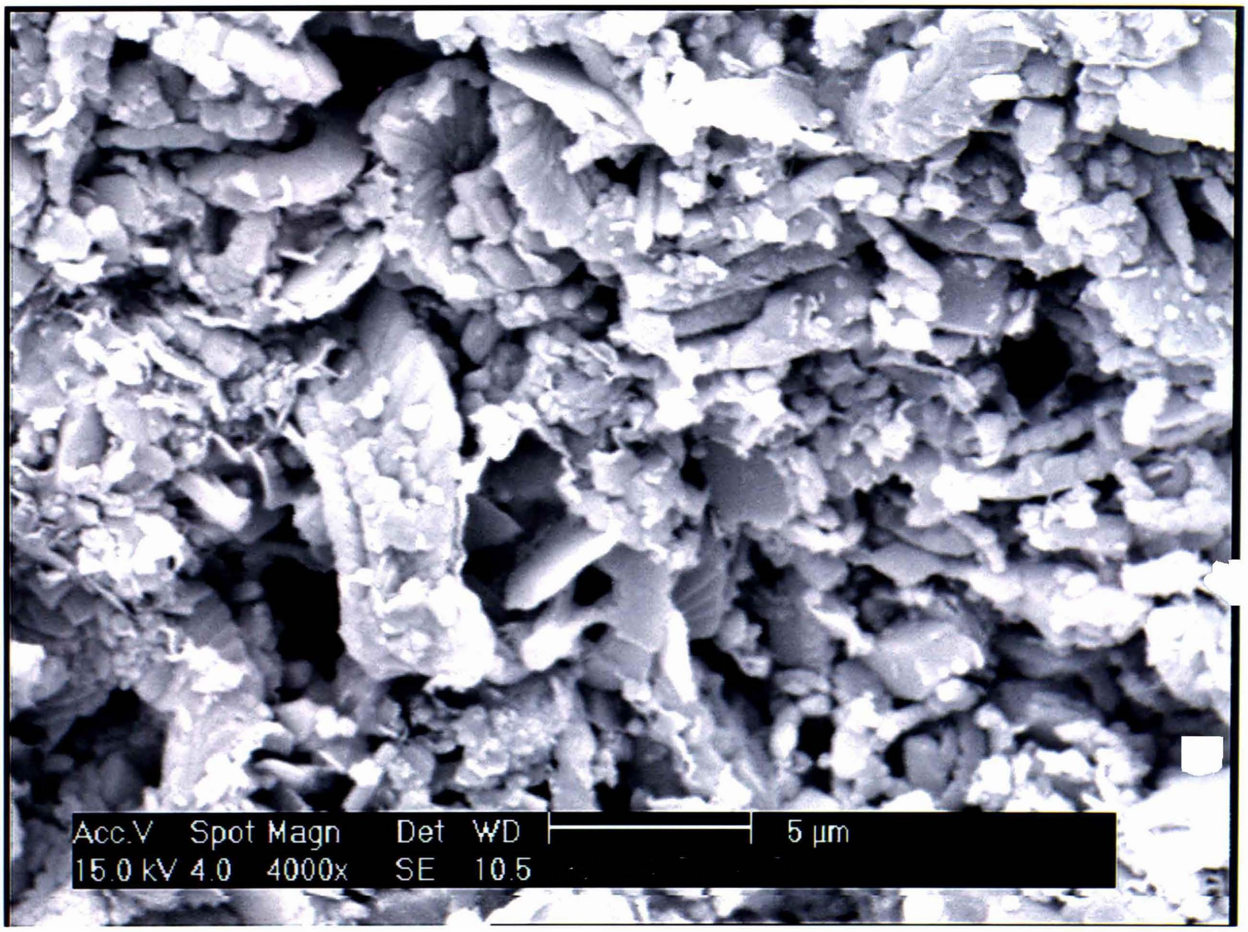

Figure V-12. SEM image of Valhall Hod Chalk.

Valhall Hod, sample 31
Multiple triaxial test

Pre-test description:

The plug appears as a relatively homogeneous chalk with burrows of *Thalassinoides.*

No lamination is observed but the plug axis is expected to be perpendicular to bedding.

Gypsum fills at the surface and ends make the plug difficult to describe. However, the plug is cut through by 2 sets of open fractures (sub-horizontal (10^{o}) and sub-vertical (70^{o}); see fig. V-13a).

Post-test description:

After test the plug is multifractured with predominant subvertical fractures (60^{o}) conjugated to the original fractures (fig. V-13b and V-14).

Two sub-horizontal fractures dipping 15^{o} are crosscut by conjugated sub-vertical fractures

The fracture surfaces are planar with a smooth-brittle surface with slickensides and mineralised surface (clay cover?).

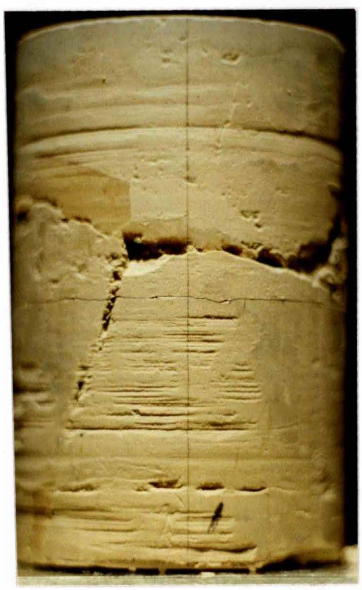

Figure V-13
a) Before test b) After test

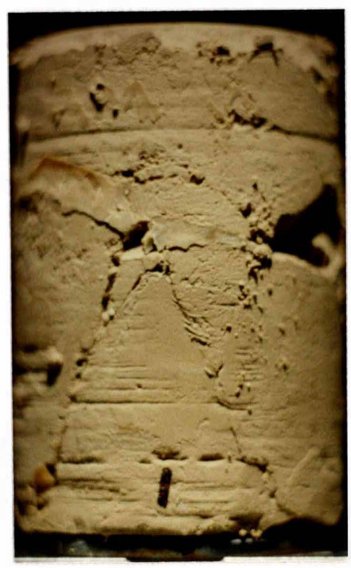

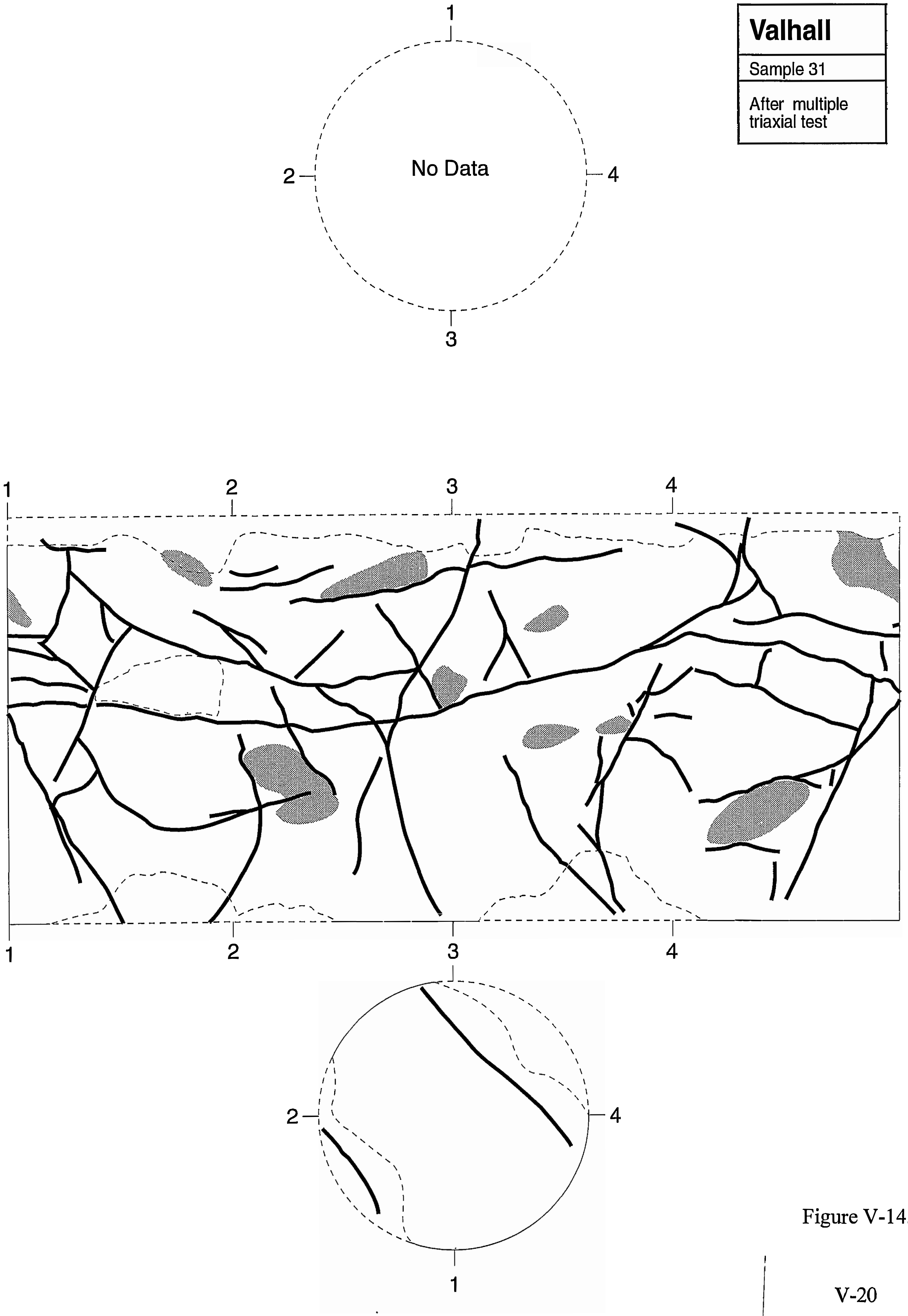
Valhall
Sample 31
After multiple triaxial test
1
2
No Data
4
3
1
2
3
4
1
2
3
4
3
2
4
1

Figure V-14.

Valhall Hod, sample 32

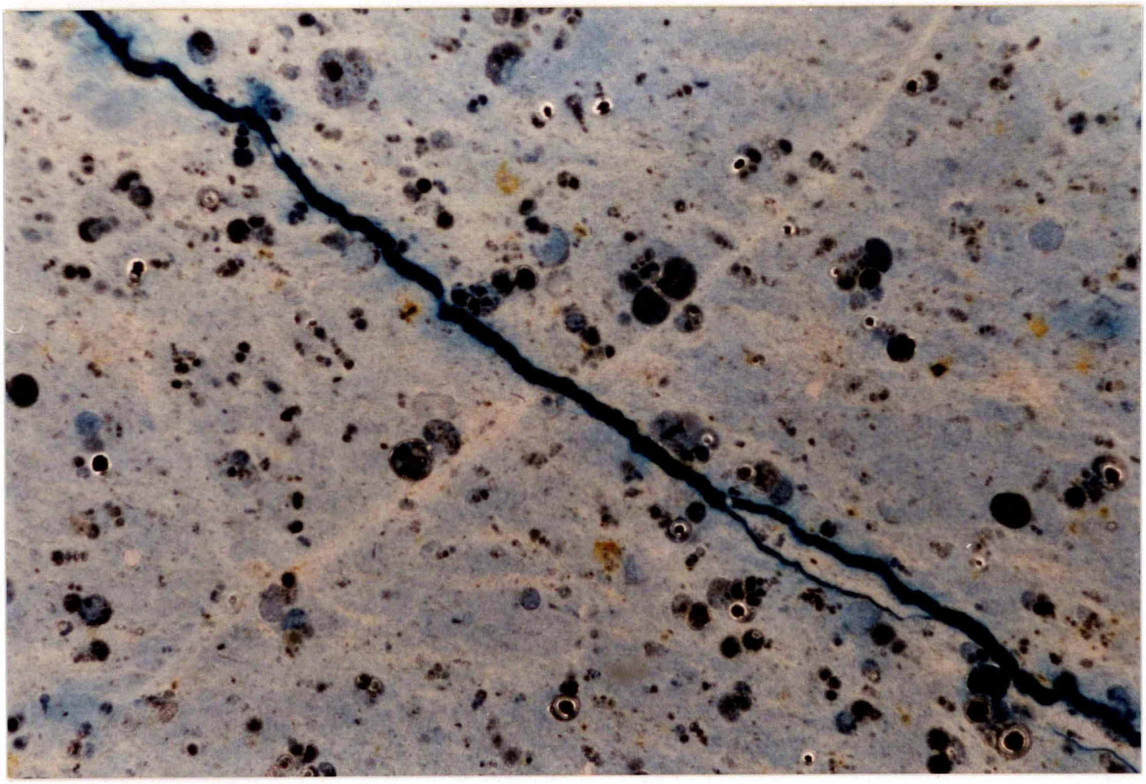

Figure V-15. Scale: ▬ 1 mm

Burrowed Laminated Chalk Mudstone

Well/location: Valhall, Norway

Formation: Hod

Depth:

M	mudstone
Cal	low argillaceous chalk
Gn	no grains
Bn	no bedding
Lpl	planar lamination (weak)
Dn	no deformation
Th	high density of trace fossils
Hm	medium hard
Cm	medium consolidation
Sn	no visible stylolites
Mn	no visible secondary minerals
Fn	no visible fractures (original rock)

Description:

Medium hard, highly bioturbated argillaceous mudstone with weak lamination.

The chalk has a sparse biomicritic wackestone texture with foraminifera as the most dominant grain component (fig. V-15). The chambers are open or filled with micrite.

The chalk is dominated by well preserved coccoliths interceded with clay flakes. An open porous framework formed by "grainbridging of coccoliths" is characteristic for this sample. The clay content is relatively high and there seems to be a relationship between clay content and the cementation. Overgrowth is rare and relatively few euhedral calcite cement crystals are present.

Trace fossils:

Ichnogeneous: *Planolites*, *Zoophycos*, *Chondrites* and *Thalassinoides*.

Insoluble residue:

19.36 %
Quartz (34 %) and kaolinite (traces of feldspar and clay)

Petrophysical properties:

Porosity:	32.71 %
Permeability (air):	0.932 mD
Density:	2.704 g/cm^3

Uniaxial strain compaction

Pre-test description:

Not available.

Post-test description:

Not available.

Valhall Hod, sample 33

Figure V-16.

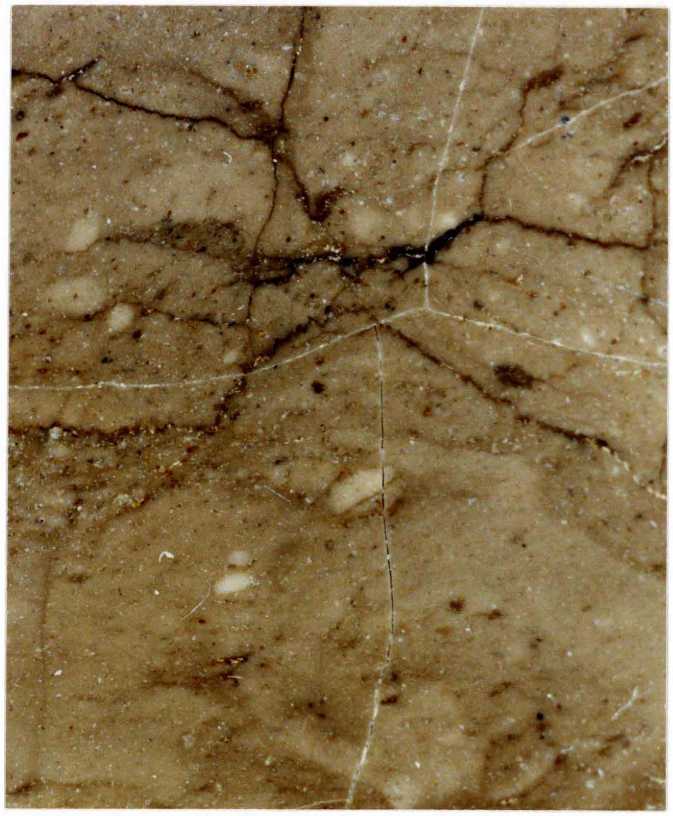

Figure V-17. Scale: 5 mm

Pebbly Chalk Wackestone

Well/location: Valhall, Norway

Formation: Hod

Depth:

Wc	coarse wackestone
Cla	low argillaceous
Gch	chalk clasts
Bn	no visible bedding
Ln	no visible lamination
Ds	sheared deformation
Tm	medium density of trace fossils
Hm	medium hard
Cm	medium consolidation
Sl	low degree of stylolites
Mn	no visible secondary minerals
Fhl	low degree of healed fractures

Description:

The sample is a medium hard, pebbly argillaceous wackestone (fig. V-16). A weak lamination partly related to pressure dissolution seams (fig. V-17).

The chalk has a sparse biomicritic wackestone texture with foraminifera as the most dominant grain component. The chambers are open or filled with micrite.

A relatively low clay content in the chalk gives rise to a higher degree of calcite cementation. Disintegration of the coccoliths is more common than in sample 31 and 32. The sample comprises a "poorly sorted" matrix with calcite cement crystal sizes ranging from < 1µm up to ~5µm.

Trace fossils:

Ichnogeneous: *Planolites*, *Zoophycos* and *Thalassinoides.*

Insoluble residue:

9.83 %
Quartz (37 %) and kaolinite (traces of feldspar and pyrite)

Petrophysical properties:

Porosity:	34.09 %
Permeability (air):	5.58 mD
Density:	2.702 g/cm^3

Valhall Hod, sample 33
Direct shear test

Pre-test description:

Not available.

Post-test description:

Not available.

Valhall Hod, sample 34

1 cm

Figure V-18.

Massive Chalk Mudstone

Well/location: Valhall, Norway

Formation: Hod

Depth:

Wc	coarse wackestone
Arl	low argillaceous
Gch	chalk clasts
Bn	no visible bedding
Lpl	planar lamination
Dn	no deformation
Tm	medium density of trace fossils
Hm	medium hard
Cm	medium consolidation
Sl	low degree of stylolites
Mn	no visible secondary minerals
Fol	low degree of open fractures

Description:

The sample is a medium hard, pebbly argillaceous wackestone (fig. V-16). A weak lamination partly related to pressure dissolution seams (fig. V-17).

The chalk has a sparse biomicritic wackestone texture with foraminifera as the most dominant grain component. The chambers are open or filled with micrite.

A relatively low clay content in the chalk gives rise to a higher degree of calcite cementation. Disintegration of the coccoliths is more common than in sample 31 and 32. The sample comprises a "poorly sorted" matrix with calcite cement crystal sizes ranging from < 1µm up to ~5µm.

Trace fossils:

Ichnogeneous: *Planolites*, *Zoophycos*, *Chondrites* and *Thalassinoides*.

Insoluble residue:

6.16 %
Quartz (39%) and kaolinite (feldspar and pyrite).

Petrophysical properties:

Porosity:	33.81 %
Permeability (air):	9.34 mD (fractured)
Density:	2.694 g/cm^3

Valhall, sample 34
Direct shear test

Pre-test description:

Not available.

Post-test description:

Not available